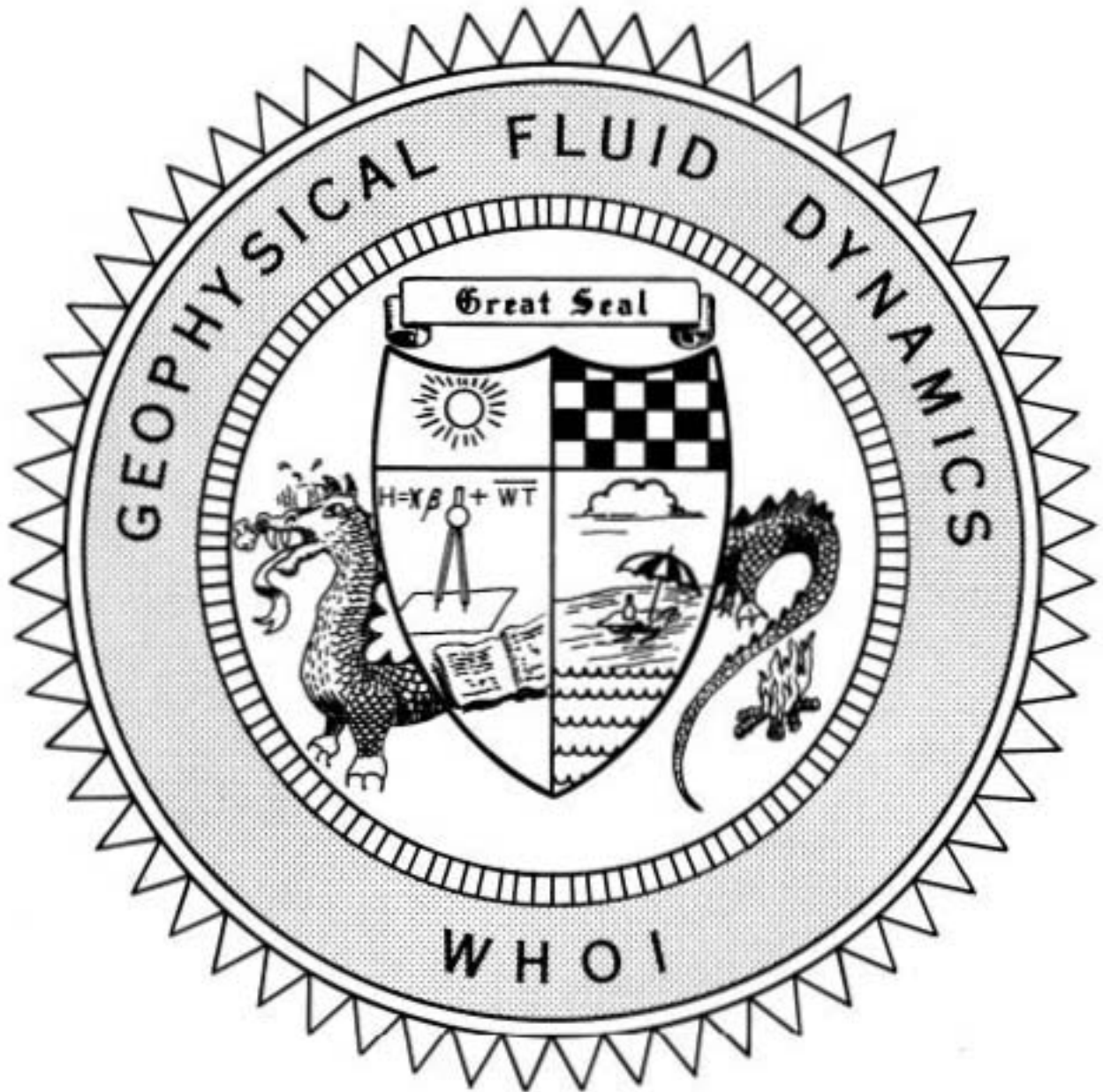


71-63

1971

VOLUME



COURSE LECTURES
AND
ABSTRACTS OF SEMINARS

Notes on the 1971
Summer Study Program
in
GEOPHYSICAL FLUID DYNAMICS
at
The WOODS HOLE OCEANOGRAPHIC INSTITUTION

Reference No. 71-63

Contents of the Volumes

Volume I	Course Lectures and Abstracts of Seminars
Volume II	Fellowship Lectures

Participants and Staff Members

Charney, Jule G.	Massachusetts Institute of Technology
de Rivas, Eugenia E.	Massachusetts Institute of Technology
Gierasch, Peter J.	Florida State University, Tallahassee
Holton, James R.	University of Washington
Howard, Louis N.	Massachusetts Institute of Technology
Ingersoll, Andrew P.	California Institute of Technology
Keller, Joseph B.	Courant Institute of Mathematical Sciences
Kraichnan, Robert H.	Dublin, New Hampshire
Leovy, Conway B.	University of Washington
Malkus, Willem V.R.	Massachusetts Institute of Technology
Moffatt, H. Keith	University of Cambridge, England
Ooyama, Katsuyuki	New York University
Prinn, Ronald G.	Massachusetts Institute of Technology
Rasool, S. I.	Institute of Space Studies, New York
Sakurai, Dr. Takeo	N.C.A.R., Boulder, Colorado
Simmons, Adrian J.	University of Cambridge, England
Smagorinsky, J.	Princeton University
Stern, Melvin E.	University of Rhode Island
Thompson, Rory	Woods Hole Oceanographic Institution
Veronis, George	Yale University
Welander, Pierre	Massachusetts Institute of Technology
Williams, R. Terry	Naval Postgraduate School, Monterey, California
Young, Richard E.	University of California at Los Angeles

Fellows

Baker, Louis	Columbia University
Bennett, John R.	University of Wisconsin
Cottrell, John W.	Stanford University, California
Dubisch, Russell	Cornell University
Roberts, Glyn O.	Courant Institute of Mathematical Sciences
Saunders, Kim D.	W.H.O.I. and Massachusetts Institute of Technology
Schneider, Edwin K.	Harvard University
Simmons, Adrian M.	University of Cambridge, England
Thiebaut, Martial L.	University of Massachusetts

Editor's Preface

A topic, such as planetary atmospheric dynamics, is necessarily a speculative one because of the extreme difficulty of obtaining detailed observations. A single datum is often responsible for several "theories". Andy Ingersoll was continually challenged during his attempts to present a coherent picture of a broad spectrum of observations and speculations about the atmospheres of the planets. He emerged somewhat battered but still intact. All of us felt rewarded by his efforts.

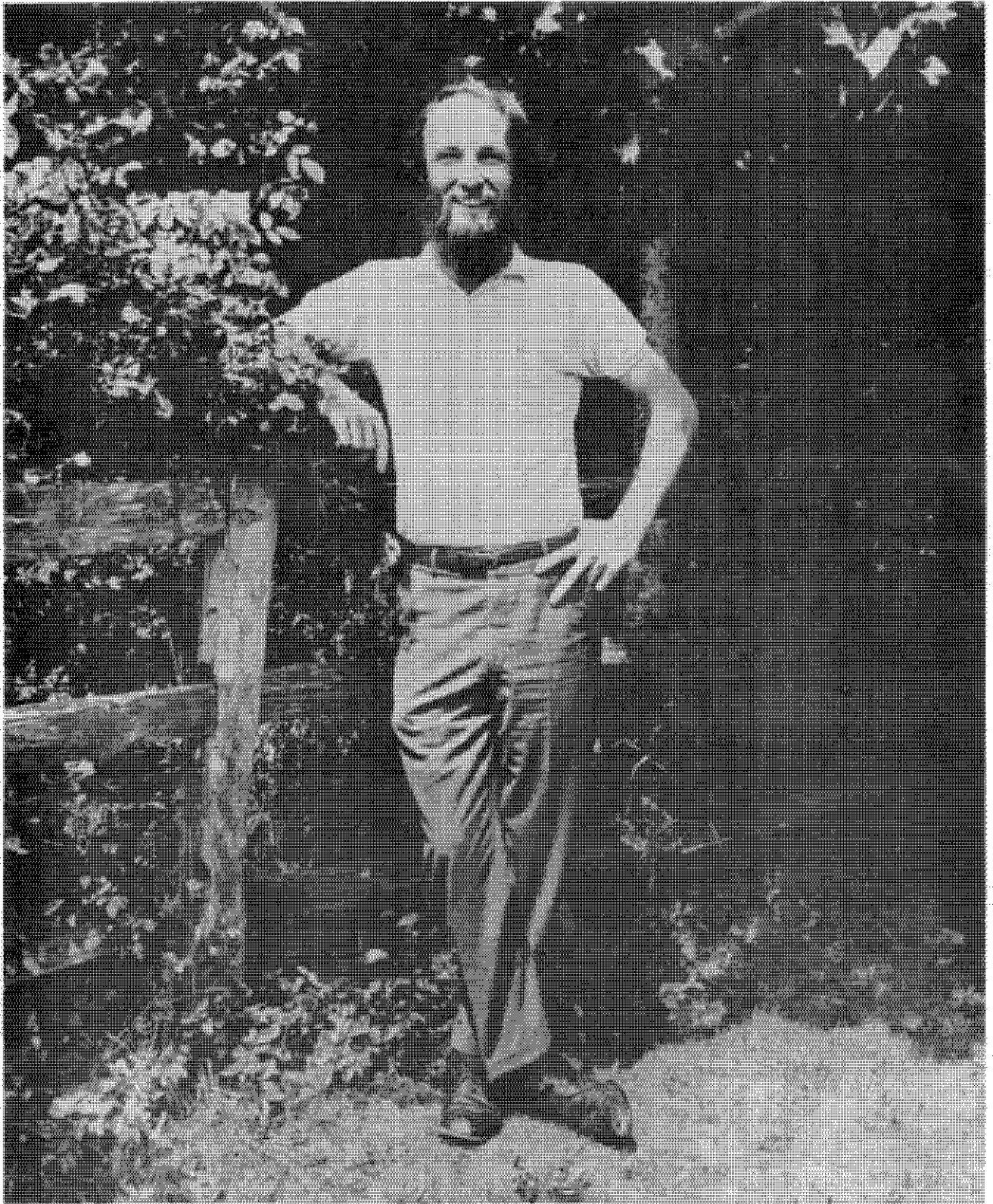
The formal lectures were followed by a microsposium on planetary atmospheres which included discussions of the latest observations, speculative theories and simple models of certain gross features.

Jule Charney's stimulating three lectures formed the basis for a two-week symposium on the general circulation of the atmosphere and the role of the intertropical convergence zone in the mean circulation,

Robert Kraichnan addressed himself to the problem of predictability of turbulent flow and discussed the topic of prediction in meteorology.

All of us who took part in this thirteenth GFD program are grateful to the National Science Foundation for its continued support. The Woods Hole Oceanographic Institution has once again encouraged us to branch out and explore topics which are not normally studied in an oceanographic institution. We are especially thankful for the continued efforts of Mary Thayer to keep the program running smoothly.

George Veronis



Andrew P. Ingersoll, Principal Lecturer
"From out of the bouche came words of wisdom".

CONTENTS OF VOLUME I

Course Lectures and Seminars

COURSE LECTURES

by

Andrew P. Ingersoll
California Institute of Technology, Pasadena

DYNAMICS OF PLANETARY ATMOSPHERES		Page No.
Lecture #1	Scaling of Atmospheric Motions for a Non-rotational Planet	1
Lecture #2	Scaling for a Rotating Planet, Introduction to the Planets	5
Lecture #3	Composition of Planetary Atmospheres: Earth and Mars	10
Lecture #4	The Atmosphere of Venus	16
Lecture #5	The Hydrostatic Approximation. Kinematics of Jupiter's Cloud Bands .	21
Lecture #6	The Heat and Vorticity Equations .	28
Lecture #7	Barotropic Models of Jupiter's Atmosphere . .	34
Lecture #8	Potential Vorticity and Baroclinic Instability . .	43
The Venusian Atmosphere (Lecture #1) Peter J. Gierasch		51
The Venusian Atmosphere (Lecture #2) Peter J. Gierasch		58
The Boussinesq Approximation in a Multi-component Fluid (Abstract) George Veronis		63
Turbulent Diffusion (Abstract) Joseph B. Keller		63
The Thermohaline Circulation (Abstract) Pierre Welander		65

CONTENTS OF VOLUME I (continued)

	Page No.
Laminar Rotating Flame Effect in a Stratified Fluid at Small Prandtl Number (Abstract)	68
Melvin E. Stern	
Physical Tracers in Oceanography (Abstract)	69
George Veronis	
Planetary Fluid Dynamics Symposium	70
A Quick Survey of Theoretical Work having Possible Relevance to the Apparent Rotation of the Upper Venus Atmosphere (Abstract)	70
Conway B. Leovy	
Consequences of Momentum and Thermal Diffusion for the Mean Shear induced by a Moving Heat Source (Abstract).	73
Richard E. Young	
The Circulation of the Atmosphere of Venus (Abstract)	74
Eugenia E. Kalnay de Rivas	
Venus Four-day Circulation as an Instability (Abstract)	75
Rory Thompson	
The Problem of the Resonant Rotation of Venus (Abstract)	77
Andrew P. Ingersoll	
Planetary Fluid Dynamics	79
Jule G. Charney	
Geostrophic Turbulence	87
Jule G. Charney	
The Circulation of the Earth's Atmosphere .	91
Jule G. Charney	
Structural and Compositional Models for the Jovian Atmosphere and Clouds (Abstract)	96
Ronald G. Prinn	

CONTENTS OF VOLUME I (continued)

	Page No.
A Moist Model of Jupiter's Cloud Bands (Abstract) , Peter J. Gierasch	98
Motion of Jupiter's Red Spot (Oceanography of Jupiter) (Abstract) George Veronis	100
Mars: The Small White Spots (Abstract) . Conway B. Leovy	100
ABC's of Convection (Abstract) Louis N. Howard	102
The Parameterization of Convection in Tropical Disturbances (Abstract) Katsuyuki Ooyama	106
Non-periodic Convection and Reversing Dynamos (Abstract) . Willem V.R. Malkus	107
Generation of a large-scale Magnetic Field by Random Fluid Motion (Abstract) H. Keith Moffatt	108
Dynamics of Tropical Cyclones (Abstract) . Katsuyuki Ooyama	110
Predictability of Fully-developed Turbulence in Two and Three Dimensions (Abstract) Robert H. Kraichnan	112
Dynamics of Isotropic Turbulence, I and II (Abstract) Robert H. Kraichnan	113
Equatorial Wave Disturbances (Part I and Part II) (Abstract) . James R. Holton	114
The Dynamics of the Polar-night Jet (Abstract) Adrian J. Simmons	116

CONTENTS OF VOLUME I (continued)

	Page No.
Numerical Simulation of the Tropical Circulation (Abstract) Joseph Smagorinsky	118
A Simple Numerical General Circulation Model (Abstract) R. Terry Williams	118
An Episode from the Study of the Solar Spin-down Problem (Abstract) Takeo Sakurai	119
Frontogenesis (Abstract) R. Terry Williams	120
The Problem of Oxygen in the Earth's Atmosphere (Abstract) Saiyed I. Rasool	123

DYNAMICS OF PLANETARY ATMOSPHERES

Andrew P. Ingersoll

Lecture #1 SCALING OF ATMOSPHERIC MOTIONS FOR A NON-ROTATIONAL PLANET

References: Golitsyn, Icarus 13: 1, 1970 and
Gierasch, Goody and Stone, GFD 1: 1, 1970.

The above references are attempts to find the relevant scales of time, velocity and temperature fluctuation for motions in planetary atmospheres, using the external parameters of the problem. The approach I am going to give basically agrees with Gierasch, Goody and Stone and differs in some important respects from that of Golitsyn. We begin by writing down the basic parameters which have to be considered in any complete theory.

$$(1) \frac{q_A}{4} = \frac{(1-A)F}{4} \quad \text{where } F = \text{solar constant} \\ \text{and } A = \text{albedo,}$$

$$(2) a = \text{radius of planet.}$$

$$(3) M = \text{mass per unit area of the atmosphere.}$$

$$(4) g = \text{gravitational acceleration.}$$

$$(5) \sigma = \text{Stefan-Boltzman constant.}$$

$$(6) c_p = \text{specific heat at constant pressure.}$$

$$(7) \gamma = \frac{c_p}{c_v} = 1 + \frac{R}{c_v}$$

$$(8) \text{latent heat parameters.}$$

$$(9) \text{transport parameters; viscosity, thermal conductivity, opacity}$$

$$(10) \Omega = \text{rotation rate.}$$

To start with we will consider only the first six. The seventh, γ , is non-dimensional and of order unity, and thus all of our results contain

factors which are functions of it, The eighth and ninth are too complicated to bring in here, The tenth, Ω , will be added later, The ultimate test of this approach is the degree to which it accounts for the observed differences among the planets.

From the six parameters $\frac{q_A}{4}$, M , σ , g , c_P one can form two non-dimensional numbers since there are four units (mass, length, time, temperature). (I will use c_P in the place of any other gas constant such as c_V or R since they are all related if γ is known, Thus the scale height, H , equal to $\frac{RT}{g}$, is proportional to $\frac{c_P T}{g}$.) The two non-dimensional combinations are

$$\delta = \frac{c_P \left[\frac{q_A}{4\sigma} \right]^{1/4}}{g a} \quad \text{and} \quad \mu = \frac{\left[\frac{q_A}{4M} \right]^{1/2}}{\left[c_P \left(\frac{q_A}{4\sigma} \right)^{1/4} \right]^{1/2}}$$

Both numbers are small for most planets although μ may be of order unity for Mars.

The combination $\left[\frac{q_A}{4\sigma} \right]^{1/4}$ is the radiative equilibrium temperature, T . The number δ is the ratio of the scale height to the radius of the planet. The number μ can be interpreted in three ways. The denominator is $(c_P T)^{1/2}$, proportional to the speed of sound, The numerator can be seen to be the typical horizontal velocity by the following scale analysis of the equations of motion:

By balancing the pressure gradient force and the acceleration term in the equation of motion, one gets

$$\frac{v_i^2}{a} \approx \frac{p_1}{\rho a}$$

where p_1 is a typical departure of pressure from the state of hydrostatic

equilibrium, and v_1 is a typical horizontal velocity,

Using the relation $\frac{p_1}{p} \approx \frac{T_1}{T}$ from the equation of state we arrive at

$$p_1 \approx \left(\frac{\gamma-1}{\gamma}\right) \rho c_p T_1, \text{ whence } v_1^2 \approx \left(\frac{\gamma-1}{\gamma}\right) c_p T_1$$

where T_1 is a typical temperature fluctuation associated with the motion.

Now suppose that advection of heat is important in the thermodynamic equation:

$$v_1 \frac{T_1}{a} \approx \frac{q_A}{4c_p M}$$

Solving these last two relations for v_1 gives

$$v_1 \approx \left[\left(\frac{\gamma-1}{\gamma}\right) \frac{q_A a}{4M} \right]^{1/2}$$

Thus, except for a factor depending only on γ , μ is the ratio of the fluid velocity to the speed of sound, i.e., the Mach number,

The second interpretation of μ is that it is the ratio of two time scales. One time scale is the dynamical time scale $\tau_1 = a/v_1$. The second is the radiative time scale

$$\tau = \frac{M c_p T}{q_A 4} = \frac{M c_p T}{\sigma T^4}$$

This is the time it would take the sun to heat up the atmosphere to the temperature T . Thus, except for factors depending on γ , we have

$$\mu \approx \left(\frac{\tau_1}{\tau}\right)^{1/2}$$

The third interpretation is that μ is the ratio of two temperatures. We have shown that T_1 is the typical temperature difference associated with the motion, where

$$T_1 \approx \left(\frac{\gamma}{\gamma-1}\right) \frac{v_1^2}{c_p}$$

Thus, leaving out an unspecified function of γ , we have

$$\mu \approx \left(\frac{T_1}{T}\right)^{1/2}$$

Note that it is impossible to derive the correct dynamical scales v_1 , T_1 and τ_1 from dimensional analysis alone. The fact that both δ and μ are $\ll 1$ suggests that certain simplifications are possible, but one must examine the equations of motion to find the appropriate scaling. We observe that in the expressions for v_1 , T_1 and τ_1 , neither the scale height $c_p T/g$, nor the sound speed $(c_p T)^{1/2}$ appears, so we conclude that neither of these quantities is relevant when both δ and μ are $\ll 1$. The condition $\mu \ll 1$ is also equivalent to the statements that radiative heat exchange occurs slowly compared to advective heat exchange, and that temperature differences associated with the motion are small compared to the mean temperature.

The following table gives the magnitude of these quantities for Earth, Venus and Mars,

	Units	EARTH	MARS	VENUS
$q_A/4$	erg/cm ² sec	2.4×10^5	1.3×10^5	2.2×10^5
T	^o K	255	218	245
M	gm/cm ²	10^3	16	10^5
g	cm/sec ²	980	380	870
a	km	6380	3400	6150
c_p	erg/gm ^o K	1.0×10^7	$.85 \times 10^7$	$.85 \times 10^7$
γ	-	1.4	1.3	1.3
H	km	7.5	11.0	5.5
v_1	m/sec	35	85	7
T_1	^o K	4	40	0.25
τ_1	sec	1.8×10^5	0.4×10^5	9×10^5
μ	-	0.11	0.32	0.025

For the Earth and Mars, the above values of v_1 are larger than the observed values, and the above values of T_1 are smaller than the observed

values, The discrepancy is probably due to neglecting effects of the planet's rotation rate. For Venus, both v_1 and T_1 given above may be smaller than the actual values, because motion may take place only near the cloud tops, for which a smaller value of M applies,

Notes submitted by
John R. Bennett

SCALING FOR A ROTATING PLANET, INTRODUCTION TO THE PLANETS

Lecture #2

In the last lecture, we considered a slowly rotating planetary atmosphere and formed two independent non-dimensional parameters from the six variables:

$$g_A/a, \sigma, M, a, c_p, g$$

From these variables we defined a mean temperature, sound velocity, and scale height:

$$T \approx \left[\frac{g_A a}{4\sigma} \right]^{3/4}, \quad v \approx (c_p T)^{1/2}, \quad H \approx c_p T/g$$

The only physical consideration was to specify that the speed of sound should not enter in the scaling. There is then one dynamic velocity

unique to a function of $\delta = \frac{H}{a}$

$$v_1 \approx \left(\frac{g_A a}{4M} \right)^{1/3} f_1(\delta)$$

and a temperature representative of the departure from the mean:

$$T_1 \approx \frac{v_1^2}{c_p} f_2(\delta)$$

A dynamic time constant based on the velocity and planetary length scale is

$$\tau_1 \approx a/v_1$$

The derivation of these parameters was based on the argument that since the Mach number $\mu = v_1/v$ is generally small (although for Mars this

argument is weak), the time constant for dynamical motion is much smaller than the radiative time constant. In this case we may equate radiative heat input to rate of potential energy generation which converts to mechanical energy and is ultimately balanced by dissipation, so that

$$\underbrace{\frac{q_A}{4}}_{\text{rad. heat in}} \sim \underbrace{M c_p T_1 / \tau_1 \sim M v_1^2 / \tau_1}_{\text{potential- + dynamic energy}} \sim \underbrace{\frac{M v_1^3}{a}}_{\text{dissipation}}$$

in which, as mentioned, the radiative time constant does not enter,

An important consideration is what meaning we should attach to the temperature T_1 . For $\mu \ll 1$, the temperature distribution is controlled by dynamics and T_1 is therefore the temperature deviation from adiabatic conditions. This implies

$$\left. \begin{array}{l} \text{vertical lapse rate} \\ \text{minus adiabatic lapse rate} \end{array} \right\} \left(\frac{dT}{dz} \right) - \left(\frac{dT}{dz} \right)_{ad} \sim T_1 / H$$

$$\text{horizontal temperature gradient} \sim T_1 / a$$

For a planet like Venus, where the condition of small Mach number is strongly satisfied, we expect the vertical lapse rate to be close to adiabatic, since T_1/H is small,

Effect of Oceans

Oceans enter by adding a seasonal time constant, thereby affecting the seasonal variation of temperature. Their effect on daily variations of temperature is much less important, since these are small for most of the atmosphere in any case. On earth, the oceans carry less than 10-20% of the poleward transport of heat,

Their second major role is in completing the water cycle whereby latent heat of vaporization is convected away from the surface at low latitudes and later released in condensation.

Effect of Rotation

Including rotation in the model introduces a new time scale $\sim \Omega^{-1}$. For our model, we have assumed

$$\tau_{\text{rad}} \gg \tau_{\text{dyn}} \gg \tau_{\text{sound}}$$

comparison of Ω^{-1} with each of these time constants yields a different flow regime. Considering first $(\Omega \tau_{\text{rad}})^{-1}$:

$$(\Omega \tau_{\text{rad}})^{-1} = (v_1 / \Omega a) (v_1^2 / c_p T) = \epsilon \mu^2$$

$$\text{where } \epsilon = v_1 / \Omega a = \text{Rossby number}$$

When $(\Omega \tau_{\text{rad}})^{-1}$ is of order one, heat may be stored from day to night instead of necessarily being convected around. As this point is passed, the predominant circulation switches from solar - antisolal to equator - pole. In this regime, since Coriolis forces are still small, a Hadley convection from equator to pole should be expected.

If the rotation is fast enough so that $(\Omega \tau_{\text{dyn}})^{-1}$ is of order one, Coriolis forces become important and must be considered in the equation of motion.

$$\frac{1}{\Omega \tau_{\text{dyn}}} = v_1 / \Omega a = \epsilon$$

Another regime is defined by the ratio of rotational time constant to sound time constant such that

$$\frac{1}{\Omega \tau_{\text{sound}}} = \frac{(c_p T)^{1/2}}{\Omega a} = v_1 / \Omega a (c_p T)^{1/2} / v_1 = \epsilon \mu^{-1} = B^{1/2}$$

where B = Burger number

When this number is of order one, a new length scale is introduced, representative of baroclinic waves in the atmosphere.

$$L_1 = \frac{(c_p T)^{1/2}}{\Omega} = \frac{\sqrt{g H}}{\Omega} = \text{Rossby radius of deformation.}$$

Another important length scale is

$$L_2 = \left(\frac{v_1 a}{\Omega} \right)^{1/2} = \left(\frac{v_1}{\beta} \right)^{1/2}$$

where β = the derivative of the Coriolis parameter with respect to the poleward coordinate, This scale determines the width of the Gulf Stream, and may be representative of the width of Jupiter's cloud bands.

A number of the above parameters are listed in Table 1.

	EARTH	MARS	JUPITER
Ω	$7 \times 10^{-5} \text{ sec}^{-1}$	$7 \times 10^{-5} \text{ sec}^{-1}$	$17 \times 10^{-5} \text{ sec}^{-1}$
a	6000 km	3000 km	70,000 km
v (observed)	15m sec^{-1}	75m sec^{-1}	50m sec^{-1}
ϵ	.03	.3	.004
β	.7	.7	.002
L_1	4000 km	3000 km	3500 km
L_2	1000 km	2000 km	5000 km

Table I

Note that whereas L_1 and L_2 are comparable to a for Earth and Mars, they are $\ll a$ for Jupiter, Thus the effects of rotation are more important for Jupiter.

Planetary Properties

In Table II are listed the density, mass and period of rotation of each of the planets,

	Merc.	Ven.	Earth	Mars	Jup.	Sat.	Ur.	Nep.	Pl.
$\rho(g/cc)$	5.5	5.5	5.5	3.9	1.3	0.7	1.7	1.6	?
M/M_{\oplus}	.056	.815	1.0	.107	318	95	14	17	?
$2\pi/\Omega$	55days	-243days	24hr	24hr	10hr	10 ⁴⁵ hr	12hr	15hr	6days

Table II

The rotation of Mercury on its axis is of interest, being $2/3$ of its period of revolution about the sun, so that the same face is presented to the sun on every other closest approach (Fig.1).

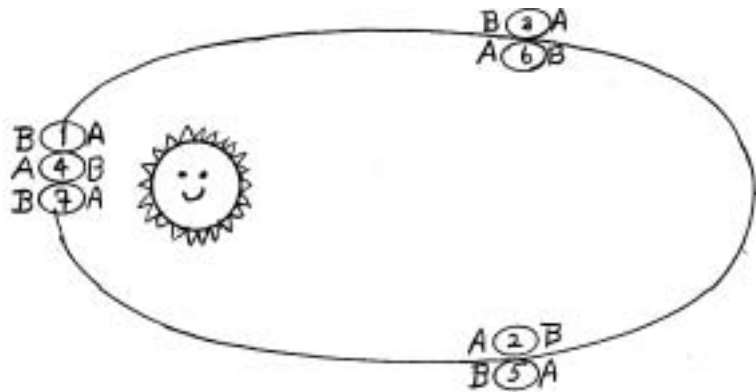


Fig.1 Rotation of Mercury through Two Solar Revolutions.

The rotation of Venus is also of interest because Venus may be locked in resonance to the Earth, a mystery because we expect the effects of the Earth on the rotation of Venus to be 10^{-6} those of the Sun. Also of interest is the preponderance of rotation periods around 10 hr. This observation is more striking if one includes the asteroids, which also have periods close to this value,

Inspection of Table II indicates that the planets fall into two categories characterized by their densities. The terrestrial planets (Mercury, Venus, Earth, Mars) are all nearly the same density as Earth, whereas the Jovian planets (Jupiter, Saturn, Uranus, Neptune) are much less dense and have densities about equal to that of water.

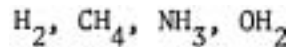
If it is assumed that the planets were originally formed from solar

material, the solar abundance of elements (Table III is of interest,

H	H	O	C	Ne	N	Si	Mg	Fe
10^7	10^6	7×10^3	3×10^3	3×10^3	10^3	3×10^2	3×10^2	10^2

Table III. Abundance of solar material relative to 10^7 atoms of hydrogen.

If a portion of solar material were cooled to 150°K , representative of the temperature on Jupiter, the excess hydrogen would combine with other elements to form molecules of



all of which are observed spectroscopically in the atmosphere of Jupiter except for water, which is frozen out below the cloud at $T = 150^\circ\text{K}$. Both Jupiter and Saturn have close to the solar composition, for if we take solar proportions for the total mass, we find the proper densities. This is not so for Uranus and Neptune, for which the observed densities are too large, and we expect these to be enriched in CH_4 , NH_3 and OH_2 .

The terrestrial planets, characterized by an excess of O relative to H_2 so that metallic oxides are formed, consist mainly of SiO_2 , MgO , FeO , Si, Fe, Mg. Their atmospheres are observed to consist mainly of H, C, O, N in compounds such as H_2O , CO_2 , N_2 , O_2 , etc., which indicate an excess of oxygen to hydrogen,

Notes submitted by
John W. Cottrell

COMPOSITION OF PLANETARY ATMOSPHERES: EARTH AND MARS

Lecture #3.

I, The Earth's Atmosphere

There are two important features of the earth's atmosphere which require further discussion: a significant absence of noble gasses and a large abundance of carbon dioxide in the earth's sedimentary rocks,

The Absence of the Noble Gases

The relative abundances of the atmospheric gases of the planets may be studied by comparing the abundances relative to those occurring in the sun. The ratios of concentration of various metals to each other are approximately the same for the earth and the sun. To compute the relative abundance of another element, the ratios of its abundance to that of a typical metal on the earth and the sun may be compared. If X is such an element a "deficiency factor" may be defined:

$$-D(X) = \log_{10} (X/Si)_{\text{earth}} - \log_{10} (X/Si)_{\text{sun}}$$

Some deficiency factors (from Mason) are given below,

X	D(X)
Ne	10.6
N	5.9
H	6.6
C	4.0
O	0.8

The large deficiency factor for Neon is typical of the other noble gases. In general, all elements which have gaseous phases at planetary temperatures are more depleted (in relation to the solar atmosphere) than those elements which form solid compounds. Apparently, the deficiency factor is an inverse measure of the tendency of the element to form solid compounds with the earth's major constituents. This indicates that

- a) The earth's atmosphere is not a remnant of the solar atmosphere and
- b) The earth's atmosphere was originally bound to the solid phase and has formed by outgassing.

The Abundance of Carbon Dioxide

The principal volatiles in the earth's atmosphere and crust are CO_2 , H_2O , N_2 and O_2 . Their abundance is given below.

Volatile	Abundance (kg cm^{-2})
H_2O	300
CO_2	40-100
N_2	0.8
O_2	0.2

The largest portion of carbon dioxide is bound in the form of limestone, CaCO_3 . This has been deposited by the reaction



in the oceans. If there were no carbonates, the earth's atmosphere would have roughly the same abundance of CO_2 as Venus.

II Physics of the Martian Atmosphere

The average radiative equilibrium temperature of Mars is about 225°K . At Martian temperatures, both CO_2 and water may occur either as solid or vapor. The abundance of the gaseous phase is governed by the saturation vapor pressure at the temperature of some point on the surface or in the atmosphere. (Note: at earth temperatures in the presence of liquid water, the CO_2 composition of the atmosphere is governed by chemical processes in the oceans such as the equilibrium with carbonates discussed above.) The typical horizontal temperature difference T_1 for Mars is observed to be about 100°K . This large value of T_1 is due to the small mass of the Martian atmosphere and its consequent lack of ability to transport heat ($\mu_{\text{Mars}} \approx \frac{1}{3}$).

A Mechanism for the Control of p_{CO_2} on Mars

Leighton and Murray (1966) constructed a model of the Martian atmosphere based on the assumption that there is an average radiative equilibrium at the poles, and that atmospheric heat transport is negligible. The average absorbed sunlight at the poles over one Martian year is $F(\sin\theta/\pi)(1-A)$, where θ is the angle of inclination of the axis of Mars' pole to its ecliptic pole. This leads to an "average" temperature

$$T_p = \left[\frac{F(1-A)\sin\theta}{\pi\sigma} \right]^{1/4}$$

Taking $A = 0.7$ (the value for frost), $T_p = 148^\circ\text{K}$. At this temperature, the vapor pressure of the solid phase of CO_2 is the same as that observed for the Martian atmosphere, about 6 mb.

Mars has two polar "ice" caps, one seasonal, the other permanent. This asymmetry results from the eccentricity of Mars' orbit. During the Martian summer, the sun heats the pole, evaporating the CO_2 . As it is evaporated, the latent heat of evaporation cools the surface. If the total change in CO_2 pressure is small, the process acts to keep the temperature at the permanent pole constant throughout the year. The total amount of CO_2 freezing during one seasonal cycle depends only on the heat deficiency between summer and winter and the latent heat of CO_2 . This amount has been estimated as 10% - 20% of the total mass of the atmosphere (about one meter depth at the pole), so the atmospheric pressure cannot change by more than this. As carbon dioxide is the major component of the Martian atmosphere, when any is evaporated from the polar cap, the pressure change is transmitted through the whole atmosphere at the speed of sound, the adjustment time

being $\propto (c_p T)^{-1/2}$. No local concentrations of CO₂ vapor can build up as in the case of water vapor on the earth,

It was also noted that CO₂ coming in to replace frozen out CO₂ brings sensible heat from the equator but this is small since

$$\text{latent/sensible heat} = \frac{\lambda}{c_p T} \approx 10.$$

Water in the Martian Circulation

Water is a minor atmospheric constituent on Mars, and its concentration is not locked to the pole temperature as is CO₂. The mechanism for controlling the amount of water in the Martian atmosphere is not the same as on earth, for Mars has no oceans. Measurements of the amount of water in the Martian atmosphere indicate that the observed gas pressure of water vapor is consistent with an equilibrium temperature of 200-225°K. If there were no source of water at or above this temperature, water would freeze out of the atmosphere until it reached a vapor pressure in equilibrium with a temperature of 148°K (the temperature of the permanent pole).

One possible solution to this problem is that the time needed for the water to freeze out of the atmosphere is very long. The Martian pole of rotation precesses with a period of 50,000 years. Thus, once every 25,000 years the permanent pole changes. During this time the water that is frozen in the permanent cap could evaporate and then slowly be frozen out again during the next precessional cycle. This mechanism could work if the time scale for freezing out the excess water at the permanent cap is longer than 25,000 years,

Two other ideas have been presented to explain the source of the water: underground rivers and juvenile water. They suffer from the same

difficulty as the aforementioned mechanism: the rate of freezing out at the permanent pole must be extremely slow. Otherwise, we would have to explain why the sources have not dried up, and why there are not vast deposits of H_2O at the polar cap. Clearly the water cycle on Mars is still a mystery.

Liquid Water on Mars

Finally, we consider whether there can be any liquid water on Mars. Liquid water will not condense directly out of the atmosphere: the partial pressure of H_2O is too low. Thus liquid water requires the melting of ice. Daytime temperatures at the equator exceed $0^\circ C$, but it is unlikely that any overnight accumulation of frost (~ 10 microns thick) would last more than a few minutes, even at temperatures well below the melting point. On the surface, such an accumulation would last approximately five minutes at $T = -10^\circ C$ (Ingersoll, 1970) and we expect it to take longer than this in going from $T = -10^\circ C$ to $T = 0^\circ C$. In soil interstices, the lifetime at $-10^\circ C$ depends on the accumulation time (~ 12 hours) and on the ratio of the pressure difference during accumulation (p_{H_2O} in the atmosphere minus p_{H_2O} in the soil at night) to the pressure difference during evaporation (p_{H_2O} at $-10^\circ C$ minus p_{H_2O} in the atmosphere]. Thus

$$\text{Lifetime at } -10^\circ C \approx (12 \text{ hrs}) \frac{p_{H_2O} (\text{atmos.})}{p_{H_2O} (-10^\circ C)} \sim 10 \text{ minutes}$$

which again implies that liquid water is not likely to occur. Note that these arguments apply only to water in equilibrium with the atmosphere; there might be juvenile liquid water at sufficient depth below the surface. Also, liquid saline solutions might occur at the surface if sufficient amount of salts were present,

References

- Allen, C. W. 1963 Astrophysical Quantities, University of London, The Athlone Press.
- Brown, H. 1949 "Rare Gases and the Formation of the Earth's Atmosphere", in The Atmospheres of the Earth and the Planets, Kuiper (ed.), The University of Chicago Press, Chicago, Illinois.
- Ingersoll, A. P. 1970 Science **168**: 972,
- Leighton, R. B. and B. C. Murray 1966 Science **166**: 136.
- Mason, B. 1966 Principles of Geochemistry (third edition).

Notes submitted by
Kim D. Saunders

THE ATMOSPHERE OF VENUS

Lecture #4

Andrew P. Ingersoll

The Properties of the Atmosphere Near the Surface

The temperature of the surface is found by both microwave radio emission and the Soviet Venera 7 probe. The best value to date of the temperature of surface is $747 \pm 20^\circ\text{K}$. The pressure at the surface has been determined by extrapolating the occultation data from the U. S. Mariner flyby. The best surface pressure data is $p_{\text{sfc}} = 95 \pm 15 \text{ atm}$. The composition of the major constituent is obtained from the Soviet probe and gives $P_{\text{CO}_2}/P = 0.95 - 0.97$. The data from the Mariner flyby have shown that at least to the level where the signal is cut off, the lower atmosphere is adiabatic to within a few percent: $\left| T_z/(T_z)_{\text{ad}} - 1 \right|$ is no more than 1 - 2%. This is true for pressures between about 0.5 atm. and 27 atm.

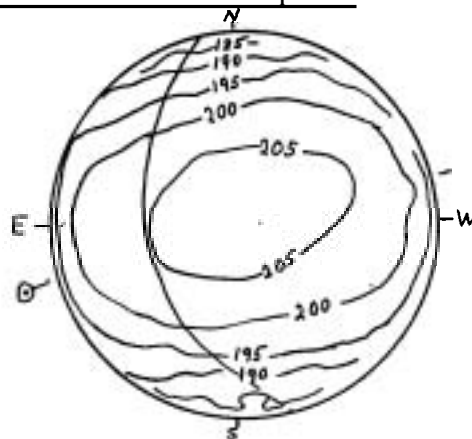
The composition of the clouds is unknown. The observations are consistent with both water clouds and dust clouds.

Explanation of the Adiabatic Gradient

In order to obtain an adiabatic atmosphere, it is necessary to stir the atmosphere. At least three mechanisms have been proposed:

1. Part of the radiation from the sun reaches the surface of the planet, causing thermal convection (provided the atmosphere is opaque to the outgoing radiation),
2. Heat is trapped by atmosphere and supplied by the solid planet.
3. The Goody-Robinson mechanism where the fluid is heated in a thin region high in the atmosphere and stirs the entire atmosphere by planetary-scale convection. (It was pointed out that this mechanism would be similar to the driving mechanism for the earth's oceans, implying that lateral thermal gradients in the oceans should be small. This is not the case, however. Stern commented that he thought the scaling was not right for this type of driving and gave the example of H. T. Rossby's experiments, which indicated that a thin absorbing layer would give rise to large lateral gradients which are not observed on Venus.)

Infrared Observations of the Venus Atmosphere



A thermal map of Venus (made from I, R. observations) is shown above. The circular pattern is a result of the phenomenon of limb darkening: for

the infrared signal to pass through the same amount of mass at the limb, it must originate at a higher, colder level than at the center of the disk. The effect of limb darkening may be removed by a fitting-residual method. This has been done by Goody (Harvard). The results obtained are:

1. The poles may be colder than the equator by 10°K and
2. The subsolar point is 2°K colder than the antisolar point. The meaning of these numbers is not clear since the pressure surfaces from whence the radiation originates may differ between equator and pole, and between subsolar and antisolar points.

Four-Day Circulation

Observations at 0.5μ do not show any features in the Venusian clouds, but features are observed when the planet is viewed in the near U. V. at 0.35μ . These features remain coherent and move in a retrograde direction with a "rotation" period of four days. Traub (Harvard) has measured Doppler shifts of CO_2 absorption lines (in the near I. R.) near the terminator and the limb. He has seen motion at the morning terminator, but not at the evening terminator. This is still a tentative result,

Since this ultraviolet radiation is reflected sunlight rather than blackbody radiation from the atmosphere, the features are not due to temperature differences, but may be due to differences in cloud composition or in cloud height,

Vertical Temperature Structure

Though the lower Venus atmosphere is adiabatic, there remains the problem of how the particular adiabat is chosen. We know the cloud top temperature which the planet must have to reradiate heat in equilibrium:

$$T = \left(\frac{q_A}{4\sigma} \right)^{1/4} \sim 240^\circ \text{K}$$

The question is: What is the pressure at this temperature?

Knowing this, the entire vertical temperature structure is determined.

We suggest two models:

1. a radiative equilibrium model, and
2. a condensate model

In the first model, it is assumed that near the top of the cloud where motion ceases, the radiation time constant is comparable to the convective time constant. Above this level, a radiative temperature gradient replaces the adiabatic temperature gradient. In this case

$$\tau_{\text{rad}} \sim \frac{M_c c_p T}{\sigma T^4} \sim \frac{a}{v_i} \sim \tau_{\text{conv}}$$

where M_c is the mass of atmosphere above the cloud deck. Now how do we determine the convective velocity? If we use M_c in our previous scaling formulas, a pressure of about 15 mb is obtained:

$$v = \left(\frac{q_A a}{4M_c} \right)^{1/3} \Rightarrow p = 15 \text{ mb}$$

Instead, if the convective velocity is based on the mass of the total atmosphere, we find $p \sim 1000$ mb. So, depending on the form of v_i taken, the pressure level where $T \sim 240^\circ \text{K}$ can be between 15 and 1000 mb, corresponding to a surface temperature variation of a factor of two,

In the second [condensate model], we suppose that the partial pressure of water in the Bower atmosphere is proportional to that of carbon dioxide:

$$\eta = \frac{p_{\text{H}_2\text{O}}}{p_{\text{CO}_2}} = \text{const} \sim 10^{-3} - 10^{-2}$$

according to the Soviet spacecraft results.

(Note: spectroscopic results indicate less water than this,]

Now if it is assumed that the equilibrium temperature corresponds to a level in the clouds where water condenses, we have

$$P_{\text{CO}_2} \text{ (cloud deck)} = \frac{1}{\eta} P_{\text{H}_2\text{O}}^{\text{sat}} \quad (T = 240^\circ)$$

This method also poses severe difficulties, for the saturation vapor pressure is extremely sensitive to temperature, changing by a factor of two as the temperature increases from 240°K to 250°K.

If the equilibrium temperature is too high, the condensate model breaks down completely. Assuming radiative equilibrium above the cloud tops, the temperature is constant while the pressure drops with altitude. The integral of $\rho_{\text{H}_2\text{O}}$ over altitude determines the total amount of water vapor above the cloud top, which is proportional to $p_{\text{H}_2\text{O}}$ at the cloud top.

$$P_{\text{H}_2\text{O}} \text{ (cloud top)} \sim g \int \rho_{\text{H}_2\text{O}} dz$$

If the total amount of water vapor above the cloud deck is large enough, the upper atmosphere is no longer transparent to infrared radiation, and the planet radiates from a higher, colder level, in spite of the fact that equilibrium requires that it radiate at the cloud top temperature. So there is a temperature for which the model breaks down, about 280°K or 10 mb of H₂O above cloud tops. If T_{eq} were above this, the cloud would have to evaporate completely before equilibrium could be established. On Venus today, where there is a limited amount of water vapor in the atmosphere, this would pose no difficulties. However, if an ocean of water were initially present on Venus, raising the equilibrium temperature above 280° would lead to catastrophic changes: evaporation of the ocean and a water vapor atmosphere.

It is significant that a planet with the earth's albedo ($A \approx 0.3$) at the orbit of Venus would have an equilibrium temperature of about 305°K , well beyond the critical point. We shall not discuss the chemical evolution of a water vapor atmosphere, but it is possible that Venus was once a watery planet which lost its oceans by photodissociation of water, escape of hydrogen, and formation of oxides,

References

- Ingersoll, A. P. 1969 "The Runaway Greenhouse: A history of water on Venus", J.Atm.Sci., 26: 1191.
- Ingersoll, A. P. and C. B. Leovy 1971 "The Atmospheres of Mars and Venus", Annual Reviews of Astronomy and Astrophysics 9: 147-182.

Notes submitted by
John W. Cottrell

THE HYDROSTATIC APPROXIMATION. KINEMATICS OF JUPITER'S CLOUD BANDS

Lecture #5

Andrew P. Ingersoll

We begin this lecture with a discussion of the simplifications which are possible for describing motions whose horizontal scale is large compared to the vertical scale. We start out with the no-rotation case, and then introduce rotation.

The essence of the hydrostatic (thin shell) approximation is that forces leading to vertical acceleration of the fluid are small compared to the buoyancy forces. We consider as a prototype the motion determined by the following (non-rotational) equations:

$$\frac{du}{dt} = -\frac{1}{\rho} \frac{dp}{dx} \quad (1)$$

$$\frac{dw}{dt} = -\frac{1}{\rho} \frac{dp}{dz} - g \quad (2)$$

where

$$\frac{d}{dt} = \frac{\partial}{\partial t} + u \frac{\partial}{\partial x} + w \frac{\partial}{\partial z} \quad (3)$$

u = horizontal velocity

w = vertical velocity

x = horizontal coordinate

z = vertical coordinate

We have ignored the y -coordinate in the above equations, along with the corresponding velocity v ; it may be assumed that all scalings will apply to y and v as apply to x and u . One might believe that as long as

$$\frac{dw}{dt} \ll g,$$

we could obtain the full advantage of the hydrostatic approximation for this system, but this is not the case. Instead, we must show that $\frac{dw}{dt}$ is small compared to the pressure term in the vertical momentum equation, taking into account the pressure fluctuations associated with the motion. We consider the pressure to be a sum of p_0 (in hydrostatic balance) plus p_1 (a small perturbation from hydrostatic equilibrium,

$$p = p_0(z) + p_1(x, z, t) \quad (4)$$

and similarly for the density

$$\rho = \rho_0(z) + \rho_1(x, z, t) \quad (5)$$

so that

$$\frac{dp_0}{dz} = -\rho_0 g. \quad (6)$$

Then the condition we want is

$$\frac{dw}{dt} \ll -\frac{1}{\rho_0} \frac{\partial p_1}{\partial z} \quad (7)$$

This inequality is not hard to establish.: we use the scaling

$$\frac{d}{dt} \sim \frac{v_1}{L} \quad (8)$$

$$\frac{du}{dt} \sim \frac{v_1^2}{L} \sim \frac{1}{\rho_0} \frac{P_1}{L}$$

Thus $\rho_0 v_1^2 \sim P_1$.

Now, by use of the continuity equation we can show that $w \sim \frac{H}{L} v_1$. We write the continuity equation in the form

$$\frac{\partial \rho}{\partial t} + \frac{\partial}{\partial x} (\rho u) + \frac{\partial}{\partial z} (\rho w) = 0 \quad (9)$$

The magnitudes of the terms are, respectively,

$$\frac{v_1}{L} \rho, \quad \frac{v_1}{L} \rho, \quad \text{and} \quad \frac{w}{H} \rho, \quad (10)$$

provided the motions of interest take place on the convective time scale L/v_1 . The third term cannot be larger than the other terms, so we have

$$w \lesssim \frac{H}{L} v_1$$

Thus $\frac{dw}{dt} \sim \frac{v_1}{L} w \sim \frac{v_1^2}{L} \left(\frac{H}{L}\right),$

so that

$$\frac{dw}{dt} \sim \frac{H^2}{L^2} \left(-\frac{1}{\rho} \frac{\partial P_1}{\partial z}\right) \quad (11)$$

which agrees with (7), provided $H/L \ll 1$.

If we now consider a rotating system, this introduces Coriolis terms into (1) and (2)

$$\left. \begin{aligned} \frac{du}{dt} - 2\Omega v \cos \theta &= -\frac{1}{\rho} \frac{\partial p}{\partial x} \\ \frac{dv}{dt} + 2\Omega u \cos \theta &= -\frac{1}{\rho} \frac{\partial p}{\partial y} \\ \frac{dw}{dt} - 2\Omega u \sin \theta &= -\frac{1}{\rho} \frac{\partial p}{\partial z} - g, \end{aligned} \right\} \quad (12)$$

(θ = colatitude)

where the y coordinate and velocity v have now been included. The w -term in the Coriolis force has been dropped because $w \sim \frac{H}{L} v \ll v$.

Now in a rapidly rotating system $\frac{dw}{dt}$ will be small compared to $2\Omega v \cos \theta$, except near the equator. This leads to the approximate relations,

$$\frac{p_1}{\rho} \sim L\Omega u \sim L\Omega v.$$

Thus the ratio of terms in the vertical momentum equation is

$$\frac{2\Omega u \sin \theta}{\frac{1}{\rho} \frac{\partial p_1}{\partial z}} \sim \frac{\Omega u}{p_1/(\rho H)} \sim \frac{H}{L} \ll 1.$$

At the equator, we have $v \sim \frac{p}{\rho}$ and thus $\frac{2\Omega u \sin \theta}{\frac{1}{\rho} \frac{\partial p_1}{\partial z}} \sim \frac{\Omega H}{v}$, where typically $H\Omega \sim 1 \text{ m/sec}$ (atmosphere), $\sim 10 \text{ cm/sec}$ (oceans). Thus Coriolis terms may be important in the vertical momentum equation at the equator.

If we can neglect the $2\Omega u \sin \theta$ term compared to the $\frac{1}{\rho} \frac{\partial p_1}{\partial z}$ term, then we will still have the hydrostatic approximation in the rotating system.

The $\frac{dw}{dt}$ term is smaller than the $u \sin \theta$ term by the factor $\frac{H}{L} \frac{v}{\Omega L} \ll 1$.

Note that the condition $H/L \ll 1$ ensures that only the vertical component of the rotation vector enters in the dynamics. This important result is independent of the magnitude of Ω , and holds whether the Rossby number is large or small.

The hydrostatic approximation which we have just discussed allows us to use pressure coordinates to simplify our equations. We transform to the following set of variables:

$$\begin{aligned} \text{coordinates:} & \quad x, y, p, t \\ \text{dependent variables:} & \quad u, v, z, \end{aligned}$$

where $\omega \equiv \frac{dp}{dt} = \frac{\partial p}{\partial t} + \vec{v} \cdot \vec{\nabla} p$. The total time derivative is then defined as

$$\frac{d}{dt} = \frac{\partial}{\partial t} + u \frac{\partial}{\partial x} + v \frac{\partial}{\partial y} + w \frac{\partial}{\partial p},$$

where $\frac{\partial}{\partial x} \equiv \left(\frac{\partial}{\partial x}\right)_p$, etc.

The continuity equation can be found by the following: consider a differential mass $dm = \rho \, dx \, dy \, dz$. By the hydrostatic approximation $dm = \frac{1}{g} \, dx \, dy \, dp$. Since g is constant, the fluid is incompressible in x, y, p - space, so the continuity equation is

$$\frac{\partial u}{\partial x} + \frac{\partial v}{\partial y} + \frac{\partial w}{\partial p} = 0 \quad (13)$$

In transforming the momentum equations, we note that

$$-\frac{1}{\rho} \frac{\partial p}{\partial x} = g \frac{\partial p}{\partial x} / \frac{\partial p}{\partial z} = -g \left(\frac{\partial z}{\partial x}\right)_p,$$

so our system of equations is

$$\left. \begin{aligned} \frac{du}{dt} - 2\Omega v \cos \theta &= -g \left(\frac{\partial z}{\partial x}\right) \\ \frac{dv}{dt} + 2\Omega u \cos \theta &= -g \left(\frac{\partial z}{\partial y}\right) \\ \frac{1}{\rho} &= -g \frac{\partial z}{\partial p} \end{aligned} \right\} \quad (14)$$

along with the continuity equation (13). To close the system we need a heat equation, which we will discuss in the next lecture.

Application to Jupiter

Now we will attempt to apply the above equations to the analysis of the kinematics of Jupiter's cloud bands [see Ingersoll and Cuzzi, J.Atm.Sci. 26 (1969)]. We consider a system of coordinates having x increasing to the east, y to the north. Dissipative forces will be ignored in the following analysis.

The most striking thing about Jupiter when one looks at it through a telescope of moderate resolution ($\geq 4''$ diameter) is the axial symmetry. There are at least 10 identifiable belts (dark bands) and zones (light bands) which circle the planet at fairly well-defined latitudes. The typical wavelength of these features is $10''$ of latitude, or about 10^4 km, which is five times the size of the smallest features resolvable from the earth. The markings are extremely long-lived by terrestrial atmospheric standards; most of the main features have been observed for the last 70 years. Nevertheless, from spectroscopic and other data it is clear that these are merely colored clouds; the solid planet, if there is one, lies thousands of kilometers below the visible cloud surface.

The motions of observable features in Jupiter's atmosphere have been recorded by observers and compiled by B. M. Peck (The Planet Jupiter, London, Faber & Faber, 1955) in the form of the mean rotation periods of spots in the individual belts and zones. In general, the middle of belts and zones have periods close to the mean rotation period (i.e. close to the magnetic period $9^{\text{h}}55^{\text{m}}30^{\text{s}}$). The poleward edges of zones have somewhat shorter periods (down to $9^{\text{h}}49^{\text{m}}$), while the equatorward edge of zones have somewhat longer periods (up to $9^{\text{h}}59^{\text{m}}$). This is consistent with the above equations if we make the following assumptions:

(a) No y-velocity: $v = 0$.

(b) No variation with longitude or time: $\frac{\mathbf{a}}{\partial x} = \frac{\mathbf{a}}{\partial t} = 0$.

(c) The deep atmosphere is in solid rotation with the mean rotational period of the planet ($9^{\text{h}}55^{\text{m}}30^{\text{s}}$).

(d) The zones are hotter than the belts on surfaces of constant pressure. We then have

$$2\Omega \left(\frac{\partial u}{\partial p} \right) \cos \theta = \frac{\partial}{\partial y} \left(\frac{1}{\rho} \right)_p = \frac{R}{P} \left(\frac{\partial T}{\partial y} \right)_p,$$

where we have assumed the ideal gas law $p = \rho RT$. Then we may calculate

$$2\Omega \left(\frac{\partial u}{\partial z} \right) \cos \theta = -\frac{g}{T} \left(\frac{\partial T}{\partial y} \right)_p = \frac{g}{aT} \left(\frac{\partial T}{\partial \theta} \right)_p,$$

where a = radius of planet. This is then integrated to get the horizontal velocity,

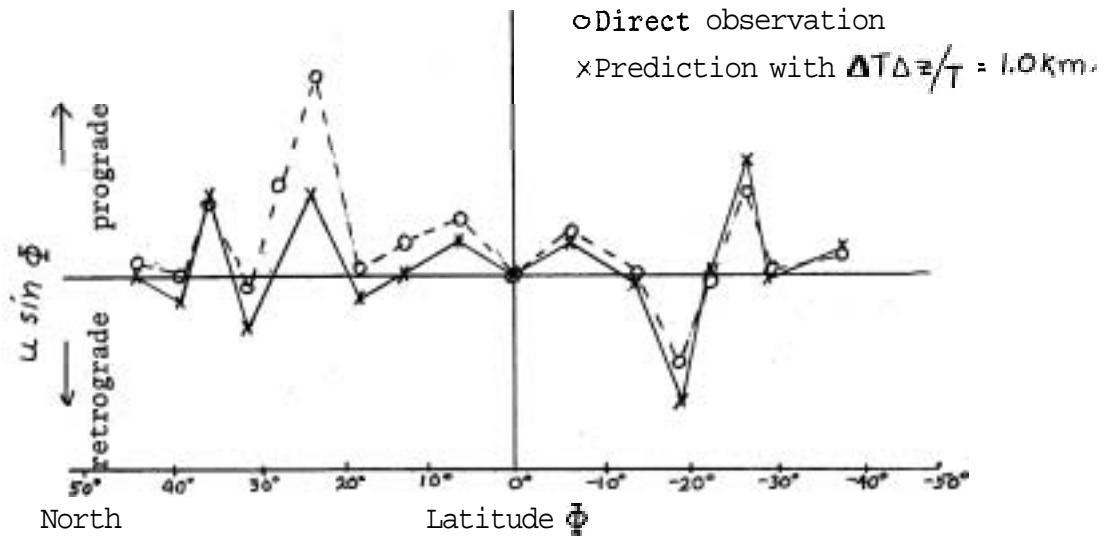
$$2\Omega u \cos \theta = \int_{-\infty}^{z_{cloud}} \frac{g}{aT} \left(\frac{\partial T}{\partial \theta} \right)_p dz \approx \frac{g}{a\Delta\theta} \left(\frac{\Delta T \Delta z}{T} \right) \begin{pmatrix} +1 \\ 0 \\ -1 \end{pmatrix} \quad (15)$$

The quantity $\Delta\theta$ is the observed width of the current and is taken to be $\frac{1}{2}$ the angular distance from the middle of a belt to the middle of the adjacent zone. The multiplier $\begin{pmatrix} +1 \\ 0 \\ -1 \end{pmatrix}$ is +1 at the north edge of a zone (south edge of a belt), 0 at the middle of a belt or zone, and -1 at the south edge of a zone (north edge of a belt). The quantity $\left(\frac{\Delta T \Delta z}{T} \right)$ will be considered as a single parameter, to be determined by a best fit to Peck's data. Such a fit gives

$$\left(\frac{\Delta T \Delta z}{T} \right) = 1.2 \text{ km} \pm 0.2 \text{ km.}$$

(See figure on next page,)

The fit is excellent, as these things go, and indicates that zones are hotter than belts on surfaces of constant pressure. This would imply rising motion in the zones and sinking motion in the belts, which is consistent with the lighter-colored zones being cloudy areas and the darker-colored belts being relatively clear areas. The infrared observations give the temperature of the cloud tops, which is almost certainly not a constant pressure surface. They indicate that the atmosphere is much more transparent over the belts than over the zones. For example, at 5μ wavelength,



the zones are at $T \sim 125^{\circ}\text{K}$ while the belts are at $T \sim 250^{\circ}\text{K}$. The most reasonable interpretation is that the zones are the cloudy areas, which is consistent with our dynamical picture. It is possible that the differences in cloud height are driven by the differences in radiative cooling: the belts radiate more heat, causing them to cool and sink, which leads to clearing of the clouds, and further radiant cooling.

Notes submitted by
Russell Dubisch

THE HEAT AND VORTICITY EQUATIONS

Lecture #6

Andrew P. Ingersoll

1. The Heat Equation in Pressure Coordinates

Define \dot{Q} by the relation

$$\dot{Q} = T \frac{ds}{dt}$$

where \dot{Q} is heat per unit mass per unit time, s is entropy per unit mass.

\dot{Q} represents the effects of radiation, dissipation of kinetic energy,

thermal conduction, and Patent heat exchange. Radiative effects include the conversion of solar radiation into heat, and emission and absorption of infrared radiation,

For an ideal gas,

$$\begin{aligned} Tds &= c_v dT + pd \left(\frac{1}{\rho} \right) \\ &= c_p dT - \frac{1}{\rho} dp \\ \text{heat} &= \Delta[\text{internal energy}] + \text{work} \end{aligned}$$

Leaving out Patent heat effects, and using $p = \rho RT$, we obtain

$$\begin{aligned} ds &= c_p \frac{dT}{T} - R \frac{dp}{p} \\ \text{or } s &= c_p \ln(Tp^{-R/c_p}) \\ &= c_p \ln \left[\frac{T}{T_s} \left(\frac{p_s}{p} \right)^{\frac{\gamma-1}{\gamma}} \right] \end{aligned}$$

where T_s and p_s are reference values for T and p .

We now define the potential temperature θ , a quantity with the dimensions of temperature and which is a function of s only:

$$\theta = T \left(\frac{p_s}{p} \right)^{\frac{\gamma-1}{\gamma}}$$

$$\text{Then } s = c_p \ln \left(\frac{\theta}{T_s} \right)$$

In terms of potential temperature the heat equation becomes

$$\dot{Q} = c_p \left(\frac{p}{p_s} \right)^{\frac{\gamma-1}{\gamma}} \frac{d\theta}{dt} \quad (1)$$

In terms of θ , the hydrostatic equation becomes

$$\frac{1}{\rho} = \frac{R}{p_s} \left(\frac{p_s}{p} \right)^{\frac{1}{\gamma}} \theta = -g \left(\frac{\partial z}{\partial p} \right)_{x,y,t} \quad (2)$$

We now have a closed system: five equations in five unknowns. The five equations include continuity, heat, hydrostatic, and two horizontal momentum relations. These equations differ from the Boussinesq in that we now have pressure-dependent equivalent specific heat and thermal coefficient of expansion, associating like terms in the two systems. In the Boussinesq system the u-momentum equation is

$$\frac{du}{dt} = -\frac{1}{\rho_s} \left(\frac{\partial p}{\partial x} \right)_{y,z}$$

the vertical momentum equation is

$$-\alpha g T = -\frac{1}{\rho_s} \left(\frac{\partial p}{\partial z} \right)_{x,y}$$

Here α , the coefficient of thermal expansion is defined by

$$\alpha = -\frac{1}{\rho} \left(\frac{\partial \rho}{\partial T} \right)_p = \text{constant} = \frac{1}{T_s}$$

for an ideal gas. The new buoyancy term is almost the same as the buoyancy term for a Boussinesq fluid if $\frac{p}{p_s}$ constant. This approach can be generalized for any compressible system going to infinity in z , whose scale height is much less than the horizontal scale,

To get the compressible equations from the Boussinesq equations we make the following associations:

$$\begin{aligned} z &\rightarrow p \\ \frac{1}{\rho_s} p &\rightarrow gz \\ T &\rightarrow \theta \\ \alpha g &\rightarrow \frac{R}{p_s} \left(\frac{p_s}{p} \right)^{\frac{1}{\gamma}} \\ c_p &\rightarrow c_p \left(\frac{p}{p_s} \right)^{\frac{\gamma-1}{\gamma}} \end{aligned}$$

Scaling for a non-rotating system

$$\frac{du}{dt} = -g \frac{\partial z_1}{\partial x}$$

where z_1 is the part of z depending on x , y , and t , i.e. the height of a constant pressure surface,

$$z = z_1(x, y, p, t) + z_0(p)$$

Scale $\frac{d}{dt} \sim \frac{v_1}{L}$. Then from the above momentum equation, we have

$$\frac{v_1^2}{L} \sim g \frac{z_1}{L} \implies v_1^2 \sim g z_1$$

Now, scale equation (1) in a region where p/p_s is of order one. Then

$$\dot{Q} \sim \frac{q_A}{4M} \sim c_p \theta_1 \frac{v_1}{L}$$

where θ_1 is the departure of θ from adiabatic. Subtracting off the hydrostatic and adiabatic part from the vertical momentum equation (2), and equating the magnitudes of the remaining terms,

$$R \theta_1 \sim g z_1 \text{ and } R \sim c_p$$

$$v_1 \sim \left[\frac{q_A L}{4M} \right]^{1/3}, \theta_1 \sim \frac{v_1^2}{c_p}$$

Then

$$z_1 \approx \frac{v_1^2}{c_p T} H = \mu^2 H \text{ where } H = \frac{c_p T}{g} \text{ is the scale height.}$$

II. Boundary Conditions

The top of the atmosphere is $p = 0$. (Note that the above scaling may not be valid near there.) We set

$$\omega = \frac{dp}{dt} = 0 \text{ at } p = 0,$$

First consider a flat bottom, i.e. $\frac{dz}{dt} = 0$. We show that

$$\omega \Big|_{\text{lower boundary}} \sim \mu \dot{\omega} \Big|_{\text{interior}} \text{ i.e., } \dot{\omega} \Big|_{\text{boundary}} = 0,$$

$$\frac{d\mathbf{z}}{dt} = \frac{\partial \mathbf{z}_1}{\partial t} + u \frac{\partial \mathbf{z}_1}{\partial x} + v \frac{\partial \mathbf{z}_1}{\partial y} + \omega \frac{\partial \mathbf{z}_1}{\partial p} = 0$$

The ratio

$$\frac{u \frac{\partial \mathbf{z}_1}{\partial x}}{\omega \frac{\partial \mathbf{z}_1}{\partial p}} \sim \frac{v_1 \frac{z_1}{L}}{p \frac{v_1}{L} \frac{1}{\rho g}} \sim \frac{g z_1}{RT} \sim \mu^* \ll 1$$

since $\frac{1}{\rho} = -g \frac{\partial \mathbf{z}_1}{\partial p}$ and $\omega \sim p \frac{v_1}{L}$. Therefore $\omega = 0$ on $p = p_s$ to lowest order,

If the bottom were not flat, for example if there were a mountain at the bottom, we would have

$$-\omega = u \frac{\partial \pi}{\partial x} + v \frac{\partial \pi}{\partial y}$$

where π is the height of the mountain in pressure coordinates:

$\pi = h g A \left(\frac{p}{p_s} \right)^6$ where h is the (x, y, z) height of the mountain. When h is not too large ($h/H \ll 1$), $\pi = h/H_s p_s$ at $p = p_s$ where $H_s = \frac{RT_s}{g}$, T_s the typical ground temperature.

III. Vorticity Equation for a Rotating System

So far we have talked about $H \ll L, \mu \ll 1$. For a rapidly rotating system, the latter condition is replaced by $v \ll \Omega L$, where Ω is the rotation rate. We shall further consider only motions for which $L \ll a$, where a is the planetary radius.

The condition $\frac{L}{a} \sim \frac{v}{\Omega L}$ is allowed, giving $L \sim \left(\frac{va}{\Omega} \right)^{1/2}$. It will be suggested that this L is the typical width of Jupiter's cloud bands in the next lecture. Keeping away from the equator, we define $f = 2 \Omega \cos \theta$.

$$\frac{1}{f} \frac{df}{dy} \sim \frac{1}{a}$$

Exactly, $\frac{1}{f} \frac{df}{dy} = \frac{\beta}{f}$ where $\beta = \frac{2\Omega \sin\theta}{a}$. Thus f varies by a fraction L/a of itself in distance L . So for motions of the scale being considered, we may assume $f = \text{const.}$ to a first approximation. The horizontal momentum equations are

$$\begin{aligned} \frac{du}{dt} - fv &= -g \frac{\partial z}{\partial x} \\ \frac{dv}{dt} + fu &= -g \frac{\partial z}{\partial y} \end{aligned}$$

Under the above assumption we find, to a first approximation

$$\begin{aligned} -fv &= -g \frac{\partial z}{\partial x} \\ fu &= -g \frac{\partial z}{\partial y} \end{aligned}$$

These are the familiar geostrophic equations, in plane geometry since

$$L/a \ll 1$$

To find the next approximation without going through a formal expansion, use the exact vorticity equation. Define $\zeta = \frac{\partial v}{\partial x} - \frac{\partial u}{\partial y}$ as the vertical component of relative vorticity. After cross differentiating the horizontal momentum equations

$$\frac{d}{dt} \zeta + v \frac{d\zeta}{dy} + (u_x + v_y)(\zeta + f) = \underbrace{\frac{\partial \omega}{\partial y} \frac{\partial u}{\partial p} - \frac{\partial \omega}{\partial x} \frac{\partial v}{\partial p}}_{(5)}$$

Estimate the magnitudes of the terms:

$$\frac{(1)}{L^2} v^2$$

$$\frac{(2)}{a} v\Omega$$

$$\frac{(3)}{L^2} v^2$$

$$\frac{(4)}{L} \Omega v$$

$$\frac{(5)}{L^2} v^2$$

$$(1) \sim (2) \text{ if } L^2 \sim \frac{va}{\Omega}$$

$$(4) \gg (1), (2), (3) \text{ and } (5) \text{ since } \frac{v}{\Omega L} = \epsilon \ll 1.$$

Then to lowest order, $(u_x + v_y)f = 0$, or $u_x + v_y = 0$, which is consistent with the geostrophic equations with $f = \text{const.}$ Substituting $-\omega_p$ for $u_x + v_y$ in the vorticity equation we see that ω_p must be of order $\left(\frac{v}{L}\right)$

times $\left(\frac{L}{a} \text{ or } \frac{v}{\Omega L}\right)$. Since $\omega=0$ at $p=0$, we then have

$$\omega \sim p \frac{v}{L} \left(\frac{L}{a} \text{ or } \frac{v}{\Omega L}\right),$$

and therefore

$$(5) \sim \frac{v^2}{L^2} \left(\frac{L}{a} \text{ or } \frac{v}{\Omega L}\right) \text{ which is } \ll (19 \text{ and } (2)).$$

Now define

$$\left(\frac{d}{dt}\right)_h = \frac{\partial}{\partial t} + u \frac{\partial}{\partial x} + v \frac{\partial}{\partial y}.$$

Then since $u \frac{\partial}{\partial x} \gg \omega \frac{\partial}{\partial p}$ to this order, and since $v \frac{df}{dy} = \left(\frac{d}{dt}\right)_h f$,

the second approximation to the vorticity equation is

$$\left(\frac{d}{dt}\right)_h (\zeta + f) - \frac{\partial \omega}{\partial p} f = 0.$$

We assume that all terms in the above equation are no greater than

$$\left(\frac{v^2}{L^2}\right) \text{ or } \left(\frac{v\Omega}{a}\right).$$

Notes submitted by
Edwin K. Schneider

BAROTROPIC MODELS OF JUPITER'S ATMOSPHERE

Lecture #7

Andrew P. Ingersoll

There is some evidence that the horizontal temperature differences at the Jovian cloud tops (Lecture #5) are due to the latent heat of water vapor (Gierasch and Barillon, J.Atm.Sci., 1970). In this model, the condensation of water in the uprising areas (zones) provides the heat to determine the temperature excess ΔT of the zones. The quantity $\int \Delta T dz \sim \Delta T \Delta z$ may then be computed from our knowledge of the amount of water in the Jovian atmosphere (based on the assumption of solar composition). The value of $\Delta T \Delta z$ computed in this way agrees with the value $\sim 100 \text{ km}^0 \text{K}$ computed in

Lecture #5 from observations of cloud motions.

Today we discuss the stability of the observed cloud motions in Jupiter's atmosphere. We shall use a barotropic model, neglecting gradients of potential temperature on constant pressure surfaces. The stability criterion is thus the barotropic stability criterion discussed by Kuo (J. Meteor. 6, 1949). This barotropic model violates the description of Jupiter's atmosphere given in Lecture #5, but we have to make this assumption to get a sufficiently tractable problem. Also, the observations indicate that the barotropic stability criterion may be relevant on Jupiter, as we shall see.

The vertical momentum equation is

$$\frac{R}{p_s} \left(\frac{p_s}{p} \right)^{\frac{1}{\gamma}} \theta = -g \frac{\partial z}{\partial p} \quad (1)$$

and for the special case of a barotropic fluid, we have $\theta = \theta(p)$, independent of x, y, t . Then from the equations of geostrophic balance we get

$$\begin{aligned} -f \frac{\partial v}{\partial p} &= -g \frac{\partial}{\partial x} \left(\frac{\partial z}{\partial p} \right) = 0 \\ +f \frac{\partial u}{\partial p} &= -g \frac{\partial}{\partial y} \left(\frac{\partial z}{\partial p} \right) = 0 \end{aligned} \quad (2)$$

Thus $\frac{\partial u}{\partial p} = \frac{\partial v}{\partial p} = 0$, so from the continuity equation we have $\frac{\partial^2 \omega}{\partial p^2} = 0$.

We also assume the boundary conditions $\omega = 0$ at $p = 0$ and $p = p_s$, so that

ω is identically zero throughout. Plugging this into the equation of conservation of vorticity,

$$\left(\frac{d}{dt} \right)_h (f + \zeta) - \frac{\partial \omega}{\partial p} f = 0$$

we get

$$\left(\frac{\partial}{\partial t} \right)_h (f + \zeta) = 0 \quad (3)$$

This equation constitutes our present approximate model for determining the stability of flow on Jupiter,

To make use of equation (3), we separate u and v into a finite-amplitude basic state plus an infinitesimal perturbation:

$$u = U(y) + u'$$

$$v = v'$$

u' and v' are given by the geostrophic equations

$$u' = -\frac{g}{f} \frac{\partial z'}{\partial y} = -\frac{\partial \psi}{\partial y}$$

$$v' = \frac{g}{f} \frac{\partial z'}{\partial x} = \frac{\partial \psi}{\partial x}$$

so that the relative vorticity is given by

$$\zeta = \frac{\partial v}{\partial x} - \frac{\partial u}{\partial y} = \nabla_h^2 \psi - \frac{dU}{dy} \quad (4)$$

(The variation of f introduces corrections of order L/a in the expression for ζ , and we may assume $L/a \ll 1$.) If we then call $\beta = \frac{df}{dy}$, we get

$$\left(\frac{\partial}{\partial t} + U \frac{\partial}{\partial x} \right) \nabla_h^2 \psi + \frac{\partial \psi}{\partial x} (\beta - U'') = 0 \quad (5)$$

which follows from the vorticity equation (Note: $U'' \equiv \frac{d^2 U}{dy^2}$). Stability may be determined by obtaining a solution of the form

$$\psi = \phi(y) e^{ik(x-ct)} \quad (6)$$

where $\text{Im}(c) > 0$ implies instability, since this will lead to growth of the perturbation in time. Inserting (6) into (5) gives

$$(U-c)(\phi_{yy} - k^2 \phi) + (\beta - U'') \phi = 0 \quad (7)$$

If we divide by $(U-c)$, multiply by ϕ^* , and integrate with respect to y , we get

$$-\int (|\phi_y|^2 + k^2 |\phi|^2) dy + \int \frac{(\beta - u'')(u - c^*)}{|u - c|^2} |\phi|^2 dy = 0, \quad (8)$$

where the term $\phi_y \phi^* \Big|_{y_1}^{y_2}$ has been assumed to vanish. Taking the imaginary part of (8) yields

$$\text{Im}(c) \int (\beta - u'') \frac{|\phi|^2}{|u - c|^2} dy = 0 \quad (9)$$

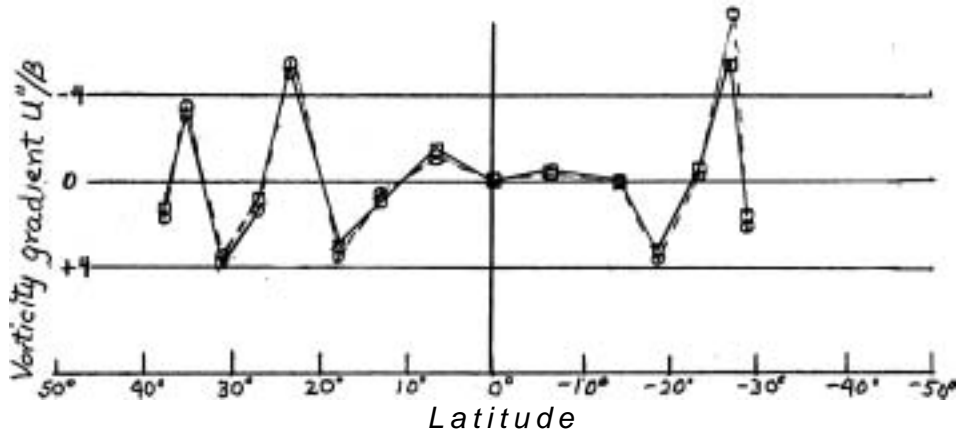
A sufficient condition for stability is thus that $(\beta - u'')$ not change sign.

Now

$$\begin{aligned} \beta &= \frac{df}{dy} = -\frac{1}{a} \frac{d}{d\theta} (2\Omega \cos \theta) \\ &= \frac{2}{a} \Omega \sin \theta > 0, \end{aligned}$$

so our condition for stability is that

$$\frac{u''}{\beta} \leq 1. \quad (10)$$



U'' has been calculated by fitting the three points (two edges + interior) of each band to a parabola. The results show that the inequality (10) is always satisfied, although sometimes just barely, suggesting that the flow may be limited to a velocity ($U \leq U_{crit}$) dependent on the width of the band. In addition, there is apparently some process tending to make U/L^2 as large as possible consistent with stability. Another way of

saying the same thing is that the width of the bands, estimated from the above stability criterion and Peek's data, is

$$L \sim \left(\frac{U}{\beta}\right)^{1/2} \sim \left(\frac{Ua}{\Omega}\right)^{1/2} \sim 5000 \text{ km,}$$

which is in good agreement with the observed widths,

We will now attempt to apply some of this physics to the Great Red Spot. Before starting, we review some of the observed properties of the GRS:

(a) Although the GRS somewhat [but not exactly] resembles the belts in color, unlike the belts it does not show enhanced 5μ emission. At 10μ , while the belts are slightly warmer than the average disk temperature, the GRS is slightly colder (by several $^{\circ}\text{K}$). In the ultraviolet, the GRS shows up as a prominent dark feature on a relatively featureless disk.

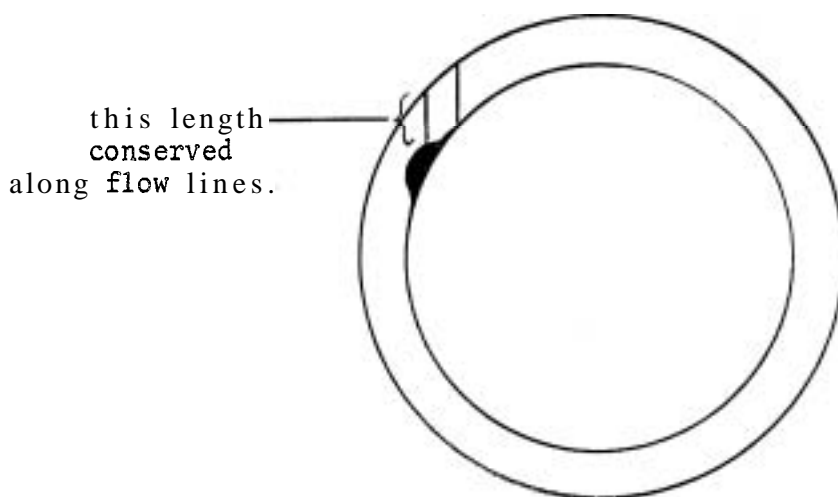
(b) Its lifetime is at least several hundred years, perhaps much longer, as it has been observed by even the earliest observers,

(c) Its rotational period is variable and slower than the magnetic period by five to ten seconds. Over long periods its longitude varies by as much as 4° from its mean longitude, that is, it may rotate ahead or behind its mean position by up to about two revolutions, as measured over a 100-year period. There is also a small oscillation of about one degree longitude with a 90-day period.

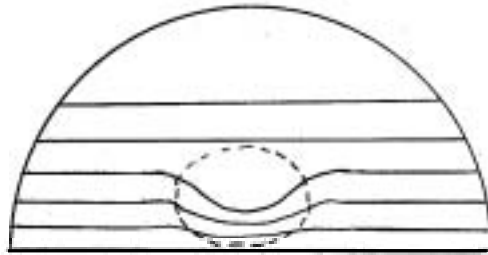
(d) The GRS is located in a region of large anticyclonic vorticity. Poleward of the Spot, prograde motion is observed. Equatorward of the Spot, there is large retrograde motion, five times greater than the retrograde flow at other points on the planet. In addition, this retrograde flow seems to be deflected toward the equator as it approaches the GRS, forming the Red

Spot Hollow in the adjacent belt. Several spots have been observed to circulate around the GRS in the anticyclonic sense with periods of four to five days.

The following qualitative argument is presented in an **attempt** to account for the above features of the GRS. It is reproduced in greater detail in Ingersoll, J.Atmos.Sci. 26, 1969. The most striking features of the GRS are its extremely long life and its relatively constant latitude over a long period of time. This suggests that the GRS may be due to some solid permanent feature of the atmosphere (its variable period probably precludes a surface feature, although it could be, for example, a **solid** mass of material floating at some level in the atmosphere). Qualitatively, the presence of a bump will perturb the flow due to the fact that the fluid tends not to compress along the rotation axis. Thus fluid will tend to flow along lines of constant length along the rotation axis (from the top of the atmosphere to the surface or bump):



The flow lines therefore will look something like this



that is, streamlines are deflected toward the equator. This is consistent with the presence of the Red Spot Hollow equatorward of the Spot.

To show this effect quantitatively, we consider the vorticity equation:

$$\left(\frac{d}{dt}\right)_h (f + \zeta) - f \frac{\partial \omega}{\partial p} = 0 \quad (11)$$

Again we assume barotropic flow, more for the sake of mathematical simplicity than because it is justified *a priori*. As we showed earlier in this lecture, barotropic flow implies $\frac{\partial^2 \omega}{\partial p^2} = 0$, or that ω is a linear function of p . The boundary conditions are

$$\begin{aligned} \omega &= 0, \quad \text{at } p = 0 \\ \omega &= -\left(\frac{p_s}{H_s}\right) \left(u \frac{\partial}{\partial x} + v \frac{\partial}{\partial y}\right) (h - z_1), \quad \text{at } p = p_s \end{aligned} \quad (12)$$

where h is the height of the topographic feature (bump] at mean pressure p_s , and H_s is the value of the mean scale height at the level where $p = p_s$.

Therefore we have

$$\frac{\partial \omega}{\partial p} = -\left(\frac{1}{H_s}\right) \left(u \frac{\partial}{\partial x} + v \frac{\partial}{\partial y}\right) (h - z_1).$$

The vorticity equation is then

$$\left(\frac{d}{dt}\right)_h \left(f + \zeta + f \frac{h}{H_s} - f \frac{z_1}{H_s}\right) = 0. \quad (13)$$

Gradients of f (with respect to y) are comparable to gradients of ζ for Jupiter, so we keep both f and ζ in the vorticity equation. In effect, we are making use of the observation discussed earlier that the length scale $L \sim (\frac{u}{\beta})^{1/2} \sim 5000$ km gives a good estimate of the widths of Jupiter's cloud bands and of the diameter of the GRS.

Since we are considering steady flow,

$$\left(\frac{d}{dt}\right)_h = u \frac{\partial}{\partial x} + v \frac{\partial}{\partial y} = \frac{g}{f} \left(-\frac{\partial z_1}{\partial y} \frac{\partial}{\partial x} + \frac{\partial z_1}{\partial x} \frac{\partial}{\partial y} \right),$$

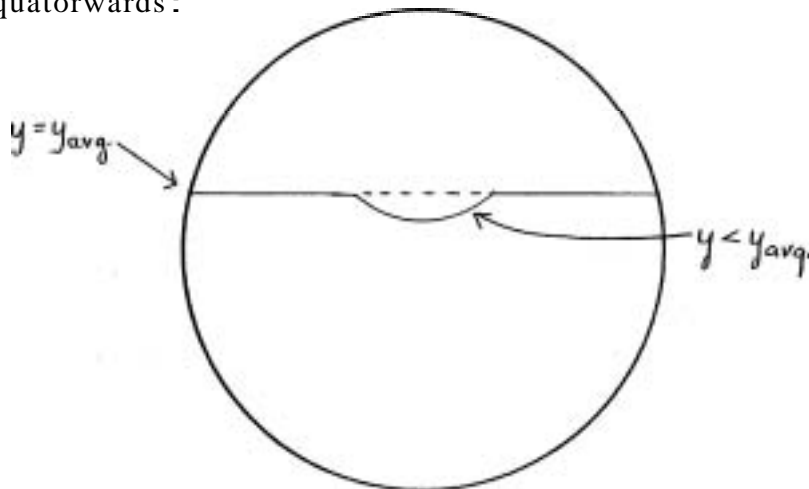
from the geostrophic equations, Now if F is any function of z_1 only, then

$$\left(\frac{d}{dt}\right)_h F = \frac{g}{f} \frac{dF}{dz_1} \left(-\frac{\partial z_1}{\partial y} \frac{\partial z_1}{\partial x} + \frac{\partial z_1}{\partial x} \frac{\partial z_1}{\partial y} \right) = 0,$$

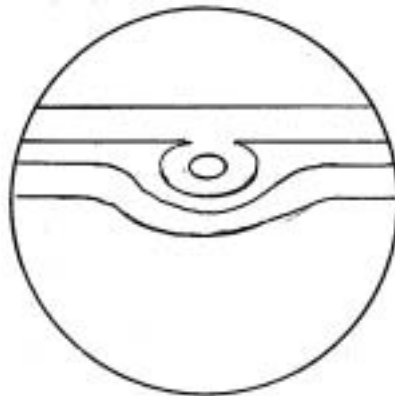
so that any function $F(z_1)$ will satisfy (13). Thus we have

$$\frac{g}{f} \nabla_h^2 z_1 + \beta y + f \frac{h}{H_s} = F(z_1) = \beta y_{avg}(z_1), \quad (14)$$

where we have assumed $\zeta = h = 0$ far upstream and downstream. Now qualitatively, if we consider the balance to be between the right-hand side and the last two terms on the left-hand side of (14), we can see that for a bump ($h > 0$), we have $y < y_{avg}$. This means that a streamline will be perturbed equatorwards:

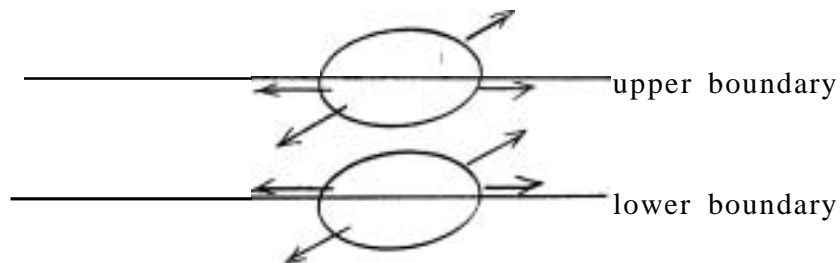


A small bump ($\frac{h}{H} \sim \frac{\Delta L}{f} \sim \frac{L}{\alpha}$) will produce a pattern of streamlines which are perturbed toward the equator. A larger bump will produce closed loops:



This brings up the following problem: the quantity on the left-hand side of (14) is conserved along streamlines. For open streamlines, its value may be determined from the flow at infinity, but closed loops are essentially a degenerate system - we have no boundary conditions, We may, however, make the following argument:

If there is positive (negative) circulation along a closed streamline, then



arrows show Ekman flow for $\zeta < 0$.

these will be a net inward (outward) flow through the Ekman Payer at the top and bottom boundaries. This precludes a steady-state solution. Thus we assume that within closed streamlines there is no motion. In particular, there can be no motion at the edge of the critical streamline. This free-surface boundary condition arises because the region inside the critical streamline "spins-down" as a result of friction with the bottom. Outside the critical streamline, we neglect friction under the assumption that

the spin-down time is long compared to the advection time L/v_1 . This free surface boundary condition, together with the condition at $x^2 + y^2 \rightarrow \infty$, completely determines the solution of the inviscid equation (14) for the flow outside the critical streamline. We will not pursue this subject further in these lectures; solved examples can be found in Ingersoll (J. Atm. Sci., 26, 1969). The application to the GRS is uncertain, partly because we do not know whether there is a solid surface or not, and partly because no one has formulated a theory with stratification, baroclinicity, non-uniform flow at infinity, or any of the other possible complications taken into account.

Notes submitted by
Russell Dubisch

POTENTIAL VORTICITY AND BAROCLINIC INSTABILITY

Lecture #8

Andrew P. Ingersoll

a) Scaling

We make the assumptions

- 1) scale height $H \ll$ horizontal scale $L \ll$ planetary radius a
- 2) Rossby number $\epsilon = \frac{v}{\Omega L} \ll 1$
- 3) $L/a \leq \epsilon$

The last assumption is made to retain the possibility of including the β -effect..

In the vorticity equation

$$\left(\frac{d}{dt}\right)_h \zeta + v \frac{d\zeta}{dy} = f \frac{\partial \omega}{\partial p},$$

$$u = -\frac{g}{f} \frac{\partial z}{\partial y}, \quad v = \frac{g}{f} \frac{\partial z}{\partial x}, \quad \zeta = \frac{\partial v}{\partial x} - \frac{\partial u}{\partial y} = \frac{g}{f} \nabla_h^2 z,$$

the second term is no larger than the first, from assumption 3) above.

Then comparing the third term and the first term, and using the boundary conditions $\omega = 0$ at $p = 0$, we have

$$\frac{\omega}{p} \sim \frac{v^2}{L^2 \Omega} = \epsilon \frac{v}{L}.$$

This insures that vertical advection of vorticity is negligible compared to horizontal advections. On the other hand, vertical advection of heat may be comparable to horizontal advections if vertical differences of θ (over an interval $\Delta p \sim p$) are a factor $\frac{1}{\epsilon}$ greater than horizontal differences of θ (over an interval $\Delta x \sim L$). In fact, this condition determines the baroclinic length scale L . Let θ_1 and θ_v be typical horizontal and vertical potential temperature differences, respectively. Then from either of the thermal wind relations, e.g.

$$f \frac{\partial v}{\partial p} = \frac{R}{p_s} \left(\frac{p_s}{p} \right)^{\frac{1}{\gamma}} \frac{\partial \theta}{\partial x},$$

we have

$$\Omega v \sim \frac{R \theta_1}{L}.$$

The condition $\theta_v \sim \frac{1}{\epsilon} \theta_1$, then becomes

$$1 \sim \epsilon \frac{\theta_v}{\theta_1} \sim \frac{v}{\theta_1} \frac{\theta_v}{\Omega L} \sim \frac{R \theta_v}{\Omega^2 L^2} \sim \frac{g H}{\Omega^2 L^2} \frac{\theta_v}{\theta_1},$$

which gives the length scale L for unstable waves in a stratified baroclinic atmosphere,

b) Equation for potential vorticity

We assume zero heating function \dot{Q} , so that $\frac{d\theta}{dt} = 0$.

We define a basic hydrostatic state θ_0, z_0 such that

$$\left. \begin{aligned} \theta &= \theta_0(p) + \theta_1(x, y, p, t) \\ z &= z_0(p) + z_1(x, y, p, t) \end{aligned} \right\} \frac{R}{p_s} \left(\frac{p_s}{p} \right)^{\frac{1}{\gamma}} \theta_0 = -g \frac{dz_0}{dp}$$

The heat equation then becomes

$$\left(\frac{d}{dt} \right)_h \theta_1 + \omega \frac{d\theta_0}{dp} = 0.$$

Vertical advections of θ_1 are negligible because $\omega/p \sim \epsilon v/L$ as described above. The basic equations in the three unknown variables z_1 ,

ω are now

$$\begin{aligned} \left(\frac{d}{dt} \right)_h \zeta + v \frac{d\zeta}{dy} &= f \frac{\partial \omega}{\partial p} \\ \left(\frac{d}{dt} \right)_h \theta_1 + \omega \frac{d\theta_0}{dp} &= 0 \\ \frac{R}{p_s} \left(\frac{p_s}{p} \right)^{\frac{1}{\gamma}} \theta_1 &= -g \frac{\partial z_1}{\partial p} \end{aligned}$$

where

$$\begin{aligned} \left(\frac{d}{dt} \right)_h &= \frac{\partial}{\partial t} + u \frac{\partial}{\partial x} + v \frac{\partial}{\partial y} \\ u &= -\frac{g}{f} \frac{\partial z_1}{\partial y}, \quad v = \frac{g}{f} \frac{\partial z_1}{\partial x} \\ \zeta &= \frac{\partial v}{\partial x} - \frac{\partial u}{\partial y} = \frac{g}{f} \nabla_h^2 z_1 \end{aligned}$$

These equations can be combined to a single non-linear equation in the variable z_1 . Eliminate θ_1 to obtain

$$\omega = - \left(\frac{d}{dt} \right)_h \left(\frac{p_s^2}{L^2} \frac{g}{f^2} \frac{\partial z_1}{\partial p} \right)$$

where we have defined

$$L^2(p) = \frac{R}{f^2} \left(\frac{p_s}{p} \right)^{\frac{1}{\gamma}} p_s \left| \frac{d\theta_0}{dp} \right|, \quad \frac{d\theta_0}{dp} < 0.$$

Then it can be shown that

$$\frac{\partial \omega}{\partial p} = - \left(\frac{d}{dt} \right)_h \left[\frac{\partial}{\partial p} \left(\frac{p_s^2 g}{f^2 L^2} \frac{\partial z_1}{\partial p} \right) \right] - \left(\frac{\partial u}{\partial p} \frac{\partial}{\partial x} - \frac{\partial v}{\partial p} \frac{\partial}{\partial y} \right) \left[\frac{p_s^2 g}{f^2 L^2} \frac{\partial z_1}{\partial p} \right]$$

which becomes

$$\frac{\partial \omega}{\partial p} = - \left(\frac{d}{dt} \right)_h \left[\frac{\partial}{\partial p} \left(\frac{p_0^2 g \partial z_1}{f^2 L^2 \partial p} \right) \right].$$

The other terms cancel, using the above expressions for u and v in terms of z_1 . Then substituting for $\frac{d\omega}{\partial p}$ in the vorticity equation, we obtain

$$\left(\frac{d}{dt} \right)_h \left[\frac{g}{f} \nabla_h^2 z_1 + f + \frac{g}{f} \frac{\partial}{\partial p} \left(\frac{p_0^2}{L^2} \frac{\partial z_1}{\partial p} \right) \right] = 0$$

The quantity in brackets, which is conserved along streamlines, is called potential vorticity,

c) Vertical stratification and boundary conditions

1) For simplicity, take

$$\theta_0(p) = \theta_s - \theta_v \left(\frac{p}{p_s} \right)^{\frac{1+\gamma}{\gamma}},$$

where θ_s and θ_v are constants. For this case we have

$$L^2 = \frac{R \theta_v}{f^2} \left(\frac{1+\gamma}{\gamma} \right) = \text{constant}$$

2) At the same time, drop the β -plane term $\beta v = \left(\frac{d}{dt} \right)_h f$.

This requires

$$\frac{L}{a} \ll \epsilon = \frac{v}{\Omega L}.$$

Again, we make this assumption for the sake of mathematical simplicity.

3) The boundary condition at the top is

$$\omega = 0 \text{ at } p = 0.$$

Assuming no bottom topography, the lower boundary condition is

$$0 = \frac{d}{dt} (z_0 + z_1) = \omega \frac{dz_0}{dp} + \left(\frac{d}{dt} \right)_h z_1, \text{ at } p = p_s.$$

The ratio of the two terms is

$$\frac{\omega \frac{\partial z_0}{\partial p}}{\left(\frac{d}{dt} \right)_h z_1} \sim \frac{(\epsilon \frac{v}{L} p) \left(\frac{1}{p g} \right)}{\frac{v}{L} z_1} \sim \epsilon \frac{H}{z} \sim \frac{v H}{\Omega L z_1} \sim \frac{g H}{\Omega^2 L^2} \sim \frac{\theta_s}{\theta_v}$$

where the last step follows since

$$\frac{g H}{\Omega^2 L^2} \frac{\theta_v}{\theta_s} \sim 1.$$

We assume that $\frac{\theta_s}{\theta_v} \gg 1$, implying that the atmosphere is close to neutral stratification. Again this assumption is made for the sake of mathematical simplicity. The boundary conditions are now $\omega = 0$ at $p = 0, p_s$, from which we obtain

$$\left(\frac{d}{dt}\right)_h \left(\frac{\partial z_1}{\partial p}\right) = 0, \text{ at } p = 0, p_s.$$

The problem as we have now formulated it was first considered by Eady (Tellus, 1949).

d) The steady symmetric state

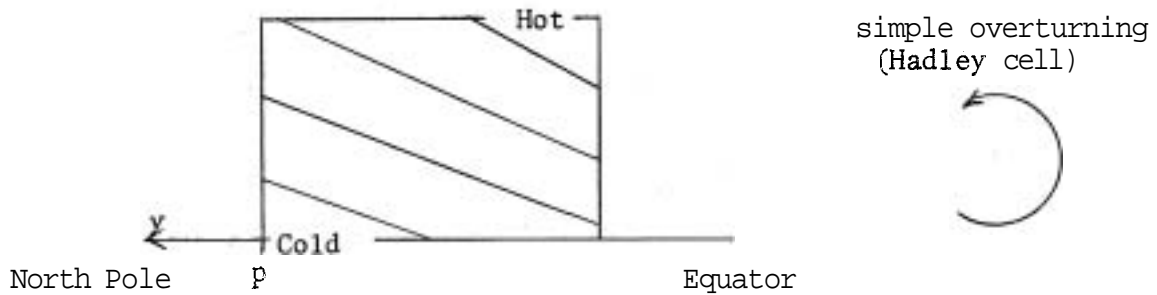
Assume a basic state $z_1(y, p), \bar{\theta}_1(y, p)$, independent of time and of the eastward coordinate x . Then the velocity is eastward; $\left(\frac{d}{dt}\right)_h = \bar{u} \frac{\partial}{\partial x}$ is identically zero; and the equations and boundary conditions are automatically satisfied. Assume further that

$$\bar{u} = -\frac{g}{f} \frac{\partial \bar{z}_1}{\partial y} = U_0 \left(\frac{1}{2} - \frac{p}{p_s}\right),$$

so that the eastward velocity is independent of latitude, increases linearly as p decreases upward, and has zero mean.

$$\begin{aligned} \bar{z}_1 &= -\frac{f U_0 y}{g} \left(\frac{1}{2} - \frac{p}{p_s}\right) \\ \bar{\theta}_1 &= -\frac{g p_s}{R} \left(\frac{p}{p_s}\right)^{\frac{1}{2}} \frac{\partial \bar{z}_1}{\partial p} = -\frac{f U_0 y}{R} \left(\frac{p}{p_s}\right)^{\frac{1}{2}} \\ \frac{\partial \bar{\theta}_1}{\partial y} &= -\frac{f U_0}{R} \left(\frac{p}{p_s}\right)^{\frac{1}{2}} \end{aligned}$$

Thus the temperature decreases northward (in the northern hemisphere, with f positive), and as the figure shows, a simple overturning motion will release gravitational potential energy. But north-south velocities require $\frac{\partial z_1}{\partial x} \neq 0$, because of the rotational (quasi-geostrophic) constraint,



Thus the basic state is unstable, because of the possibility of releasing potential energy, but as we shall see, the instability manifests itself as a wave periodic in x .

e) Stability of baroclinic wave disturbances

Now study the stability of the basic state $\bar{z}_1(y, p)$ to a small disturbance

$$z_1' = \phi(p) \exp i k (x - ct),$$

$$u' = -\frac{g}{f} \frac{\partial z_1'}{\partial y}, \quad v' = \frac{g}{f} \frac{\partial z_1'}{\partial x}$$

Replacing z_1 by $\bar{z}_1 + z_1'$ in the non-linear equation and boundary conditions

$$\left(\frac{d}{dt}\right)_h \left\{ \nabla_h^2 z_1 + \frac{p_s^2}{L^2} \frac{\partial^2 z_1}{\partial p^2} \right\} = 0,$$

$$\left(\frac{d}{dt}\right)_h \left\{ \frac{\partial z_1}{\partial p} \right\} = 0 \text{ at } p=0 \text{ and at } p=p_s,$$

and linearising in the primed quantities, gives

$$(\bar{u} - c) \frac{\partial}{\partial x} \left\{ \nabla_h^2 z_1' + \frac{p_s^2}{L^2} \frac{\partial^2 z_1'}{\partial p^2} \right\} = 0$$

$$(\bar{u} - c) \frac{\partial}{\partial x} \left\{ \frac{\partial z_1'}{\partial p} \right\} + v' \frac{\partial}{\partial y} \left\{ \frac{\partial z_1'}{\partial p} \right\} = 0 \text{ at } p=0, p_s.$$

In terms of $\phi(p)$

$$\left(\frac{d^2}{dp^2} - \frac{L^2 k^2}{p_s^2} \right) \phi = 0,$$

$$\left(\pm \frac{1}{2} - \frac{c}{\bar{u}_0} \right) \frac{d\phi}{dp} + \frac{\phi}{p_s} = 0 \text{ at } p = \frac{p_s}{2} (1 \mp 1),$$

Writing

$$\phi = \sinh \frac{Lk p}{P_s} + A \cosh \frac{Lk p}{P_s}$$

substituting in the boundary conditions, and eliminating A, gives

$$\left(\frac{ckL}{U_0}\right)^2 = 1 + \left(\frac{KL}{2}\right)^2 - kL \coth kL$$

which is of order $-\frac{(KL)^2}{12}$ for small kL and is positive for kL greater than some constant of order unity. There are always unstable solutions; the growth rate kc_L is largest, of order $\frac{U_0}{L}$, for kL of order unity.

f) Scaling arguments with applications to our atmosphere

The unstable waves which we have just described are a model of the cyclones and anti-cyclones which dominate the circulation at mid-latitudes in the earth's atmosphere. It is observed, for these waves, that kL is of order unity, and the traditional view is that the stratification determines the wavelength $2\pi/k$ through the parameter $L = \left(\frac{g}{N^2}\right)^{1/2}$ where $\theta_v = \theta(\sigma) - \theta(p_s)$. However, these waves release energy by convecting heat upward, and thus act to increase the stratification parameter θ_v . Thus it is equally possible that the wavelength of the baroclinic waves determines the stratification parameter, and not the reverse, as is usually assumed. For an independent wavelength scale, we have the barotropic stability criterion, which yields

$$L \sim \left(\frac{va}{\Omega}\right)^{1/2}$$

where v is a characteristic velocity. Assume that the NS and EW speeds are comparable in the real atmosphere. Then the velocity can be estimated as follows:

$$\frac{q_A}{4M} \sim \frac{\text{horizontal heat advection}}{\text{unit mass}}$$

$$= \frac{v}{L} c_p \theta_1$$

$$= \frac{v}{L} R \theta_1 \quad \text{since } R = c_p - c_v$$

$$= \frac{v}{L} g z_1 \quad \text{from hydrostatic balance}$$

$$= \frac{v}{L} \Omega v L \quad \text{for geostrophic flow}$$

Thus

$$v \sim \left(\frac{q_A}{4M\Omega} \right)^{1/2} \sim 15 \text{ m/sec.},$$

using estimates for the earth's atmosphere. With this velocity scale, the barotropic length scale is

$$L = \left(\frac{va}{\Omega} \right)^{1/2} \sim 1000 \text{ km.}$$

whence the wavelength of baroclinic waves is

$$2\pi L \sim 6000 \text{ km.}$$

These numbers are in excellent agreement with observation, but a mechanistic theory has yet to be worked out.

It may be significant that this scaling is also the one for which the vertical change of potential temperature θ_v is comparable to the equator-to-pole change θ_h . This follows from the relation $\theta_1 \sim \epsilon \theta_v$ derived at the start of this lecture. Since θ_1 is the change of θ over an interval $\Delta x \sim \Delta y \sim L$, it follows that

$$\theta_h \sim \frac{a}{L} \theta_1$$

However, the scaling $L \sim (va/\Omega)^{1/2}$ implies

$$\frac{a}{L} \sim \frac{\Omega L}{v} = \frac{1}{\epsilon}$$

So we have

$$\theta_h \sim \frac{1}{\epsilon} \theta_1 \sim \frac{1}{\epsilon} \theta_1 \sim \theta_v$$

These ideas do not constitute a theory. The important point is that the stratification of the atmosphere at mid-latitudes and the upward energy transport in the baroclinic waves are coupled in a non-linear fashion, the details of which have yet to be fully explained.

Notes submitted by
Glyn O. Roberts

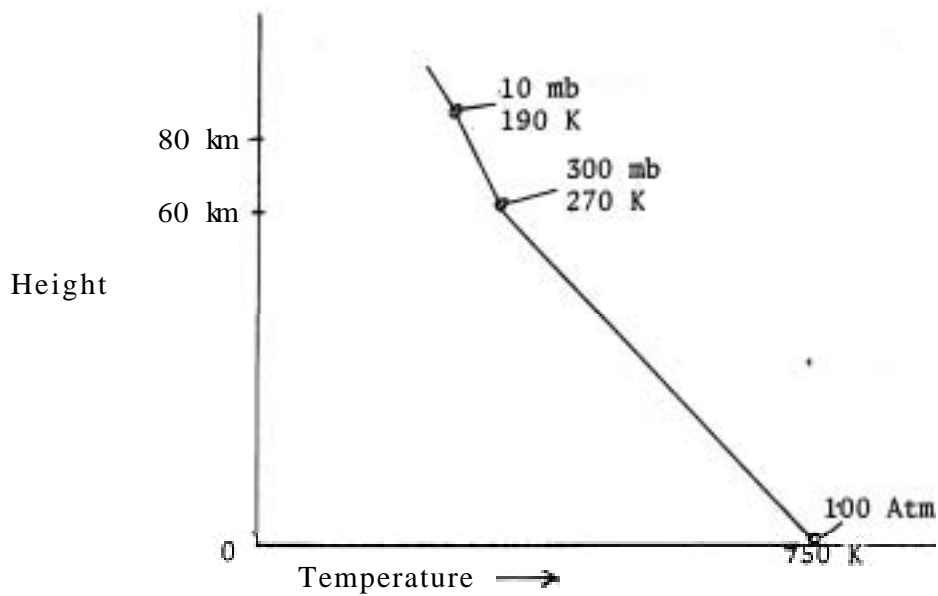
THE VENUSIAN ATMOSPHERE

Peter J. Gierasch

I. Physical properties

A. General

The Venus atmosphere is more than 90% CO_2 . The temperature profile in the vertical and values of the pressure at a few levels are roughly as indicated in the sketch below, according to data obtained by Soviet Venera probes and USA Mariner flybys (Rasool and Stewart, 1971).



Below 60 km, the lapse rate is approximately adiabatic ($\sim 10 \text{ K km}^{-1}$); between 60 and 80 km it is approximately one-half the adiabatic. The surface pressure is about 100 atm, corresponding to a total atmospheric amount of about 10^5 gm cm^{-2} .

Temperatures on the night side and on the day side seem to differ very little. Variation of infrared emission from the clouds suggests that the poles could be about 10 K cooler than the equator, however (Goody, 1965).

Surface topography, over the small area which has been explored by radar, seems to be similar in magnitude to terrestrial topography.

B. Clouds

The cloud composition is unknown. J. Lewis has pointed out that the high surface temperature would drive a large number of volatiles into the atmosphere if the soil composition is similar to the Earth's. He has performed a chemical equilibrium calculation, based on the assumption which predicts a multitude of cloud decks at different levels (Lewis, 1969). The planet's infrared spectrum is nearly featureless, indicating emission primarily from cloud, but providing no clue to the nature of the cloud (Hanel *et al.*, 1968).

The height of the cloud top is also ambiguous. Solar radiation scattered back from the clouds seems to penetrate to a level where the pressure is about 200 mb, judging from the strength of CO_2 absorption lines (Belton, 1968). On the other hand grazing solar radiation observed during transits of Venus across the Sun seems to be interrupted at a level where the pressure is only about 10 mb (Goody, 1967). Goody speaks of a deep haze rather

than a sharp cloud top, Others have proposed several distinct cloud layers, The location of the cloud bottom (if any) is unknown (both Gierasch and Ingersoll agree that it would be appreciated if the next Venera probe would carry a photometer),

The planet's albedo, approximately 0.75, is probably due primarily to the clouds.

C. Rotation

Ingersoll discusses this subject in a later lecture, and we shall at this point only mention the few basic facts which are needed for our dynamics review. The planet has a 225 day orbital period, The rotation about the planet's axis, from radar data, is retrograde with a period of about 243 days. These two rotations add to produce a solar day (sunrise to sunrise time) of about 117 days,

Venus is featureless in visible light. Photographs in the ultraviolet do show markings, however, and these markings move in a way which suggests an approximately solid body rotation of the cloud deck in the retrograde sense, with a period of about four days (Boyer and Suerin, 1969). If this observation is due to an actual wind, it is about 100 m s^{-1} in magnitude, It is in the opposite direction to the motion of the subsolar point on the planet and about 30 times faster.

II. Review of Ideas of Venusian Circulation

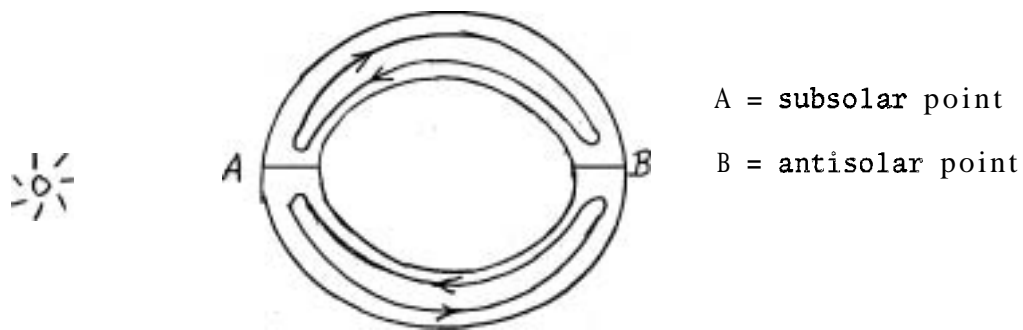
A, Introduction

Motions of only two scales have been anticipated by theoreticians: very small scale turbulent convection of some sort, with a characteristic length of one scale height or less, and very large scale Hadley cell over-

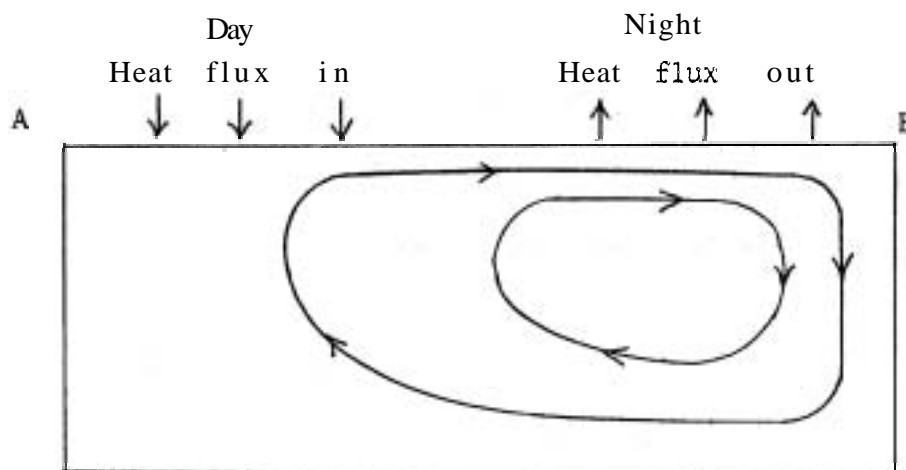
turning driven by solar heating, with a characteristic horizontal length equal to the planet's radius. Motions of intermediate scale are not expected because of the planet's small rotation rate. However, it should be borne in mind that if the atmosphere is really rotating with a four-day period at some level, then our ideas may need revision. Also, it is interesting that the ultraviolet markings have a scale which is less than the planet's radius.

B. Large scale stationary Hadley cells

Goody and Robinson (1966) investigated the nature of a hypothetical Hadley circulation between subsolar and antisolar points, as sketched below.



Spread out, the cell is as below,



They used the Boussinesq approximation in their model, with eddy diffusivities for heat and momentum taken as $10^4 \text{ cm}^2 \text{ s}^{-1}$. The lower boundary is rigid and insulating, The upper one is a free surface with heat flux boundary conditions as shown, The flow, which is deduced by scaling arguments, is characterized by a thin upper boundary layer and a thin downwelling region. Velocities in the upper boundary layer are about 30 m s^{-1} , and the temperature contrast predicted along the top is about 40 K. The temperature distribution through the interior is adiabatic, and they conclude that a high surface temperature can be produced in this way even though in the model no solar heat penetrates directly to the surface (see however the De Rivas and Schneider papers later in this volume).

A scaling by Gierasch, Goody and Stone (1970) of radiatively-driven Hadley cells on non-rotating planets (in which there will not necessarily be a boundary layer structure) predicted velocities on the order of 8 m s^{-1} and temperature contrasts of about 3 K for Venus conditions,

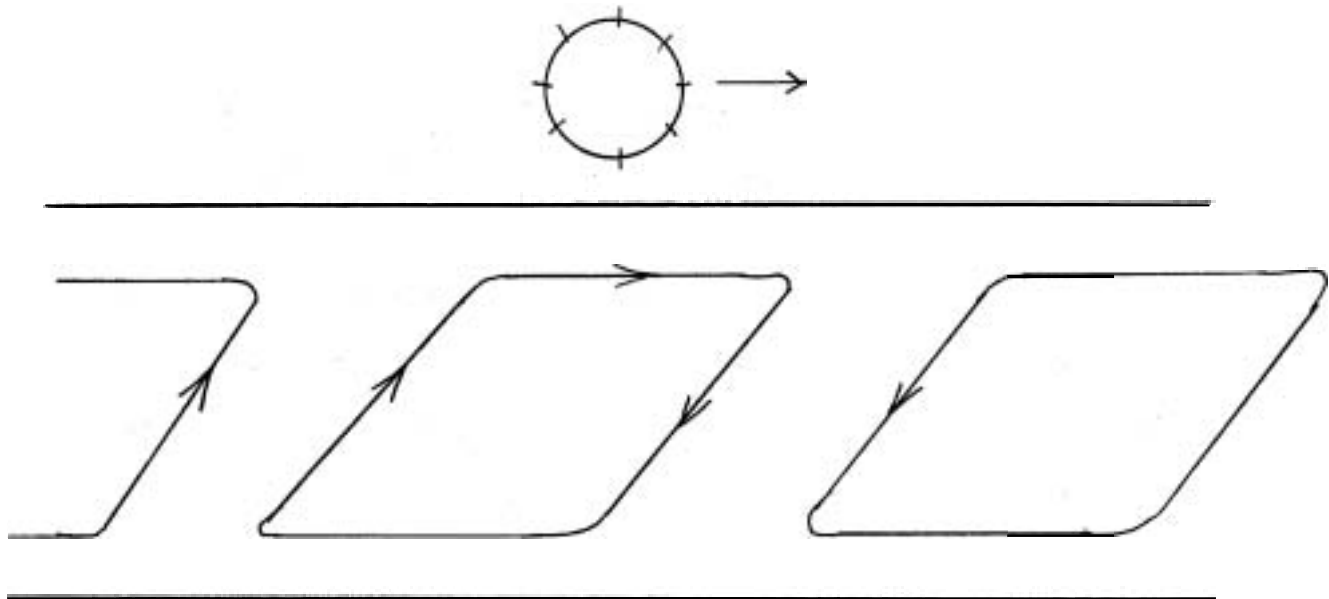
C. The moving Sun

We move on now to the question of how simple Hadley flows will be modified by motion of the heat source, In the case of a rotating planet, there are two limiting possibilities in which simple Hadley cell circulations are still possible: very slow and very rapid rotation rates, If the velocity of the solar heat source [the velocity of the subsolar point on the planet) is much slower than the response time of a Hadley circulation, then the flow can continually adjust to the changing position of the Sun, and the result can be a subsolar point to antisolar point cell, following the Sun while the planet rotates beneath it, On the other hand if the velocity

of the subsolar point is much larger than the Hadley cell response time, then the flow cannot adjust and will see the time-averaged Sun. In this case a simple Hadley cell is still possible but the orientation would be from equator to pole,

On Venus, unfortunately, there are reasons to believe that Hadley cell response times are the same order as the solar motion time scale, Particle cycle times according to the scalings mentioned above are about equal to a solar day, Also, radiative time constants are on the order of one solar day at cloud top level, We must therefore expect phase lags of different magnitudes at different levels in the atmosphere, and this is the basis of recent work on the explanation of a four-day circulation by Schubert and Whitehead, Young, Hinch, Thompson and others (see papers by Young and Thompson later in this volume). The idea is as follows:

Suppose the top of the cell follows the solar motion more closely than the bottom, as sketched below:



Reynolds stresses will accelerate the tops and bottoms of the cells differently, A mean circulation could be driven, but boundary conditions would be crucial and these models have been highly idealized,

Tidal acceleration of the upper atmosphere by the sun has also been suggested, the bulge in the atmosphere caused by the fact that the hottest time of day is not noon but afternoon (see Ingersoll, Venus lecture), This too could drive a mean circulation.

References

- Belton, M. J. S. 1968: Theory of the curve of growth and phase effects in a cloudy atmosphere. J.Atmos.Sci., 25: 569-609.
- Boyer, C. and P. Guerin 1969: Etude de la rotation retrograde, en 4 jours, de la couche exterieure nuageuse de Venus. Icarus, 11: 338-355.
- Gierasch, P. J., R. M. Goody and P. Stone 1970: The energy balance of planetary atmospheres. Geophys.Fluid Dyn. 1: 149-166,
- Goody, R. M. 1965: The structure of the Venus cloud veil, J.Geophys.Res., 70: 5471-5481.
- Goody, R. M. 1967: The scale height of the Venus haze layer. Planetary Space Sci., 15: 1817-1819.
- Goody, R. M. and A. R. Robinson 1966: A discussion of the deep circulation of the atmosphere of Venus, Astrophys.J., 146: 339-355.
- Hanel, R., M. Forman, G. Stambach and T. Meiller 1968: Preliminary results of Venus observations between 8 and 13 microns, J.Atmos.Sci., 25: 586-595,
- Lewis, J. S. 1969: Geochemistry of the volatile elements on Venus, Icarus, 11: 367-385.
- Rasool, S. I. and R. W. Stewart 1971: Results and interpretation of the S-band occultation experiments on Mars and Venus. J.Atmos.Sci., 28, to appear in September issue,

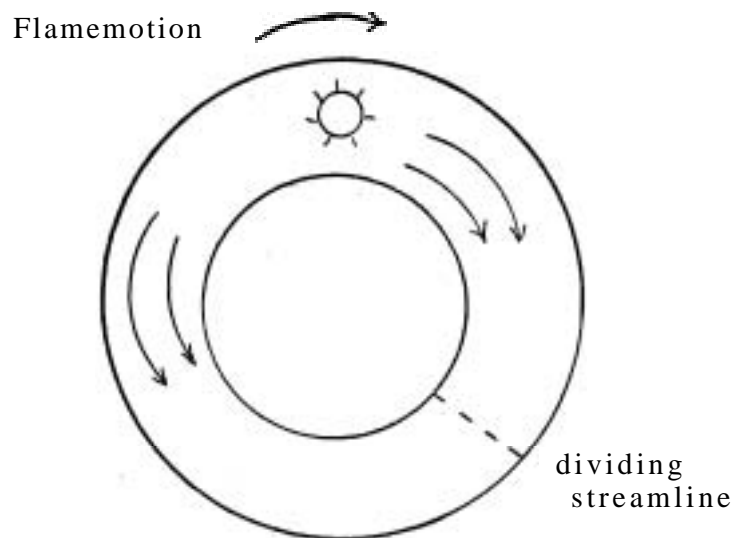
Notes submitted by
Louis Baker and
John R. Bennett

VENUSIAN ATMOSPHERE (Lecture II)

Peter J. Gierasch

D. Large scale motions, further comments.

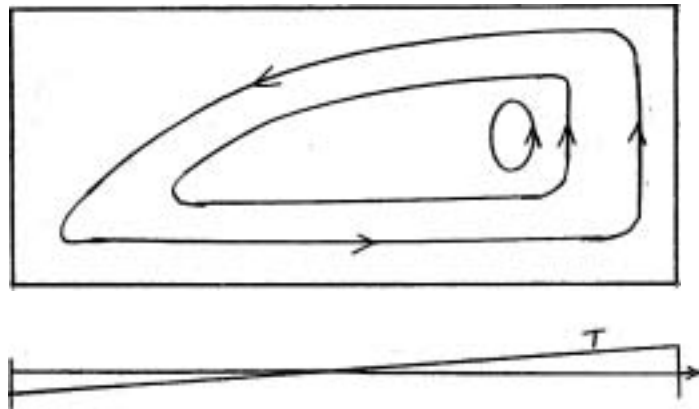
Peter Gierasch and R. Krishnamurti have studied an annulus heated by a moving heat source (similar to Fultz's experiments with a moving flame and a stationary annulus). The result, as sketched below



is that the dividing streamline is not 180° from the source. This effect on Venus, if important, might drive a mean flow of the upper atmosphere, or might by itself account for the observations.

The downwelling region in the atmosphere, according to the Goody-Robinson model, is suggested to be a thin plume. G. Veronis cited T. Rossby's experiments with an insulated box with uniform temperature gradient on one side, as sketched below. A thin rising plume developed on the hotter end!

We shall close our large-scale circulation review by noting a fact which emphasizes the complexity we must expect in the actual atmosphere.



This is that the radiative time constant for the atmosphere (the time it takes for radiative transfer to significantly change the temperature), based on a length scale equal to a scale height, varies greatly with height through the lower atmosphere, It is much greater than a solar day at levels where pressure > 10 atmospheres, and much less than a solar day for pressure ≤ 100 mb. This suggests different flow regimes at different levels, with the cloud level falling in the middle where things are most complicated,

E. Small-scale motions: the Richardson's number near cloud tops.

We have no observational information about small-scale motions in the Venus atmosphere, Telescopic resolution is simply not good enough. Estimates of the Richardson's number characterizing the atmosphere provides information about the energetics of small-scale motions, however,

The Richardson's number is defined as

$$R_i = \frac{g \left(\frac{\partial T}{\partial z} + \frac{g}{c_p} \right)}{T \left(\frac{\partial u}{\partial z} \right)^2}$$
$$= \frac{\text{energy in static stability}}{\text{energy in wind shear}}$$

where u is wind speed, T is temperature, z measures height, g is the acceleration of gravity, and c_p is heat capacity at constant pressure, The adiabatic lapse rate (rate of decrease of temperature with height) is g/c_p , and hence $\frac{\partial T}{\partial z} + \frac{g}{c_p}$ measures static stability. Observations in the terrestrial atmosphere, and to some extent theory, indicate that for $Ri \geq 0.25$ the atmosphere is **stable** to small-scale disturbances, for $-0.02 \leq Ri \leq 0.25$ "forced" convection dominates, and for $Ri \leq -0.02$ "free" convection dominates, In "forced" convection the kinetic energy comes **predominantly** from the wind shear and in "free" convection it is supplied by buoyancy.

The following table gives values of Ri for several values of wind shear and static stability.

wind shear	Ri		
$3 \frac{m \cdot s^{-1}}{km}$	21.	4.1	-4.1
$10 \frac{m \cdot s^{-1}}{km}$	1.9	.37	-.37
$30 \frac{m \cdot s^{-1}}{km}$.21	.041	-.041
$\frac{\partial T}{\partial z} + \frac{g}{c_p}$	5.3 K km^{-1}	1 K km^{-1}	-1 K km^{-1}

The left-hand column corresponds to a lapse rate of about half the adiabatic, roughly what is indicated by occultation measurements for heights where pressure ≤ 300 mb. The middle and right-hand columns are slightly stable or unstable lapse rates respectively, A slightly **stable** value seems indicated by occultation profiles for values of pressure ≥ 300 mb. The shear of $30 \text{ m s}^{-1} \text{ km}^{-1}$ in the bottom row is the value reached in the Goody-Robinson upper boundary layer and can probably be regarded as an upper limit,

We see that the most probable values of Ri near the cloud tops (the four values toward the upper left) correspond to stability, and among these the most plausible for pressure ≤ 300 mb is the far upper left value $Ri \approx 21$, indicating quite large stability.

This of course does not say that flow in the Venus atmosphere is not turbulent, merely that lack of turbulence is consistent with what we know about thermal structure and winds. Disturbance³ could obviously propagate into these regions from elsewhere, for example,

F. Latent heat release

If latent heat release is important within the cloud deck then we should expect cumulus convection. This is an extremely complicated subject but I believe we can make a plausible argument that it will not happen.

The temperature increase of a parcel of gas upon condensation of a minor constituent is

$$\Delta T = \frac{\rho_v L_v}{\rho c_p}$$

where ρ_v and ρ are the densities of the minor constituent and the atmosphere itself, and L_v is the latent heat. We wish to know if this temperature increase is sufficient to affect dynamics. We may obtain an indication by comparing this energy to the energy of a typical atmospheric static stability, and this can be done by comparing a lapse rate $\Delta T/H$, where $H = RT/g$ is a scale height, to the adiabatic lapse rate g/c_p :

$$A = \frac{\Delta T/H}{g/c_p} = \frac{\rho_v L_v}{\rho RT}$$

This is essentially a ratio of the difference between wet and dry adiabatic and dry adiabatic lapse rates to the dry one,

For most substances which have been suggested as cloud constituents (e.g. NH_4Cl , HgCl_2) this ratio is extremely small because the saturation vapor pressures are small (p_v must be evaluated at saturation for a typical cloud temperature). For water, which is also a contender, the situation is more marginal. Values of A for three temperature and pressure combinations taken from the atmospheric profile (Fig.1) are:

Temperature	200 K	250 K	300 K
Atmospheric pressure	14 mb	130 mb	600 mb
A	3.2×10^{-3}	0.13	1.0

At 250 K the wet and dry adiabats differ by about 10%, and at 300 K they would differ by a great deal if water were abundant enough to saturate. This seems unlikely, however. To reach saturation at 250 K the abundance would need to be about 1%, which is already somewhat greater than the Venera measurements indicated.

G. The coupling of clouds with dynamics.

We close by stressing the fact that the Venus clouds themselves are part of the dynamical problem. Cloud density depends upon motions; in the absence of motions particles would fall out or fall to a level where evaporation would occur. The question of why the cloud top is where it is is thus a dynamical problem. It is an extremely complicated one, because the radiative heating which drives motions is controlled by the cloud. Dynamics thus supports the cloud which in turn controls the dynamics. This aspect of the problem was studied, in terms of a radiative-convective model, by Gierasch and Goody (1969), but more needs to be done.

References

Gierasch, P. and R. M. Goody, 1969: Models of the Venus clouds,
J. Atmos. Sci., 26: 224-245,

Notes submitted by
John R. Bennett and
Louis Baker

THE BOUSSINESQ APPROXIMATION IN A MULTI-COMPONENT FLUID (Abstract)

George Veronis

The Boussinesq equations for a multi-component such as seawater can lead to difficulties with the interpretation of the potential density which is derived. By deriving the equations for seawater, it is shown that the linear equation of state (a natural part of the Boussinesq approximation) requires that the coefficients of thermal expansion and salt compression be functions of pressure. Since the equation of state thereby becomes non-linear, the preferable approach may be to take the coefficients as slowly varying functions of depth. The problem becomes more complicated but it remains linear,

TURBULENT DIFFUSION (Abstract)

Joseph B. Keller

1. Introduction

Turbulent diffusion is the dispersal of matter or energy by the turbulent motion of a fluid. Our goal is to obtain equations governing the first and second moments of the concentration of a conserved passive diffusant, assuming that the turbulent motion is prescribed. First, by using the two time perturbation method, we shall solve this problem for a single

velocity field. The result is that on a long time scale, the concentration $C(\mathbf{x},t)$ satisfies a diffusion equation and the product $C(\mathbf{x},t)C(\mathbf{y},t)$ satisfies a similar diffusion-like equation. The coefficients in these equations are coefficients of turbulent diffusion, which are given in terms of integrals of the velocity field. The virtue of these equations is that they pertain to a single velocity field, and therefore also to the mean concentration and two-point one-time moment in an ensemble of similar fields,

The disadvantage of our first results is that they describe only the slow changes of these moments which occur on a time scale long compared to the correlation time of the velocity. This is all that can be expected in the case of a single velocity field, but for an ensemble it also is possible to describe more rapid changes. Therefore by considering a stochastic velocity field from the outset, and using a different method, we obtain a second pair of equations for the moments $\langle C(\mathbf{x},t) \rangle$ and $\langle C(\mathbf{x},t)C(\mathbf{y},t) \rangle$. These second equations are integro-differential equations in t , involving the two-point two-time velocity correlation in the coefficients. They have the virtue that they describe the rapid changes in the moments as well as the slow ones, and they reduce to the previous equations for slowly changing moments.

THE THERMOHALINE CIRCULATION

Pierre Welander (Abstract)

The time-mean large-scale oceanic circulation is set up in response to the wind stress and to thermohaline effects acting at the top. The first effect can be described as a momentum flux, the second as a buoyancy flux (comprised of a heat flux and a salinity flux) through the sea surface.

The theory for the wind-driven circulation in a homogeneous ocean has been developed analytically for a nearly geostrophic ocean, the necessary friction effects being modelled by laminar-like expressions. The problem of the thermohaline circulation, set up in the absence of wind, is a more difficult problem due to the presence of the non-negligible non-linear advection terms for the temperature and salinity, but certain solutions of interest have been found.

In the standard model for this circulation it is assumed that the ocean is in geostrophic-hydrostatic balance, and that vertical mixing of heat and salt can be described by a single, constant diffusivity K . Assuming further, a Boussinesq approximation, the temperature and salinity effects can be combined, and the problem be formulated in terms of an effective temperature $\Theta = T - \frac{\gamma}{\alpha} S$, where T , S are temperature and salinity, and the equation of state is taken to be $\rho = \rho_0 [1 - \alpha T + \gamma S]$. The equations on a spherical earth are then

$$-fv = -\pi_x, \quad fu = -\pi_y, \quad \pi_z = g\alpha\Theta \quad (1, 2, 3)$$

$$u_x + \frac{1}{\cos^2\varphi} (v \cos\varphi)_y + w_z = 0 \quad (4)$$

$$u\Theta_x + v\Theta_y + w\Theta_z = K\Theta_{zz} \quad (5)$$

where $f = 2 \Omega \sin \varphi$ is the Coriolis parameter, $dx = R \cos \varphi d\lambda$, $dy = R d\varphi$ giving longitude, latitude and height. π, θ are perturbations from a basic, uniform state, and the basic density is incorporated in $\bar{\rho}$. If $\Delta\theta, u, w, L, \delta$ stand for the characteristic temperature variation (taken to be the same horizontal, and vertical), horizontal velocity, vertical velocity, horizontal scale and vertical scale, respectively, the classical thermocline scaling is obtained from the order of magnitude relations:

$$\begin{aligned} \frac{f_0}{\delta} &\sim g \alpha \frac{\Delta\theta}{L} && \text{(thermal wind)} \\ \frac{v}{L} &\sim \frac{w}{\delta} && \text{(continuity)} \\ \frac{w}{\delta} \Delta\theta &\sim \frac{K \Delta\theta}{\delta^2} && \text{(heat transport)} \end{aligned}$$

This gives

$$\begin{aligned} \delta &\sim \left(\frac{L^2 f_0 K}{g \alpha \Delta\theta} \right)^{1/3}, \quad w \sim \left(\frac{g \alpha \Delta\theta K^2}{L^2 f_0} \right)^{1/3} \\ v &\sim \left[\frac{(g \alpha \Delta\theta)^2 K}{f_0^2 L} \right]^{1/3} \end{aligned}$$

For $k \sim 1 \text{ cm}^2 \text{ s}^{-1}$ the thermocline depth becomes a few hundred meters, which is a reasonable value. As $K \rightarrow 0$ the thermocline depth obviously goes to zero. An exact solution which has been discussed in some detail (see G. Veronis, Deep-Sea Res. 17: p.421) is the exponential one, where the temperature varies as $\theta_0(\lambda, \varphi) e^{-kz/\mu m \varphi}$, where k is a constant. This is, however, a degenerate case, since K does not appear, and it can as well describe an ideal fluid thermocline, valid when $K = 0$.

In the case where the wind is also considered, and an Ekman vertical velocity $w_E(\lambda, \varphi)$ thus is added, it can be shown that the thermocline solution splits up in two regimes for small K . There will be a thin diffusive

thermocline of thickness $\delta_1 \sim \frac{K}{W_E}$ at the top, and a deeper ideal fluid thermocline below, of thickness

$$\delta_2 \sim \left(f \frac{L^2 W_E}{g \alpha \Delta \theta} \right)^{1/2}$$

In the real oceans K is probably small enough to cause such a split. The result can be understood in terms of the vertical velocity. The previous thermocline scaling gives $W \propto K^{2/3}$. For small K the prescribed Ekman vertical velocities cannot be matched, and the ideal fluid regime must be called in. Numerical experiments carried out by Killworth in Cambridge (personal communication) indicate that the split does occur, when K comes below $1 \text{ cm}^2 \text{ s}^{-1}$.

The picture for the vertical circulation in oceans will be essentially different for large and small K . In the first case water sinking into the deep sea at high latitudes can rise through the main thermocline. In fact, this upwelling combined with the downward heat diffusion produces the thermocline. In the second case the upper warm and lower cold water masses are connected only through certain singular regions. The deep water cannot penetrate the thermocline, but must come up at the equator, in coastal regions, etc. The water in the thermocline is formed by the downward Ekman pumping in the subtropical gyre. It flows along the isopycnals (density surfaces) with little mixing until it can be pumped up by the wind or reaching a singular region. Which of these two pictures comes closest to the truth is still unknown. To resolve the question direct measurements of K in and below the thermocline are highly wanted.

LAMINAR ROTATING FLAME EFFECT IN A STRATIFIED FLUID
 AT SMALL PRANDTL NUMBER (Abstract)

Melvin E. Stern

A cylindrical annulus filled with mercury is heated uniformly from the top and cooled uniformly from below. However, a periodic distribution of thermal inhomogeneities (e.g. air gaps) are embedded in the top half of the top plate so as to "screen" the uniform heat flux. By rotating the top half of the top plate a small amplitude fluctuating temperature field is superimposed on the basic static stability. The temperature fluctuations in the thermal boundary layer of the fluid generate internal waves, if the "heat source" frequency is less than the Brünt frequency. These waves transfer energy and momentum (of the same sense as the rotation of the "heat source") downwards and the amplitude of the wave decays slowly due to thermal conductivity, but it is assumed that the depth of the lower boundary is sufficiently great so that there is no reflected wave.

Linear Theory is used to compute the Reynolds stress averaged in the horizontal and integrated over the vertical. The result when divided by the viscosity (2) is equal to the following "characteristic" velocity

$$\bar{u}(0) = \frac{K}{2\nu} \frac{(g\alpha\Delta T)^2}{Ngs}$$

where K is the conductivity of the fluid, T is the amplitude of the temperature wave (assumed to be a pure harmonic) imposed on the top surface ($z = 0$),

is the propagation speed of the thermal wave, s is the basic static stability, and α is the thermal expansion. The calculations have been simplified using the approximations $\frac{K}{\nu} \gg 1$

$$\left(\frac{gs}{K^2}\right)^{1/2} \gg v \gg \left(\frac{gsK^2}{\nu K}\right)^{1/3}$$

where $2\pi/k$ is the horizontal wave length of the forced heat source, This calculation is valid for either rigid or slip boundaries at $z = 0$. The significance of $\bar{u}(0)$ is that it gives the rectified surface velocity (opposite to the propagation direction of the heat source) for the case of a slippery upper boundary condition, For the experimentally realizeable case of a rigid boundary at $z = 0$ this quasi-linear theory implies a net fluid momentum in the same direction as the heat source. In this case it is argued that the maximum mean velocities are limited by the formation of a critical layer, i.e. the fluid cannot move much faster than the heat source.

PHYSICAL TRACERS IN OCEANOGRAPHY (Abstract)

George Veronis

Hydrographic station data, consisting principally of temperature and salinity determinations, have been used by physical oceanographers to develop a climatological picture of the distribution of these quantities in the oceans of the world. Density as determined by Knudsen's formula, taken together with hydrostatic and geostrophic dynamics, also provides a crude picture of oceanic flow, However, the data probably contain substantially more information than has been derived from them in the past.

The quantity which is orthogonal to potential density curves in the σ_θ plane is suggested as a useful variable to complement the information contained in potential density. The derivation of this quantity, denoted by τ in this paper, is straightforward. A polynomial expression for τ which is suitable for computer calculations of τ from hydrographic station data is given, Two examples are shown of hydrographic station data from the Atlantic plotted on the τ - σ_θ diagram. The information contained in the τ - σ_θ diagram

shows many of the features exhibited in the TS plane. Vertical sections of τ appear to provide information about mixing in different parts of the Atlantic. The distribution of τ for abyssal waters at selected stations of the oceans of the world resembles the distribution of abyssal density as plotted by Lynn and Reid (1968). From the data presented it appears that τ may serve as a good tracer for abyssal water movements.

Since τ is defined to be orthogonal to σ_θ , the expectation is that τ is a dynamically passive variable. However, since σ_θ does not correlate with abyssal densities, it appears to lose dynamical significance at great depth and τ assumes dynamical significance because of its orthogonality to σ_θ .

PLANETARY FLUID DYNAMICS SYMPOSIUM

A QUICK SURVEY OF THEORETICAL WORK HAVING POSSIBLE RELEVANCE TO THE APPARENT ROTATION OF THE UPPER VENUS ATMOSPHERE (Abstract)

Conway B. Leovy

Ground-based observations of Venus in the ultraviolet ($\lambda < 4400 \text{ \AA}$.) show very large-scale dark features which rotate from east to west (retrograde) at an extremely consistent speed near 100 m/s. Preservation of the features over several planetary rotations suggests solid rotation. Polarization evidence indicates that the ultraviolet features occur near the 50 mb level. Very high resolution infrared observations of the illuminated west limb of Venus give Doppler sights indicating retrograde velocities of very nearly 100 m/s at somewhat lower heights. Similar measurements of the illuminated east limb of Venus do not yield a consistent Doppler shift.

A physical mechanism which might account for a strong zonal flow on a slowly rotating planet is suggested by the moving flame experiments of Fultz, Stern, Whitehead and others. These have been analyzed theoretically by Stern, Davey, Schubert, Young, Hinch and Malkus.

In its simplest form, applied to a fluid with high thermal conductivity, the thermal wave due to the moving flame penetrates the entire fluid with very little phase change with depth. For weak thermal conduction (or a very deep fluid), the conductive wave would produce convective cells tilting toward the flame, and transporting momentum toward the fluid surface (either the upper or lower surface) closest to the flame. On the other hand, if the thermal wave penetrates the fluid rapidly enough that there is no phase shift of the thermal wave with depth, the primary convective circulation will have no tilt. A secondary circulation resulting from convergence in the oscillating viscous boundary layer produced by the primary circulation will transport retrograde momentum of the primary circulation away from any rigid boundaries. Because this eddy momentum flux can only be balanced by viscous momentum transport down the gradient of the mean zonal flow, a steady flow in the retrograde sense will be set up near a free surface, or in the interior of a fluid between rigid upper and lower boundaries. Scale analysis suggests that for moderately large values of the Froude Number

$$F = \frac{gH\alpha\Delta T}{U^2},$$

the zonal flow is of order $UF^{2/3}S^{1/6}$, where H is depth, α is the thermal expansion coefficient, ΔT is the temperature perturbation due to the flame, and U is the flame speed. The parameter S is the product of flame frequency

and diffusion time scale. If the moving flame results are applicable to Venus, three conditions must be satisfied: (1) the thermal wave must penetrate rapidly through the fluid, (2) a source of secondary circulation analagous to that driven by the boundary layer in the experiments must exist, (3) the effect of motions at scales smaller than that of the primary convective circulation must be to transport momentum down the gradient of the mean zonal wind. It is not clear that any of these conditions are satisfied on Venus.

Gierasch has pointed out that the thermal wave produced by solar heating of Venus will, in fact, tilt toward the sun with increasing height, if there were no mean motion. This is because radiative transfer, the dominant heat transfer mechanism, acts most rapidly at the highest levels of the Venus mesosphere. Gierasch found a novel solution in which zonal retrograde shear balances this tilting effect without the requirement for any viscous momentum transfer. This solution could provide a mechanism for the apparent rotation if its stability can be demonstrated,

A third possible mechanism has been demonstrated by Thompson and by Malkus. They have shown the existence of non-linear instabilities in stationary heated fluids by means of which zonal flows can be produced by the original convective motion,

A fourth possibility: that the observed ultraviolet features indicate phase motion in a planetary scale internal gravity wave, has apparently not yet been investigated.

References

Davey, A. 1967 The motion of a fluid due to a moving source of heat at the boundary, J.Fluid Mech., 29, Part I: 137-150.

- Fultz, D. *et al.*, 1959 Studies of thermal convection in a rotating cylinder with some implications for large-scale atmospheric motions, Meteorol.Monog., 4(21).
- Gierasch, P. 1970 The four-day rotation in the stratosphere of Venus: a study of radiative driving, Icarus: 25-33.
- Malkus, W. 1970 Hadley-Halley circulation on Venus, J.Atmos.Sci. 27: 529-535,
- Schubert, G. 1969 High velocities induced in a fluid by a travelling thermal source. J.Atmos.Sci., 26: 767-770.
- Schubert, G. and J. Whitehead, 1969 The moving flame experiment with liquid mercury: possible implications for the Venus atmosphere. Science, 163: 71-72.
- Schubert, G. and R. E. Young. 1970 The four-day Venus circulation driven by periodic thermal forcing, J.Atmos.Sci. 27: 525-528.
- Smith, B. 1967 Rotation of Venus: continuing contradictions. Science, 158: 114-116.
- Stern, M. 1959 The moving flame experiment. Tellus 11: 175-179.
- Thompson, R. 1970 Venus' general circulation is a merry-go-round. J.Atmos.Sci., 27.

CONSEQUENCES OF MOMENTUM AND THERMAL DIFFUSION
FOR THE MEAN SHEAR INDUCED BY A MOVING HEAT SOURCE (Abstract)

Richard E. Young

Depending on the value of the Prandtl number for a given value of the parameter $S = \frac{\omega h^2}{\nu}$, the average velocity imparted to a layer of Bous-sinesq fluid by traveling thermal waves applied at the upper free surface can be either in the same or in the opposite direction as that of the moving thermal wave. In the above expression for S, ω is the frequency of the wave, h is the fluid layer thickness, and ν is the kinematic viscosity.

Mean field calculations by E. J. Hinch give an approximate expression for the mean flow at the top surface, which although not completely justifiably, can be used to give an estimate of the magnitude of the mean flow the moving flame mechanism might produce on Venus.

Finally, a simple model with radiative heat transfer described in a manner analogous to that used by Gierasch (1970) demonstrates that the

inviscid mean flow profile is not the correct limit the mean flow approaches as the viscosity goes to zero.

References

- 1, Schubert, G., R. E. Young, E. J. Hineh 1971 Prograde and retrograde motion in a fluid layer: consequences for thermal diffusion in the Venus atmosphere, J.Geoph.Res., 76:2126-2130.
2. Hinch, E. J. 1971 The moving flame: a dynamical model for Venus¹ four-day circulation. Monog. submitted for the Smith and Rayleigh prizes.
3. Gierasch, P. J. 1970 The four-day rotation in the stratosphere of Venus: a study of radiative driving. Icarus, 13: 25-33.

THE CIRCULATION OF THE ATMOSPHERE OF VENUS (Abstract)

Eugenia E. K. de Rivas

The circulation of the atmosphere of Venus is simulated by means of two-dimensional numerical models. Two extreme cases are considered: first, rotation is neglected and the subsolar point is assumed to be fixed; second (and probably more realistically), the solar heating is averaged over a Venus solar day and rotation is included. For each case a Boussinesq model, in which density variations are neglected except when coupled with gravity, and a quasi-Boussinesq model, which includes a basic stratification of density and a semi-grey treatment of radiation, are developed. The results obtained with the Boussinesq models are similar to those obtained by Goody and Robinson and by Stone. However, when the stratification of density is included and most of the solar radiation is absorbed near the top, the large-scale circulation is confined to the upper layers of the atmosphere and cannot maintain an adiabatic stratification in the interior. The thermal equilibrium in the interior is radiative-diffusive. When solar radiation is allowed to penetrate the atmosphere, so that at the

equator 6% of the incoming solar radiation reaches the surface, then the combination of a more deeply-driven circulation and a partial greenhouse effect is able to maintain an adiabatic stratification.

The effect of symmetrical solar heating is to produce direct Hadley cells in each hemisphere with small reverse cells near the poles. Poleward angular momentum transport in the upper atmosphere produces a shear in the zonal motion with a maximum retrograde velocity of the order of 10 m/sec at the top of the atmosphere.

The numerical integrations were performed using non-uniform grids to allow adequate resolution of the boundary layers. A study of the truncation errors introduced by the use of non-uniform grids is included, and it is shown that the use of stretched coordinates has several advantages for flows with boundary layers.

A proposal for a simple three-dimensional model, capable in principle of explaining the observed rapid zonal velocities at cloud level as well as the deep circulation, is presented,

VENUS' FOUR-DAY CIRCULATION AS AN INSTABILITY (Abstract)

Rory Thompson

Since there have been several "moving flame" models already presented here, it seems desirable to show how the concept of Thompson (1970) differs from that of Gierasch (1970), Malkus (1970) or Schubert and Young (1970).

Smith (1967) presented a convection that the clouds of Venus rotated with a period of four or five days, despite radar evidence that

the solid planet rotated very slowly. Smith thought these observations were incompatible. However, temperature observations indicated heat is transported from the light to the dark side quite efficiently. Intuitively, the easiest way to move the heat is simply to rotate the atmosphere around the planet; there is no need for return at a different level in the atmosphere. So, the problem was to find a way to get the angular momentum in the upper atmosphere.

So, suppose the spherical shell of gas is heated on one side and cooled on the other; one expects there to be rising motion on the front and sinking on the back. Now put in a small amount of rotation of the upper atmosphere, so there is a mean vertical shear. This will tend to push the tops of the convection cells farther than the bottom, giving them a **tilt**, so when particles are going up, they are going forward, and **contra-**wise. Then the Reynolds stress tends to reinforce the original mean vertical shear.

Thus, the picture proposed is that of a non-linear instability, with emphasis on the tilting of cells by the fluid motion. This is in contrast to the "moving flame" theories, which emphasize the **tilt** in the isotherms induced by the motion of the heat source.

Another contrast of the picture presented to the others is that here the heating is internal, rather than conductive through a boundary. In part, this is due to the scaling of the model. Here, the vertical scale is taken to be that of the short-wave radiational heating in the top of the clouds. Under the scaling assumptions used by Thompson (1970), the velocity scale, independent of the particular model, must be of the order of 100 m/sec, as observed,

While the model considered is only two-dimensional, addition of the third dimension may not be disastrous. The stratification is stable, so there is no obvious source of energy for longitudinal cells. Conservation of angular momentum will also act as a constraint.

A certain skepticism should be maintained about all of the models of Venus' circulation. For instance, all observations of the apparent rotation of the clouds are from the light side of the sphere, so it is conceivable that the dark side acts differently. For another, all studies so far have used an upper boundary condition of $w = 0$ at the top, $\zeta = 0$, despite the scaling requiring $w + u \zeta$ at $\zeta = \zeta$. The external gravity waves excluded thereby could carry a lot of momentum.

References

- Gierasch, Peter J. 1971 The Four-day Rotation in the Stratosphere of Venus. Icarus,
Malkus, Willem V.R. 1970 Hadley-Halley Circulation on Venus. J.Atmos.Sci., 27: 529-535,
Schubert, Gerald and R. E. Young 1970 The Four-day Venus Circulation driven by Periodic Thermal Forcina. J.Atmos.Sci. 27: 523-528.
Thompson, Rory 1970 Venus' General Circulation is a Merry-go-round. J.Atmos.Sci., 27: 1107-1116.

THE PROBLEM OF THE RESONANT ROTATION OF VENUS (Abstract)

Andrew P. Ingersoll

Venus is observed to rotate once every 243.1 ± 1 days in a direction opposite to its orbital revolution. The best estimates of this period (from ground-based radars) indicate that Venus' rotation may be controlled by the Earth, as Venus shows the same face to the Earth at times of closest approach. One expects, however, that the solar gravitational torque on the solid planet would be 10^6 times that of the Earth, and would bring Venus into a direct rotation, synchronous with its orbital revolution,

In an effort to explain these observations, several people have tried to estimate the gravitational torque on the thermally-driven solar tide in the atmosphere of Venus, Gold and Soter pointed out that if this tide had the same amplitude and phase as the solar semi-diurnal tide in the Earth's atmosphere, it would produce a torque in approximate equilibrium with the gravitational torque on the solid body. Hinch and Ingersoll have attempted to identify those models of the Venus atmosphere for which a thermally-driven tide of the proper amplitude and phase might occur.

The behavior of the atmospheric tide depends on the stratification parameter B , where

$$B = \frac{gH}{4\Omega^2 a^2} \frac{\Delta\theta}{\theta} \quad (1)$$

Here g is the acceleration of gravity, H is the atmospheric scale height, Ω is the angular velocity based on one-half the solar day, a is the radius of the planet, and $\Delta\theta$ is the change of potential temperature in one scale height. For $B \ll 1.4$, there is negligible phase shift of the wave height, and the peak pressure of the wave at the surface is

$$p_s = \frac{2F(1-A)g}{3\pi c_p T_s \Omega} \quad (2)$$

where F is the solar constant, $(1-A)$ is the fraction of solar power absorbed in the atmosphere, c_p is the specific heat, and T_s is the surface temperature. The peak pressure occurs at 9 a.m. and 9 p.m., leading to a torque in the desired direction, accelerating the planet away from synchronous rotation. For Venus, the condition $B \ll 1/4$ implies $\Delta\theta/\theta \ll 10^{-3}$ a very stringent condition, Nevertheless, this condition is consistent with observations of the Venus atmosphere from $p = 0.5$ atm to $p = 100$ atm. For $(1-A = 0.3$, the peak pressure of the wave for Venus is $p_s \sim 15$ mb, which is an order of magnitude greater than the value necessary to balance the solid body time,

For $B \approx 1/4$, a resonance occurs, and the peak pressure of the thermal tide is much larger than the value given by Eq. (2). Apparently, the semi-diurnal tide in the Earth's atmosphere satisfies this condition. For $B \approx 1.4$, the amplitude is again given approximately by Eq. (2), but the phase depends on the details of the thermal forcing and the stratification. These details are not known for Venus, so a definitive theory is impossible at the present time.

References

- Gold, T. and S. Soter 1969 Icarus, 11: 356.
Gold, T. and S. Soter 1971 Icarus, 14: 16.
Hinch, E. J. 1970 GD Summer Study Notes, W.H.O.I.

PLANETARY FLUID DYNAMICS

Jule G. Charney

1. Introduction

Solar heating produces motions of planetary length and time scales; only a small proportion of this energy cascades to smaller scales. Typical instantaneous summer and winter height contours for the sea level, 500 mb, 100 mb, and 10 mb surfaces, for the northern hemisphere, and similar charts for the mean heights for January and July for sea level and 500 mb, display the following main features of the general circulation:

- (i) A circumpolar westerly vortex in the upper layers is stronger in winter,
- (ii) Oceans are anticyclones in summer (high pressure) and cyclones in winter,
- (iii) Standing and transient waves are superimposed on the mean circumpolar vortex right up to high levels, and
- (iv) The 10 mb flow is radically different from that at 100 mb, simpler, unrelated and apparently undated.

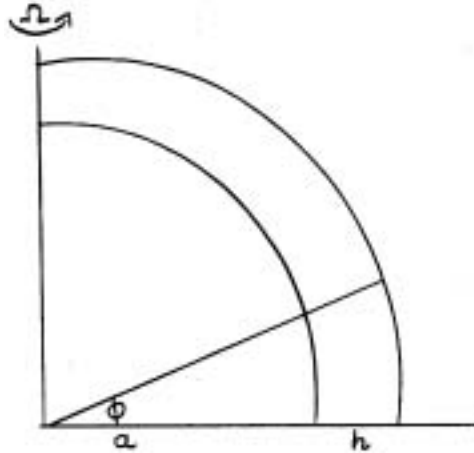
The dominant flow can be described as an axially symmetric vortex, mainly eastward and strongest in winter and at 200 mb. The corresponding axially symmetric temperature is largest at the surface equator, 25°C , and smallest, -80°C , in the equatorial stratosphere; vertical gradients are much smaller at the poles. On this axially symmetric situation wave and vortex perturbations are superimposed. It is therefore natural to study first the dynamics of an axially symmetric vortex, secondly small amplitude perturbations of this vortex, and thirdly their non-linear interactions on each other and on the original vortex, and the finite amplitude motions which will ultimately develop.

Comparisons of the observed mean north-south transfer of zonal momentum and temperature by the axisymmetric north-south motions and by the non-axisymmetric north-south motions show that the symmetric transport is roughly twice the eddy transport. Both the momentum transport and the mean north-south wind have boundary layer structure, being strongest at 200 mb and at 950 mb.

The possible hydrodynamic instabilities of the mean flow can be classified according to the forces producing them. Various combinations of buoyancy forces of different origins, centrifugal force, Coriolis force, shear inertial force and viscous stress have been studied in an extensive literature, and attempts have been made to relate the results to the non-systematic part of the motions and temperature in our atmosphere, at different regions of latitude and height,

2, Systematic Circulations in an Idealized Model

(a) Equations



Consider a Boussinesq fluid contained between concentric spheres rotating with angular velocity Ω . The temperature is $T_0(\phi)$ at the lower boundary $r = a$, and $T_0(\phi) + \delta T$ at the upper boundary $r = a + h$, where ϕ is the latitude.

We assume a zonal velocity of order of magnitude U , for the scale analysis. The associated Coriolis force $2\rho\Omega U$ is matched by the horizontal pressure gradient corresponding to a pressure scale $2\rho\Omega U a$ and temperature scale $2\rho\Omega U / g h \gamma$, where ρ , g and γ are the density, gravity (uniform) and coefficient of thermal expansion. Scaling the vertical coordinate $z = r - a$ by h , and vertical velocities by hU/a , and then assuming that $\frac{h}{a}$ is negligibly small, gives the following equations:

$$Ro [v(u_\phi - u \tan \phi) + w u_z] - v \sin \phi = E u_{zz} \quad (1)$$

$$Ro [v v_\phi + w v_z + u^2 \tan \phi] + u \sin \phi = E v_{zz} - p_\phi \quad (2)$$

$$T = p_z \quad (3)$$

$$v_\phi - v \tan \phi + w_z = 0 \quad (4)$$

$$\sigma Ro (v T_\phi + w T_z) = E T_{zz} \quad (5)$$

Here u , v and w are respectively the eastward, northward and upward velocity

components, and the equations are respectively the eastward, northward and vertical momentum equations, continuity, and the temperature equation. $R\sigma$, E and σ are dimensionless, and are respectively the Rossby number $U/2\Omega a$, the Ekman number $\nu/2\Omega h^2$, and the Prandtl number $\frac{\nu}{\kappa}$, where ν and κ are the constant kinematic viscosity and the constant thermal diffusivity. In these equations the possibility of horizontal variation on scales smaller than a , for example in a boundary layer at the equator, has been ignored.

The boundary conditions on the motion at $z = 0$ and 1 are

$$u(0) = v(0) = w(0) = u_z(1) = v_z(1) = w_z(1) = 0 \quad (6)$$

the upper boundary being taken as free. The temperature boundary conditions are

$$T(0) = T_0(\phi), T(1) = T_0(\phi) + \delta T, \quad (7)$$

where $T_0(\phi)$ and δT are now non-dimensional. In addition,

$$u = v = 0, \text{ at } \phi = \pi/2.$$

We now make the scaling assumptions,

$$E \ll 0(1) \quad (8)$$

$$Ro \ll 0(E) \quad (9)$$

$$\sigma = 0(1) \quad (10)$$

$$T_0(\phi) = 0(1) \quad (11)$$

$$\delta T = 0(1), \quad (12)$$

Assumption (8) implies that diffusion can only be a dominant term, in equations (1) and (2), in Ekman boundary layers of thickness $E^{1/2}$. Assumption (9) keeps the momentum terms small. Assumption (10) is excellent for gases and for turbulent fluids. The characteristic wind magnitude U is based on Eq. (11) Eq. (12) is an assumption, reasonable for the atmosphere.

Assume now that all the variables can be expanded as series in ascending powers of $E^{\frac{1}{2}}$, in forms like

$$u(\phi, z) = \sum_{n=0}^{\infty} u^{(n)}(\phi, z) E^{\frac{n}{2}} \quad (13)$$

Take $R_0 = O(E)$ in Eq. (9), without loss of generality, in expanding equations (1) to (5) in ascending powers of $E^{\frac{1}{2}}$.

(b) Interior Solutions

From Eq. (1), $v_i^{(0)}$ and $v_i^{(1)}$ are zero. From Eq. (4), $w_{iz}^{(0)}$ and $w_{iz}^{(1)}$ are zero; assume *a posteriori* that $w_i^{(0)}$ and $w_i^{(1)}$ are zero.

Equations (2), (3) and (5) then give

$$\begin{aligned} u_i^{(0)} \sin \phi &= -p_i^{(0)} & , & & u_i^{(1)} \sin \phi &= -p_i^{(1)} \\ T_i^{(0)} &= p_{iz}^{(0)} & , & & T_i^{(1)} &= p_{iz}^{(1)} \\ T_{izz}^{(0)} &= 0 & , & & T_{izz}^{(1)} &= 0. \end{aligned}$$

Assume *a posteriori* that the Ekman boundary layer flow does not affect the boundary conditions (7) on $T^{(0)}$ and $T^{(1)}$. Then

$$T_i^{(0)} = T_0(\phi) + z \delta T \quad , \quad T_i^{(1)} = 0 \quad (14)$$

$$p_i^{(0)} = p_0(\phi) + z T_0(\phi) + z^2 \delta T/2, \quad p_i^{(1)} = p_1(\phi) \quad (15)$$

$$u_i^{(0)} \sin \phi = -p_0'(\phi) - z T_0'(\phi) = u_i^{(1)} \sin \phi = -p_1'(\phi). \quad (16)$$

The functions $p_0(\phi)$ and $p_1(\phi)$ are not arbitrary, they are determined below by the consistency conditions. Finally, from Eqs. (1) and (4)

$$v_i^{(2)} = v_i^{(3)} = w_{iz}^{(2)} = w_{iz}^{(3)} = 0.$$

(c) Ekman Boundary Layers

Introduce the stretching substitutions

$$\begin{aligned} z &= \zeta_i E^{1/2} (\sin \phi)^{-1/2} \\ z-1 &= \zeta_u E^{1/2} (\sin \phi)^{-1/2} \end{aligned} \quad (18)$$

respectively, for the lower and upper boundary layers, and let boundary layer corrections to the interior flow be denoted by the tilde, Eq. (13) becomes

$$u = u_i(\phi, z) + \tilde{u}_l(\phi, \zeta_l) + \tilde{u}_u(\phi, \zeta_u) = \sum_0^{\infty} (u_i^{(n)} + \tilde{u}_l^{(n)} + \tilde{u}_u^{(n)}) E^{n/2} \quad (19)$$

Equations (1) to (5), with their interior parts subtracted out, become

$$R_0 [v(u_\phi - u \tan \phi)] + R_0 \tilde{w} u_{i,z} + R E^{-1/2} \sin^{1/2} \phi (w_i + \tilde{w}) \tilde{u}_z - \tilde{v} \sin \phi = \tilde{u}_{\zeta \zeta} \sin \phi \quad (20)$$

$$R_0 [v v_\phi + u \tan \phi] + R_0 \tilde{w} v_{i,z} + R_0 E^{-1/2} \sin^{1/2} \phi (w_i + \tilde{w}) \tilde{v}_z + \tilde{u} \sin \phi = \tilde{v}_{\zeta \zeta} \sin \phi - \tilde{p}_\phi \quad (21)$$

$$\tilde{T} = E^{-1/2} \sin^{1/2} \phi \tilde{p}_\zeta \quad (22)$$

$$\tilde{v}_\phi - \tilde{v} \tan \phi + E^{-1/2} \sin^{1/2} \phi \tilde{w}_\zeta = 0 \quad (23)$$

$$\sigma R_0 \tilde{v} \tilde{T}_\phi + \sigma R_0 \tilde{w} T_{i,z} + \sigma R_0 E^{-1/2} \sin^{1/2} \phi (w_i + \tilde{w}) \tilde{T}_z = \tilde{T}_{\zeta \zeta} \sin \phi \quad (24)$$

where the tilde quantities can be upper or lower (not both), and

$$\tilde{v} \tilde{T}_\phi = (v_i + \tilde{v})(T_{i,\phi} + \tilde{T}_\phi) - v_i T_{i,\phi} \quad ,$$

the square-bracketed quantities being similarly defined. The boundary conditions are that the tilde quantities tend to zero in the interior, and that the sums $u_i + \tilde{u}$, etc. satisfy the boundary conditions (6) and (7).

Equations (20) to (24) can now be expanded in ascending powers of $E^{1/2}$, using Eq. (19). From Eqs. (22) and (23),

$$\tilde{p}_\zeta^{(0)} = \tilde{w}_\zeta^{(0)} = \tilde{p}^{(0)} = \tilde{w}^{(0)} = 0 \quad (25)$$

Thus from the boundary condition (6), $w_i^{(0)} = 0$, justifying the first assumption above. From Eq. (24),

$$\tilde{T}_{\zeta \zeta}^{(0)} = \tilde{T}_{\zeta \zeta}^{(1)} = \tilde{T}^{(0)} = \tilde{p}^{(1)} = 0 \quad (26)$$

Thus the boundary condition on $T_i^{(0)}$ and $T_i^{(1)}$ is Eq. (7), as assumed above, and the temperature solutions (14) are valid. From Eq. (22),

$$\bar{p}^{(1)} = \tilde{p}^{(2)} = 0 \quad (27)$$

Equations (20) and (21) give the Ekman layer equations

$$(\tilde{u}^{(0)} + i\tilde{v}^{(0)})_{\zeta\zeta} = i(\tilde{u}^{(0)} + i\tilde{v}^{(0)}), \quad (\tilde{u}^{(1)} + i\tilde{v}^{(1)})_{\zeta\zeta} = i(\tilde{u}^{(1)} + i\tilde{v}^{(1)}), \quad (28)$$

Thus, using Eqs. (16) and the boundary conditions (6), including

$$u_z(1) = u_{iz}(1) + E^{-1/2} \sin^{1/2} \phi \tilde{u}_u \zeta = 0, \quad (29)$$

we obtain

$$\tilde{u}_z^{(0)} + i\tilde{v}_z^{(0)} = p'_0(\phi)(\sin \phi)^{-1} e^{-\frac{1+i}{\sqrt{2}} \zeta}, \quad \tilde{u}_z^{(1)} + i\tilde{v}_z^{(1)} = p'_1(\phi)(\sin \phi)^{-1} e^{-\frac{1+i}{\sqrt{2}} \zeta}, \quad (30)$$

$$\tilde{u}_u^{(0)} + i\tilde{v}_u^{(0)} = 0, \quad \tilde{u}_u^{(1)} + i\tilde{v}_u^{(1)} = \sin^{-1/2} \phi T'_0(\phi) \frac{\sqrt{2}}{1+i} e^{\frac{1+i}{\sqrt{2}} \zeta}, \quad (31)$$

Integrating Eq. (23) with respect to ζ gives the Ekman flux equations

$$\begin{aligned} (\cos \phi)^{-1} \frac{d}{d\phi} \left\{ \cos \phi \int_0^1 \tilde{v}_z^{(0)} d\zeta \right\} - E^{-1/2} \sin^{1/2} \phi \tilde{w}_z^{(0)}(0) &= 0 \\ (\cos \phi)^{-1} \frac{d}{d\phi} \left\{ \cos \phi \int_{-\infty}^0 \tilde{v}_u^{(0)} d\zeta_u \right\} + E^{-1/2} \sin^{1/2} \phi \tilde{w}_u^{(0)}(0) &= 0 \end{aligned} \quad (32)$$

The total northward flux $\int_0^1 2\pi \cos \phi v dz$ is zero at every latitude. So

$$\int_0^1 v_i dz + \left(\int_0^1 \tilde{v}_z^{(0)} d\zeta_z + \int_{-\infty}^0 \tilde{v}_u^{(0)} d\zeta_u \right) E^{1/2} \sin^{-1/2} \phi = 0. \quad (33)$$

The integrals in Eqs. (32) and (33) are

$$\int_0^1 \tilde{v}_z^{(0)} d\zeta_z = -2^{-1/2} p'_0(\sin \phi)^{-1}, \quad \int_0^1 \tilde{v}_z^{(1)} d\zeta_z = -2^{-1/2} p'_1(\sin \phi)^{-1}, \quad \int_{-\infty}^0 \tilde{v}_u^{(1)} d\zeta_u = -\sin^{-1/2} \phi T'_0. \quad (34)$$

So

$$p'_0 = \tilde{v}_z^{(0)} = \tilde{u}_z^{(0)} = \tilde{w}_z^{(0)} = \tilde{w}_u^{(0)} = u_i(0) = 0, \quad (35)$$

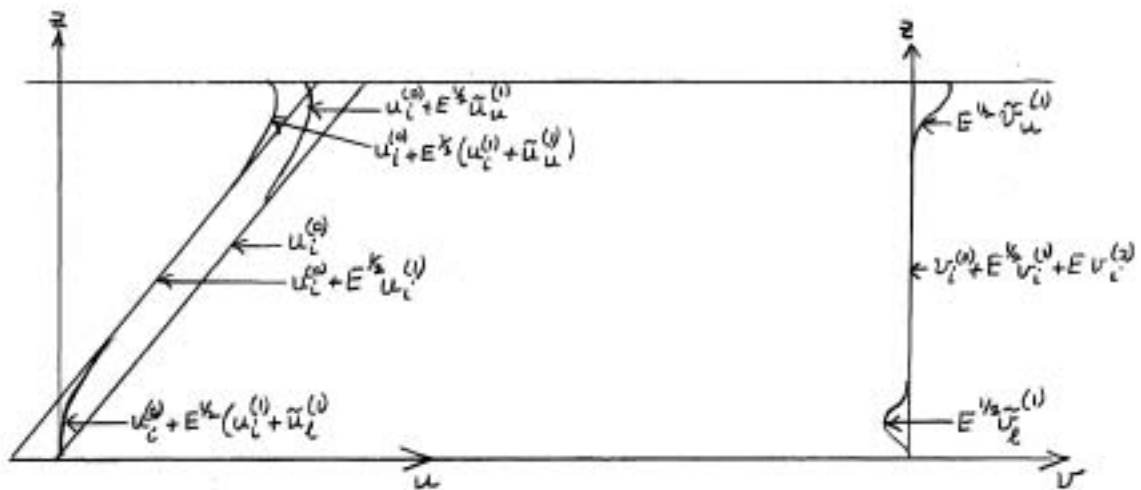
justifying the assumption above that $w_i^{(1)}$ is zero, from the boundary condition (6). Also,

$$p'_1 = -\sqrt{2} \sin^{1/2} \phi \quad 0 = -u_i^{(1)} \sin \phi, \quad (36)$$

and the complete solution to order $E^{1/2}$ has been obtained, uniquely within the assumptions already made,

The complete solution to order $\mathbb{E}^{3/2}$ can be obtained in a similar way, and then the complete solution to order $\mathbb{E}^{5/2}$, and so on. The a posteriori interior assumptions will not apply; w_i and $T(0)$ are not identically zero. But at each order, $\tilde{w}(0)$ and $\tilde{T}(0)$ can be found before w_i and T_i are needed. Thus boundary conditions (6) and (7) can be applied on the interior equations.

The nature of the circulation is shown in the figure below.



The zero order northward pressure gradient must vanish, so that the zonal motion is zero on the lower boundary, since otherwise there would be a northward flux in the bottom boundary layer with nothing to correct it. The first order pressure gradient and zonal motion take values such that the northward flux in the upper boundary layer, determined by the imposed temperature, is matched by a southward flux in the lower boundary layer.

The derivation of these solutions is invalid at the equator, since the stretching substitution (18) is invalid. Write

$$\tau_\theta(\phi) = -\tau(\sin\phi)^{\tilde{~}}$$

Then from Eqs. (32) - (36),

$$\int_{-\infty}^0 \tilde{v}_u^{(1)} d\zeta_u = - \int_0^{\infty} \tilde{v}_e^{(1)} d\zeta_e = n\tau (\sin\phi)^{n-3/2} \cos\phi$$

$$\tilde{w}_u^{(2)} = \tilde{w}_e^{(2)} = -w_e^{(2)} = -(\sin\phi)^{-1/2} (\cos\phi)^{-1} \frac{d}{d\phi} \left\{ \cos^2\phi (\sin\phi)^{n-3/2} n\tau \right\}$$

$$= \tau n \left\{ (n+\frac{1}{2})(\sin\phi)^{n-1} - (n-\frac{3}{2})(\sin\phi)^{n-3} \right\}$$

If all the velocity components tend to zero at the equator, the solution is probably valid there, asymptotically, despite the singularity. Clearly this requires only that n be more than **three**.

Notes submitted by
Glyn O. Roberts

GESTROPHIC TURBULENCE

Jule G. Charney

Quasi-geostrophic motions are characterized by the laws of conservation of entropy and conservation of potential vorticity, We combine these into a single conservation law of "pseudo-potential" vorticity, and develop an analogy between three-dimensional quasi-geostrophic motions and two-dimensional flow. We may then extend several theorems developed for the latter case, and, in particular, we are interested in a result relating to turbulence in three-dimensional quasi-geostrophic flows.

A body of theory has been developed for the problem of two-dimensional **inviscid** turbulence, The constraints of energy and mean-squared **vorticity** conservation prevent the cascade of energy from the large to the small scale which can occur in three-dimensional flow. Similarity arguments then give a k^{-3} law for the energy density in wave number space.

A similar theory can be developed for three-dimensional, quasi-geostrophic flow, starting from the conservation equation of pseudo-potential

vorticity, Its application is principally to the scales of motion in the atmosphere immediately smaller than those excited by baroclinic instability, It may also be of relevance in the meandering region of the Gulf Stream, although for most of the ocean, the β -effect is probably of sufficient magnitude to enable any energy generated to be dispersed by Rossby waves,

Consider a flow with horizontal and vertical length scales L and D , velocity scale U , and buoyancy frequency N . If a is the radius of the earth, and Ω its rotation rate, Charney and Stern (1962) have studied the scaling of the equations of motion under the conditions:

$$\begin{aligned}
 R_o &= \frac{U}{2\Omega L} \ll 1, \\
 \epsilon &= \frac{4\Omega^2 L^2}{N^2 D^2} \gg 1, \\
 L/a &\leq R_o, \\
 D/L &\leq R_o^2, \\
 \text{and } \frac{4\Omega^2 L^2}{gD} &\ll 1.
 \end{aligned}$$

To lowest order, a flow with the above characteristics may be considered to be on a plane with (x, y, z) as eastward, northward and vertical position coordinates, It is governed by the equation

$$\left(\frac{\partial}{\partial t} + \underline{v} \cdot \nabla \right) q_0 = 0 \tag{1}$$

$$\text{where } \nabla = \left(\frac{\partial}{\partial x}, \frac{\partial}{\partial y} \right)$$

$$\underline{v} = \left(-\frac{\partial \psi}{\partial y}, \frac{\partial \psi}{\partial x} \right), \text{ is the horizontal velocity,}$$

$$q_0 = \frac{\partial^2 \psi}{\partial x^2} + \frac{\partial^2 \psi}{\partial y^2} + \frac{f^2}{\rho_0} \frac{\partial}{\partial z} \left\{ \frac{\rho_0}{N^2} \frac{\partial \psi}{\partial z} \right\} + \beta y,$$

ρ_0 is the density of the mean state

$f = 2\Omega \sin \phi_0$, the Coriolis parameter at reference latitude ϕ_0 , and

$$\beta = \frac{2\Omega \cos \phi_0}{a}$$

The vertical velocity, w , is given by

$$\frac{N^2}{f} w + \left(\frac{\partial}{\partial t} + \mathbf{v} \cdot \nabla \right) \frac{\partial \psi}{\partial z} = 0$$

We consider the flow to be zonally periodic, and bounded by rigid vertical walls at $y = y_1$ and $y = y_2$. A rigid horizontal boundary on which

$w = 0$ is imposed at $z = 0$, and we require that the energy density $\rightarrow 0$ as $z \rightarrow \infty$. Multiplication of Eq. (1) by $\rho_3 \psi$, and integration over the whole atmosphere yields the energy equation

$$E = \iiint \left\{ \left(\frac{\partial \psi}{\partial x} \right)^2 + \left(\frac{\partial \psi}{\partial y} \right)^2 + \frac{f^2}{N^2} \left(\frac{\partial \psi}{\partial z} \right)^2 \right\} \rho_3 dx dy dz$$

$\frac{dE}{dt} = 0$, where

We similarly obtain

$$\frac{dF}{dt} = \rho_3 \iint \left(\frac{f^2}{N^2} \frac{\partial \psi}{\partial x} \frac{\partial \psi}{\partial z} \right)_{z=0} dx dy, \quad \text{where}$$

$$F = \iiint \left\{ \mathcal{L}(\psi) \right\}^2 \rho_3 dx dy dz, \quad \text{and}$$

$$\mathcal{L}(\psi) = \frac{\partial^2 \psi}{\partial x^2} + \frac{\partial^2 \psi}{\partial y^2} + \frac{f^2}{N^2} \frac{\partial}{\partial z} \left\{ \frac{\rho_3}{N^2} \frac{\partial \psi}{\partial z} \right\}.$$

We consider flows for which $\left(\frac{\partial \psi}{\partial z} \right)_{z=0} = 0$ at some instant. The lower boundary condition then implies it remains zero, and

$$\frac{dF}{dt} = 0$$

A consequence of the invariance of E and F is that there can be no cascade of energy towards smaller scales, We introduce the eigenvalues

$$\lambda_n \quad (n = 1, 2, 3, \dots) \text{ of the operator } \mathcal{L} : \mathcal{L}(\psi_n) = -\lambda_n \psi_n.$$

They are ordered such that λ_n is a non-decreasing, positive function of n . By virtue of the completeness property of the eigenfunctions,

$$\psi = \sum_1^{\infty} a_n \psi_n, \text{ giving}$$

$$2E = \sum_1^{\infty} \lambda_n a_n^2 \quad \text{and}$$

$$F = \sum_1^{\infty} \lambda_n^2 a_n^2.$$

since $\sum_M^{\infty} \lambda_n a_n^2 < \frac{1}{\lambda M} \sum_M^{\infty} \lambda_n^2 a_n^2 < \frac{F}{\lambda M}$, and F is invariant, the amount of energy in the small scales associated with $\lambda_r (r \geq M)$ is bounded, and there is no energy cascade,

We now investigate the spectral properties of quasi-geostrophic motions whose scales are small compared with those of baroclinic instability. Vertical variations in N^2 and ρ_s may then be neglected in Eq. (1), together with the β -effect.

The coordinates are transformed such that

$$d\zeta = \frac{N}{f} dz, \quad \text{and}$$

$$\chi = \rho_s^{1/2} \psi, \quad \text{and we assume that}$$

$\left(\frac{\partial \chi}{\partial x}, \frac{\partial \chi}{\partial y}, \frac{\partial \chi}{\partial \zeta} \right)$ is homogeneous and isotropic in the horizontal.

The further assumption of one statistical behaviour for all levels implies that $\left(\frac{\partial \chi}{\partial x}, \frac{\partial \chi}{\partial y}, \frac{\partial \chi}{\partial \zeta} \right)$ is homogeneous and isotropic in all three directions.

With the introduction of η , the rate of transfer of "enstrophy", F, down the wave number scale, we obtain from dimensional arguments the following form for the amount of energy, $E(k)$, between wave numbers k and $k + dk$:

$$E(k) = C \eta^{2/3} k^{-3}.$$

The above prediction may be compared with observation. A study of the energy content of the wave disturbances in the mid-latitude troposphere shows an approximate k^{-3} dependence for horizontal wave numbers 7 to 18. In detail, the decay appears to be somewhat greater than a -3 power law; this may be a consequence of non-localness in the non-linear wave interactions,

The theory also predicts an equipartition between each of the horizontal components of kinetic energy and the available potential energy.

The quasi-geostrophic equations then give a conversion factor of $\frac{N^2 \bar{T}^2}{g^2}$ between the kinetic energy and temperature variance spectra. This result is verified for longitudinal wave numbers 7 to 18 by observations at 500 mb and 40°N. A comparison for the vertical wave number spectra is more difficult, and has not yet been computed.

Reference

Charney, J. G. and M. E. Stern 1962 "On the stability of internal baroclinic jets in a rotating atmosphere," J. Atmos. Sci., 19: 159-172,

Notes submitted by
Adrian J. Simmons

THE CIRCULATION OF THE EARTH'S ATMOSPHERE

Jule G. Charney

Introduction

In the preceding lecture, the equation of conservation of pseudo-potential vorticity was used to describe the characteristics of small-scale, quasi-geostrophic motions. We now derive some consequences relevant to an understanding of the dynamics of the larger disturbances in extra-tropical regions. We introduce the phenomenon of baroclinic instability, and discuss its description of the origin of the travelling waves in mid-latitudes. We then investigate the vertical and horizontal propagation of large-scale wave motions away from a region of generation,

The Linearized Equations

The qualitative picture of the flow in the mid-latitude troposphere is one of a circumpolar current on which wave-like disturbances are superimposed. Accordingly, we find solutions of the pseudo-potential vorticity equation which take the form:

$$\Psi(x, y, z, \epsilon) = \bar{\Psi}(y, z) + \underline{\Psi}(y, z) e^{ik(x-ct)}$$

The zonal mean flow, \bar{u} , is given by $\bar{u} = -\Psi_y$, and the non-dimensional, linearized equation for the small disturbance, $\underline{\Psi}$, is

$$(\bar{u}-c) \left\{ \underline{\Psi}_{yy} - k^2 \underline{\Psi} + \frac{1}{\rho} (\epsilon \rho_z \underline{\Psi}_z)_z \right\} + \bar{q}_y \underline{\Psi} = 0, \quad (1)$$

where

$$\bar{q}_y = \beta - \bar{u}_{yy} - \frac{1}{\rho} (\epsilon \rho_z \bar{u}_z)_z$$

Baroclinic Instability

The classical baroclinic instability problem comprises a rigid horizontal boundary at the ground $z = 0$, with $\bar{u}_z = -\bar{\Psi}_y = \text{constant}$, which corresponds to a constant horizontal temperature gradient. Then $\bar{q}_y = \beta + \epsilon m$, where m is a dimensionless vertical wind shear. This problem was studied independently by Charney and Eady, who found unstable solutions ($\text{Im}(c) > 0$), with the fastest growth rates occurring when $\frac{fL}{NU} \sim 1$. Eady's model has $\beta = \epsilon = 0$, and a second horizontal boundary at $z = D$. It predicts a short-wave cut-off independent of shear. Charney's problem has \bar{q}_y as a positive constant, and an unbounded atmosphere. The flow is then unstable at almost all wavelengths, but with only a weak instability in the low wave number range.

We now discuss the energy source for the growing waves. Writing ψ' for the perturbation stream function, we can derive the following dimensionless equation for the time-development of the perturbation energy between levels z_1 and z_2 :

$$\begin{aligned} \frac{d}{dt} \left\{ \iiint_{z_1}^{z_2} \frac{1}{2} \rho \left[(\psi'_x)^2 + (\psi'_y)^2 + \epsilon (\psi'_z)^2 \right] dx dy dz \right\} = \\ = \iiint_{z_1}^{z_2} \rho \psi'_x \psi'_y \bar{u}_y dx dy dz - \iiint_{z_1}^{z_2} \epsilon \psi'_x \psi'_z \bar{\Psi}_{zy} \rho dx dy dz - \\ - \iiint_{z_1}^{z_2} \left[\rho \psi' w' \right]_{z_1}^{z_2} dx dy. \end{aligned}$$

The first term on the right-hand side describes the conversion of zonal kinetic energy into the eddy kinetic form, and is zero for the classical problem in which $\bar{u}_y = 0$. The third term is the rate of increase of energy due to work done on the fluid by the pressure at the boundaries z_1 and z_2 . It vanishes if the region of interest is the whole atmosphere. The second term represents the conversion to the eddy potential form of the available potential energy associated with the mean horizontal temperature gradients, It is this process which describes the energetics of baroclinic instability.

A necessary condition for a quasi-geostrophic instability is now derived, In order to avoid an explicit inclusion of surface integrals associated with the ground at $z = 0$, we introduce the concept of a generalized potential vorticity:

$$\hat{q} = q + \epsilon \psi_z \delta(z-0).$$

The statement that $(\frac{\partial}{\partial t} + \underline{v} \cdot \nabla) \hat{q} = 0$ throughout the fluid includes both the conservation of q in the body of the flow, and the boundary condition

$$\left(\frac{\partial}{\partial t} + \underline{v} \cdot \nabla\right) \psi_z = 0 \text{ at } z = 0.$$

A second horizontal boundary elsewhere in the flow, or a class of discontinuities in the mean flow, may be similarly included. We now consider the generalized form of the linearized equation (1). Multiplication by $\bar{\Psi}/|u-c|$ and integration over the range of y and z gives

$$\iint \rho_0 \left\{ |\bar{\Psi}_y|^2 + \epsilon |\bar{\Psi}|^2 + \kappa^2 |\bar{\Psi}|^2 \right\} dy dz = -i \Im m(c) \iint P \bar{q}_y dy dz + \iint P \{ \bar{u} - R_0(c) \} \bar{q}_y dy dz,$$

where $P = \frac{\rho_0 |\bar{\Psi}|^2}{|u-c|^2} \geq 0.$

If $\Im m(c) \neq 0$ inspection of the imaginary part shows

$$\iint P \bar{q}_y dy dz = 0.$$

As P is everywhere non-negative, it is necessary for instability that \bar{q}_y change sign. In addition, it follows from the real part that

$$\iint \bar{u} P \bar{q}_y dy dz > 0.$$

We note that in the limit of large stability ($\epsilon \rightarrow 0$), vertical motions are inhibited, and the necessary condition for instability reduces to the earlier result for barotropic flows, namely that $\beta - \bar{u}_{yy}$ should change sign,

The Application of Mid-Latitude Cyclones

Such considerations as the above give general information, but to proceed further it is necessary to solve the eigenvalue problem in detail. For parameters appropriate to mid-latitudes, it is found that the fastest growing waves have wave lengths around 5000 km, and have kinematics similar to those of the observed disturbances. Growth rates are such that the perturbations will double in two to three days. The inclusion of realistic horizontal shears does not alter the characteristic scales of the instability. The results further suggest that the eddies are such that they transport zonal momentum so as to sharpen an existing horizontal jet. A study of the mean-field equations is necessary in order to obtain the equilibrium situation.

The Propagation of Planetary Waves

Equation (1) may also be used to study the propagation of wave disturbances away from the region of their generation. We illustrate this with the case of vertical propagation, considering the simple case of a constant zonal flow, \bar{u} , with constant N , and constant density scale height, H . Working in dimensional variables, a perturbation stream function

$$\phi(z) e^{-\frac{z}{2H}} e^{i\{k(x-ct)+ly\}} \quad \text{satisfies}$$

$$\phi_{zz} + m^2 \phi = 0, \quad \text{where}$$

$$m^2 = \frac{N^2}{f^2} \left\{ \frac{f}{\bar{u}-c} - (k^2 + l^2 + \lambda^{-2}) \right\}$$

$$\text{and } \lambda = \frac{2HN}{f}$$

The waves propagate if $m^2 > 0$, and this cannot occur if $(\bar{u}-c) < 0$.

In summer, the mid-latitude stratospheric winds are easterly, and the troposphere disturbances are thus trapped, in good agreement with the observations of a zonally-symmetric circumpolar flow at high levels.

For strong westerly winds, such as those which occur in the winter stratosphere, propagation is favored for small values of k . The long waves forced in the troposphere by thermal and topographic asymmetries may thus more easily penetrate into the upper atmosphere than the shorter waves associated with baroclinic instability; wave numbers 1 and 2 appear to be only marginally trapped. This is confirmed by the predominance of these waves in the observations of the flow at the 10 mb level.

Similar results hold for horizontal propagation. In particular, waves are trapped by a flow which is westward relative to their phase speed, and it seems unlikely that mid-latitude disturbances can significantly penetrate into the easterlies which occur near the equator.

Notes submitted by
Adrian J. Simmons

STRUCTURAL AND COMPOSITIONAL MODELS FOR THE JOVIAN
ATMOSPHERE AND CLOUDS (Abstract)

Ronald G. Prinn

Current interpretations of spectroscopic observations and the expected mode of **accretion** of Jupiter from the primitive solar nebula would suggest that the planet is essentially of solar composition. There still exist problems however (McElroy, 1969). In such a solar composition model it is possible to compute approximate temperature profiles. Important heating mechanisms are the absorption of solar UV radiation by H_2 and He in the thermosphere and the absorption and re-radiation at longer wavelengths, of visible solar radiation. Absorption of this long wavelength radiation in the very broad pressure-induced dipole lines of H_2 produces a greenhouse effect to heat the upper **tropo-**sphere. Another heating mechanism not yet incorporated in current temperature profiles is the absorption of UV radiation by CH_4 in the **strato-**sphere-mesosphere which may produce an ozone-type temperature inversion in the upper atmosphere. In addition we should also consider the fact that Jupiter radiates considerably more energy than it receives from the Sun. With this internal energy source, strong dipole absorption by NH_3 near the visible clouds may become important (Trafton and Munch, 1969).

Lewis (1969) has computed the expected cloud layers in a wet adiabatic solar composition Jupiter and predicted the following principal layers: a dense liquid H_2O-NH_3 cloud with a base at 310K, a thinner solid NH_4HS cloud above this with a base at 229K, and uppermost a thin solid NH_3 cloud with a base at 168K. All these clouds would be **colorless**.

After the discovery of enhanced 5μ radiation from Jupiter, Westphal (1969 and later unpublished work) carried out high spatial resolution studies of this emission and found it to be emanating principally from visually very dark bands such as the NEB and STB, in contrast to the bright white bands across the planet. The NEB and STB themselves vary from very dark to lighter colors and it appears that the darker the band visually then the greater is its 5μ emission. Lewis and Prinn (1970) suggested that these dark bands are regions where the upper NH_3 clouds have been cleared away to expose the warmer layers below and hence explain the enhanced emission from such areas. If such a clearing did exist then calculations of the transfer of UV radiation (Prinn, 1970) indicate that UV radiation from 2300-2700A could penetrate down to the region of the next lowest cloud layer in Lewis' model composed of solid NH_4HS . The effect of this radiation on both solid NH_4HS and H_2S gas itself is to rapidly produce yellow, red and dark brown hydrogen and ammonium polysulphides. Hence a clearing of the upper clouds would result in a visual darkening of that region. The model appears consistent with observation. Westphal's observations suggested temperatures in the NEB were generally around 235K but could range up to 310K in very dark spots. Such very hot spots are interpreted as holes in the NH_4HS clouds to expose the $\text{H}_2\text{O}-\text{NH}_3$ clouds. The temperatures are certainly concordant. An alternative explanation for these high temperatures is simply that the uppermost layer has many small holes within the area of one aperture. Such a model however would give considerable limb darkening to the emission. Limb scans by Munch and Neugebauer (1970) across the NEB at 5μ indicated very little limb darkening and implied that the layer

was very uniform with a temperature around 230-250K. Finally a comment on interpreting strengths of absorption lines over various regions of Jupiter's disc is in order. McElroy (1969) has pointed out the inadequacy of the simple reflecting layer model for Jupiter. Hence more absorption over a particular area does not imply it is lower in the atmosphere. In fact, since the NEB is so much darker than say the adjacent EZ then much less multiple scattering is possible within that layer which may lead to less absorption over the NEB than the EZ even if it is lower in the atmosphere.

References

- Lewis, J. S. 1969 Icarus 10: 365.
Lewis, J. S. and R. G. Prinn 1970 Science 169: 472.
McElroy, M. B. 1969 J.Atmos.Sci. 26: 798.
Munch, G. and G. Neugebauer 1970 Paper presented at the AGU National Fall Meeting, San Francisco.
Prinn, R. G. 1970 Icarus 13: 424.
Trafton, L. M. and G. Munch 1969 J.Atmos.Sci. 26: 813.
Westphal, J. A. 1969 Astrophys.J. 157: L63, and a number of private communications,

A MOIST MODEL OF JUPITER'S CLOUD BANDS (Abstract)

Peter J. Gierasch

Ingersoll and Cuzzi (1969) showed that a consistent interpretation of Jovian motion observations is that the light-colored zones are warmer than the darker belts, and that a thermal wind is associated with the temperature gradients. In the present paper (abstracted from Barcilon and Gierasch, 1970) we suggest that the thermal wind is due to latent heat release within H₂O clouds deep in the atmosphere, with the temperature variations being produced by horizontally varying moisture abundance,

Lewis (1969) constructed a chemical equilibrium model of the vertical

structure of Jupiter's clouds, based on an assumption of solar abundances of the elements. He found that the thickest clouds are probably below the visible cloud deck and are composed mainly of H_2O . The present paper is motivated by the following interesting fact, If one assumes that the vertical temperature profile in Jupiter's atmosphere is given by a moist adiabat, and that the amount of H_2O vapor in the atmosphere varies in the horizontal (by its own order of magnitude) from belts to zones, then the resulting horizontal temperature variations near and above the H_2O cloud deck are of the correct magnitude to cause the observed thermal winds,

In order to study such a possibility, the equation describing conservation of H_2O must be added to the dynamical and thermodynamical equations describing the atmosphere, We attempted to do this, in a steady, zonally symmetric model, A vertical eddy diffusivity for heat, momentum, and moisture was assumed. Horizontal variations of the coriolis parameter were neglected and the Rossby and Ekman numbers were assumed to be small.

In the context of the model, a consistent solution, with adiabatic vertical structure, zonal winds of the observed magnitude, and a weak meridional circulation controlled by friction, is possible only if radiation warms the cloudy zones relative to the dark belts, This conclusion depends upon certain parameterizations of the latent heat release processes, however, which are not very well justified, and more work needs to be done.

References

- Barcilon, A, and P. J. Gierasch 1970 A moist Hadley cell model for Jupiter's cloud bands, J.Atmos.Sci. 27: 550-560.
Ingersoll, A, P. and J. N. Cuzzi 1969 Dynamics of Jupiter's cloud bands. J.Atmos.Sci., 26: 981-985.
Lewis, J. S. 1969 Observability of spectroscopically active compounds in the atmosphere of Jupiter, Icarus, 10: 393-409,

MOTION OF JUPITER'S RED SPOT
(OCEANOGRAPHY OF JUPITER) (Abstract)

George Veronis

A thermodynamic justification can be made for the hypothesis that a layer of hydrogen-rich solid can form at a level of a few thousand kilometers below the visible surface of Jupiter and that the solid is gravitationally stable (in the dynamic sense) at the level of formation. If a topographic or other such feature of the solid surface of Jupiter causes an accumulation of this material into a massive object and if the motion of this stable Cartesian diver is analyzed, the observed motion of the Red Spot can be rationalized in terms of the model. Vertical oscillations of the Cartesian diver are accompanied by longitudinal changes of position because of the associated changes in the angular momentum of the object. Speculation about the fluid motions caused by the motion of the diver leads to predicted changes in the size and location of the Red Spot which agree with observed changes.

MARS: THE SMALL WHITE SPOTS (Abstract)

Conway B. Leovy

Ground-based observations of Mars consistently show diurnally and seasonally varying bright spots recurring in the same locations. Several of these were seen by the Mariner '69 television cameras, and at least three such features in the tropics can be identified with ring-shaped structures with diameters 200-500 km.

The diurnal and seasonal variations are strongly suggestive of a condensation phenomenon. One possibility is that the brightenings are due

to condensed CO_2 formed by overshoot at the top of an intense convective layer, The constraints on such convective overshoot phenomena have been investigated by Gierasch.

The possibility that they are due to water ice condensing locally because the ring-shaped structures are related to subsurface moisture sources also can be considered, The rather high humidities sometimes observed in the Mars atmosphere suggest abundant moisture sources somewhere on the planet,

The difficulty with tropical subsurface moisture sources is that moisture cannot effectively escape from such a source for more than a few hundred years (probably a negligible time span) unless the moisture flux is also driven by a heat flux, A steady moisture flux, F_m , can be driven by a thermal flux, F_h , and can remain steady over long periods of time. However, an absolute upper limit can be set to such a steady moisture flux on simple thermodynamic grounds:

$$F_m = 2 \times 10^2 F_h$$

where F_m is in $\text{gm/cm}^2\text{-day}$, and F_h is in $\text{cal/cm}^2\text{-sec}$. For example, with the typical terrestrial value of $F_h \approx 10^{-6} \text{ cal/cm}^2\text{-sec}$, we find a moisture flux of two precipitable microns per day, Since this number is probably a high upper limit for the given heat flux, we conclude that the brightening of the ring-shaped objects is not likely to be due to local moisture sources, If local moisture sources are involved, the ring-shaped features must be associated with strong thermal sources as well.

References

Leovy, C. A., B. A. Smith, A. T. Young and R. B. Leighton 1971 Mariner Mars '69: Atmospheric Results, J. Geophys. Res., 26: 297-312.

Gierasch, P. 1970 The four-day rotation in the stratosphere of Venus: a study in radiative driving. Icarus, 13: 25-33,

"ABC'S OF CONVECTION" (Abstract)

Louis N. Howard

W. V. R. Malkus and I have recently been studying a variant of Welander's "Fluid loop" model of convection, with which it seems to be possible with analytical methods to obtain a somewhat more detailed picture of the motion than has been found for the original model - even by so original a mathematician as Joseph Keller. We consider a circular loop of "fluid" whose motion is characterized entirely by its angular velocity $c(t)$, but whose temperature is also a function of position on the circle $T(\theta, t)$. As a result of temperature variations the fluid is supposed to be subject to a "buoyancy" force associated with a gravitational field in the plane of the loop, though its moment of inertia is fixed. Motion of the fluid may then be driven by the net torque associated with the weight distribution; it is assumed to be resisted by a frictional torque proportional to the angular velocity. In addition to being convected around by the motion, the temperature field may be changed as a result of a heat flux proportional to the difference between $T(\theta, t)$ and a fixed but arbitrary temperature T_0 of an externally imposed heat bath. For the most part we have assumed that the temperature distribution $T \equiv T_0$ has no net torque associated with it, so that one solution (the "conductive state") is $c = 0$, $T = T_0$; this assumption is however not an essential one.

The mathematical model describing this situation consists then of

a coupled system of a partial differential equation in T and an ordinary one in c . We can show however that the complete solution to the initial value problem for this system can be written down explicitly in terms of the solution to a third order autonomous system of ordinary differential equations which is satisfied by the $\cos\theta$ and sine coefficients (a,b) of the Fourier expansion of T , and the angular velocity c . This system has in fact been studied somewhat, both analytically and numerically, by Edward Lorenz, who also arrived at it in connection with convection though from a different point of view,

In dimensionless form it contains two parameters which can reasonably be identified with a "Prandtl number" σ and a "Rayleigh number" R . One finds that if R is below a critical value every solution tends to the conductive state, but that if R exceeds the critical value the conductive state is unstable to infinitesimal perturbations. However in this case there also are two other steady (non-linear) solutions, very easily calculated for any R above critical, corresponding to steady convection in either direction. Under some conditions one can show that almost every solution tends to one or the other of these; but if $\sigma > 2$ and R exceeds a second critical value (which depends on σ , but can be obtained explicitly) these steady solutions are also unstable to infinitesimal perturbations, and no stable steady solution exists. Experiments with an electronic analogue as well as with a fluid mechanical model approximately described by the same equations indicate that under these circumstances a number of things can occur, depending both on the parameters and on the initial conditions. Sometimes a stable state is approached which is periodic in time - it may be a

unidirectional motion with pulsating speed, or a back-and-forth oscillation in which the angular displacement of a fluid particle varies periodically over an interval of less than $2\tilde{\eta}$, or a sort of combination of these in which a fluid particle goes several times around the loop in one direction, then reverses and goes several times around in the other direction, following this with a repeat of the first motion. In some cases the reverse phase may be a mirror image of the direct one, but this is not always the case, even in the simple back-and-forth oscillation - in such cases of course there is also another stable periodic solution which as a whole is a reversal of the first one. It appears that more than one such periodic motion can exist and be stable if the Rayleigh and Prandtl numbers are in the right range, and indeed there appears to be a range below the second critical Rayleigh number in which a periodic but not steady motion is stable, in addition to the two steady ones. In these cases of course the selection of the final stable state depends on the initial conditions. While analogous hysteresis phenomena to these have perhaps not been clearly observed in convection experiments, something rather similar has been seen by Donald Coles with circular Couette flow. In other ranges of the parameters it seems that not only is there no stable steady solution - there is no stable periodic solution either. The motion just goes on and on in an erratic manner, certainly reminiscent of some features of turbulence, though of course there is nothing like vortex stretching in this model.

To obtain a clear overall picture of this somewhat bewildering complexity is a challenging theoretical goal which we have not yet reached. However, in the case of very large values of the Rayleigh number asymptotic

methods become available and we have been able in this way to form a fairly clear picture of this asymptotic case, The motion is found to be essentially a **periodic** oscillation on a short time scale, described by the non-linear **pendulum** equation and characterized by a phase and two other parameters, which may be thought of as the length of the **pendulum** and the energy of **its motion**. These two parameters vary on a long time scale in accordance with a certain ~~two~~-dimensional autonomous system. By studying its critical points we can identify candidates for final states of motion, and from their stability properties see which of these final states can be regarded as stable. The results depend on the Prandtl number, but a typical situation is that beside the two steady convective and the conductive states, there are two periodic motions which can go on forever without further long-time-scale evolution, one corresponding to a unidirectional pulsation, the other to back-and-forth oscillations, Typically only the last is stable, and almost all solutions tend to it; in some cases the steady convections are **also** stable and some (**but** not all) solutions tend to one **or** the other of them, Thus in this **asymptotic** theory we can see in analytic detail **some** of the features (e.g. hysteresis) which have been seen in numerical or analogue experiments, We have not however found, say, a limit **cycle** in the long-time-scale motion which might correspond to a continuously changing, non-periodic **motion**. But we are hopeful that extensions of the **asymptotic** methods, which are **called for** in a certain singular region of the plane of the long-time-scale motion, will reveal such structure as well,

THE PARAMETERIZATION OF CONVECTION IN TROPICAL DISTURBANCES
(Abstract)

Katsuyuki Ooyama

Although various parameterization methods to formulate effects of cumulus convection for the use in large-scale numerical models have been proposed and shown to be reasonably **successful**, there is need of deriving the parameterization on a more general basis. The theory presented here is one possible approach to the problem. The basic hypothesis of the theory is that cumulus convection may be represented by an ensemble of independent buoyant elements. The behavior of a buoyant element, or a "bubble", is to be calculated with the use of a semi-empirical convection model. The effects of convection on the large-scale field are expressed in terms of the total effects of bubbles integrated over a distribution (the "dispatcher" function) of initial states of the bubbles, although little discussion on specifics of the dispatcher function is given except a greatly simplified one in a special application,

Results of the special application, expressed in terms of the **non-dimensional** heating distribution, $\eta(p)$, are employed in a linear stability analysis of tropical wave disturbances. The model for this analysis is based on the quasi-geostrophic vorticity equation on the β -plane with the zonal basic flow, $U(p)$, and the thermodynamic equation with the convective heating characterized by $\eta(p)$. Conclusions of this study are as follows:

- 1) Under the normal conditions of the tropical easterlies, the CISK mechanism is **subcritical**, or, at best, marginal,
- 2) The disturbance of wavelength less than 1000 km (the tropical cyclone **scale**) may become unstable if the lower troposphere is **much** more humid than it is in the **normal**

conditions. 3) Baroclinic instability (which may be combined with barotropic instability) gives unstable waves with a "cold core" in a wavelength range of 2000 - 4000 km (the easterly wave). 4) At large wavelengths, certain internal modes of Rossby wave may become unstable under convective heating. However, the growth rate of these long waves is very small (the e-folding time of more than two weeks) when the typical heating and a moderate vertical shear of the zonal flow are assumed.

Reference

Ooyama, K. 1971 A theory on parameterization of cumulus convection, Syōno Memorial Volume, to be published by the Meteorological Society of Japan in October, 1971.

NON-PERIODIC CONVECTION AND REVERSING DYNAMOS (Abstract)

Willem V. R. Malkus

It is shown that a homopolar dynamo with both an internal and a shunt load can exhibit non-periodic reversals of magnetic polarity when driven by a constant torque. E. Bullard was the first to study this simplest of dynamo systems. He expressed the view that an understanding of the instabilities in the mechanical dynamo could be of value in the interpretation of astrophysical magnetic fields and the geodynamo. However, Bullard did not consider internal impedance in his mathematical model and concluded that homopolar dynamos can not reverse polarity through instability. Following that work T. Rikitake devised a two-rotor dynamo system which did reverse its magnetic field in certain ranges of its defining parameters. This more complex dynamo was believed to be the very simplest system capable of reversal. The several lengthy studies of the Rikitake dynamo have depended upon numerical computations to determine its behavior when reversing. In

this study of the homopolar dynamo a non-linear asymptotic theory, valid in the inertial limit, permits a detailed exploration of the stability of the oscillation and reversal modes. For a particular choice of the parameters (when the parallel load is purely resistive) it is shown that the homopolar dynamo problem reduces to the problem of convection in a circular tube heated from below, P. Welander first proposed the tube convection problem and, with J. Keller, has written on several of its interesting properties, L. Howard has reformulated and extended that work to include solutions at arbitrarily large Rayleigh numbers. Here, the relation of those solutions to the homopolar dynamo is given. Also, a working model is exhibited which demonstrates the steady, the oscillatory, and the non-periodic reversing types of solutions.

GENERATION OF A LARGE-SCALE MAGNETIC FIELD
BY RANDOM FLUID MOTION (Abstract)

H. Keith Moffatt

A statistically homogeneous random velocity field $\underline{u}(\underline{x}, t)$ in an electrically conducting fluid can give rise to dynamo action (i.e. sustained transfer of energy to magnetic modes) provided the statistical properties of the velocity field lack reflexional symmetry. The dynamo mechanism was anticipated through physical reasoning by Parker (1955); it was given mathematical substance by Steenbeck, Krause and Rädler (1966 and subsequent papers); and it has been elucidated and systematized by Moffatt (1970). The treatment involves investigation of the development of Fourier components of the magnetic field whose wave number is small compared with those characteristic of the velocity field,

The lack of reflexional symmetry, that is crucial for dynamo action, can occur under two idealized circumstances in which it is supposed that the motion is generated by a random force field $(\underline{f}(\underline{x}, t))$; (i) the statistical properties of the \underline{f} -field may themselves lack reflexional symmetry and this property will be directly imprinted on the 2-field, or (ii) the whole system may rotate with angular velocity $\underline{\omega}$, and the statistical properties of the \underline{f} -field need then only lack symmetry about planes perpendicular to $\underline{\omega}$ (e.g. they may drive a flux of energy parallel to $\underline{\omega}$). The former possibility is artificial, but useful conceptually; the latter is more relevant as far as geophysical (or astrophysical) applications are concerned.

When circumstances are such that dynamo action occurs, the large-scale components of the magnetic field grow exponentially until they begin to react back upon the statistical properties of the velocity field through the Lorentz force. This back-reaction can be simply analyzed, for a particularly simple choice of forcing field consisting of a single helical wave at the resonance Alfvén frequency. If attention is focussed on a single growing magnetic mode (which also has a helical, force-free structure) it turns out that the exponential growth predicted on the linear theory ultimately levels off due to a progressive modification of the phase relationships between the perturbation magnetic field and the \underline{u} -field. Under the statistically steady conditions that ultimately develop, the magnetic energy density is an order of magnitude greater than the kinetic energy density in the random \underline{u} -field.

References

- Moffatt, H. K. 1970 J.Fluid Mech. 41: 435.
Parker, E. N. 1955 Astrophys.J. 122: 293.
Steenbeck, M., F. Krause and K. -H. Rädler 1966 Z.Naturforsch 21a: 369

DYNAMICS OF TROPICAL CYCLONES (Abstract)

Katsuyuki Ooyama

Among various problems associated with the dynamics of tropical cyclones, the mechanism of the development from an incipient vortex to a mature cyclone is presently one of the best understood. The mechanism is explained as a cooperative process between the cumulus convection and the cyclone-scale circulation. The former acts as vertically distributed heat sources to drive the cyclone-scale circulation, and the latter, through the frictionally induced inflow in the Ekman layer, organizes and maintains the convective activity around the center of the storm,

Because of a great difference in scales of individual cumuli and of the cyclone, it is impractical if not impossible to formulate the above mechanism on first principles of fluid dynamics and thermodynamics, which should apply to all scales of atmospheric motions, On the basis of empirical facts that the latent heat release in the tropical cyclone is mostly due to tall cumulonimbi in the eye wall and that the convection is supported mainly by convergence of the warm and moist air in the Ekman boundary layer, the effect of convection may be parametrized in terms by large-scale variables without explicit calculation of individual cumuli, Although various formulas of parametrization have been proposed, the simplest method is to assume the rate of convective heating, Q , in the form

$$Q = c_p \pi \frac{\partial \theta}{\partial p} \eta \omega_b$$

where ω_b is the vertical motion due to the Ekman pumping and the non-dimensional factor, η is the ratio of the convective mass flux at any level to that at the top of the boundary layer. For a two-layer model of the tropical cyclone, in which only one degree of freedom is allowed to Q in the unit vertical column, the value of η may be determined from the thermodynamical energy budget of the column. If the equivalent potential temperature of the boundary layer is sufficiently large so that free convection can reach the upper layer while entraining the air of the lower layer into the convective updraft (that is, $\eta > 1$), the stability analysis of a linear model shows that the cyclone-scale circulation will intensify,

To explain the structure and the energetics of a mature tropical cyclone, non-linear effects such as the variation of η , the vertical transport of angular momentum by clouds, and the evaporation from the underlying ocean, are necessary to be taken into account. Numerical models of the axisymmetric tropical cyclone have been built incorporating these effects and shown to be quite successful in simulating many observed aspects of the tropical cyclone.

Reference

Ooyama, K. 1969 Numerical simulation of the life cycle of tropical cyclones. J.Atmos.Sciences, 26: 3-40.

PREDICTABILITY OF FULLY-DEVELOPED TURBULENCE
IN TWO AND THREE DIMENSIONS (Abstract)

Robert H. Kraichnan

Although instability is perhaps the most fundamental characteristic of turbulence, it is only in the past few years that much theoretical effort has been devoted to quantitative study of instability, and the associated lack of predictability, in fully-developed turbulence. The impetus for this work has come from meteorologists seeking theoretical limits on weather predictability. One of the crucial questions, originally raised by Robinson and Lorenz, is whether perturbations in the small scales of turbulence (either actual perturbations or equivalents of uncertainties in measurement) infect successively larger scales and lead, eventually, to unpredictability of the entire inertial range of the turbulence.

The predictability problem may be studied theoretically by considering a double ensemble of flows and examining the fate of the difference-velocity field between pairs of flows. This leads to closed equations, like those for the ordinary energy spectrum function, which describe approximately the evolution of the wavenumber spectrum function of the difference velocity. Such approximate equations have been studied analytically and numerically for the $-5/3$ inertial range of three-dimensional turbulence, and for the $-5/3$ and -3 inertial ranges that have been hypothesized for two-dimensional turbulence. In all three cases, studies to date suggest that unpredictability does indeed travel through the spectrum from large to small wavenumbers, a result in qualitative

accord with computer experiments on two-dimensional atmospheric models. However, the theoretical predictions here are fundamentally less reliable than for the ordinary energy spectrum, and novel approaches are badly needed.

References

- Leith, C. E. 1971 Atmospheric predictability and two-dimensional turbulence. J.Atmos.Sci., 28: 145-161.
Leith, C. E. and R. H. Kraichnan. Predictability of turbulent flows, to be published.

DYNAMICS OF ISOTROPIC TURBULENCE, I and II (Abstract)

Robert H. Kraichnan

Turbulence in an incompressible Navier-Stokes or Boussinesq fluid is characterized by essential nonlinearity of dynamics, anomalously large transport of momentum and heat, and, perhaps most important, an hierarchy of instabilities whereby large-scale eddy motions give up their energy to smaller-scale motions. The rich variety of instabilities make impossible the detailed prediction of a turbulent velocity field from gross initial and boundary conditions and lead to the use of statistics in theoretical **description**. The statistical distribution of the velocity at a single point is found experimentally to be very nearly normal, but joint probability distributions of velocity at several points are significantly non-normal. In particular, the statistics of the small scales show strong **intermittency**. Isotropic turbulence is kinematically the kind with the simplest statistics in the sense of maximum symmetry. However, it emphasizes the role of non-linear interaction of velocity fluctuations and thereby is very hard to handle dynamically,

The initial goals of isotropic turbulence theory, as posed by Taylor and others in the 1930's, were to obtain closed equations predicting the evolution of the wavenumber energy spectrum. Substantial progress has been made toward these goals. Simple exact closed equations for the spectrum function do not exist, because the nonlinearity makes initial higher statistics important in the evolution of simpler statistics. However, closed approximate equations have been obtained which give accurate agreement with computer and laboratory turbulence experiments and which can be used as a starting point for systematically improved higher approximations.

The problems of higher statistics, intermittency in the small scales, and the precise asymptotic form of the inertial range of wavenumbers are another matter. It is unclear at the present time how to attack them successfully. One hopeful avenue is systematic bounding analysis like that of Malkus, Howard, and Busse for thermal convection.

References

- Kraichnan, R. H. 1971 Some modern developments in the statistical theory of turbulence. Proceedings of 6th IUPAP Conference on Statistical Mechanics, Univ. of Chicago Press.
- Jerring, J. and R. H. Kraichnan, Comparison of some approximations for isotropic turbulence, To be published,

EQUATORIAL WAVE DISTURBANCES (Part I and II) (Abstract)

James R. Holton

Part I: In **this** lecture I develop the linear theory for planetary scale waves on the equatorial beta-plane. Assuming a constant basic state zonal wind and solutions in the form of zonally propagating waves, the horizontal and vertical dependencies of the perturbation fields are separable. The vertical dependence is governed by the vertical structure equation of

atmospheric tidal theory, The horizontal modes are in the form of Hermite functions. The horizontal and vertical structures are related through a separation constant, called the equivalent depth, which depends on the frequency, the zonal wavenumber and the meridional mode, Depending on the equivalent depth waves may be either evanescent (i.e. exponentially decaying in the vertical) or vertically propagating. It turns out that all free oscillations are evanescent in the earth's atmosphere. But for certain wavenumber and frequency combinations forced oscillations may propagate vertically either as internal gravity waves of short vertical wavelengths, or Rossby waves of long vertical wavelengths.

Part II: In this lecture I discuss the observed structure of forced planetary scale waves in the equatorial region. We assume that the waves are forced by the heat released in cumulonimbus convection, Most of the internal gravity wave modes have very short vertical wave lengths (≤ 1 km) for synoptic time scale and are thus, not very effectively excited. However the lowest modes for which the zonal wind field is symmetric and antisymmetric about the equator (the Kelvin wave and the mixed Rossby gravity wave, respectively) have fairly long vertical wavelengths and appear to be the most energetic disturbances in the tropical stratosphere. The Kelvin wave is an eastward propagating wave which behaves like an internal gravity wave in the height-longitude plane, but is in geostrophic equilibrium in the height-latitude plane, The mixed Rossby gravity wave, on the other hand, propagates westward and resembles a Rossby wave in the horizontal plane and a gravity wave in the vertical, The observed Kelvin waves have periods of about 15 days, zonal wave number 1, and vertical wavelength of

—10 km. The observed mixed Rossby-gravity waves have periods in the four - five-day range, zonal wavenumber ~ 4 and vertical wavelength ~ 6 km. In addition to these propagating modes there are evanescent Rossby modes which appear to account for most of the disturbed weather in the ITCZ. These modes have periods of four - five days, wavelengths of about 2,000 - 4,000 km and propagate westward with phase speeds of $\sim 8 - 10$ m sec^{-1} . It is probably more proper to view the ITCZ as the *locus* of these westward propagating wave disturbances rather than a zonally symmetric Hadley type circulation,

References

- Lindzen, R. S. 1967 Planetary waves on beta-planes. Mon. Wea. Rev., 95: 441-451.
- Matsuno, T. 1966 Quasi-geostrophic motions in the equatorial area. J. Meteor. Soc. Japan, 44: 25-43,
- Wallace, J. M. Spectral studies of tropospheric wave disturbances in the tropical western Pacific, Revs. of Geophys. (in press).
- The paper by Wallace is a review article which contains an extensive bibliography.

THE DYNAMICS OF THE POLAR-NIGHT JET (Abstract)

Adrian J. Simmons

The question of baroclinic instability in the winter stratosphere has been re-examined following the recent finding of McIntyre (1971) that the continuous model of the polar-night jet considered by Murray (1960) is unstable in the short-wave limit. The model is found to be unstable at all but a finite number of wavelengths, which divide regions of relatively strong and weak instability. The fastest growth rates occur for wave numbers 5 to 9, with no sharp selectivity, and give doubling times of the order of a week. The vertical scale of the disturbances is only a few kilometers,

The removal of the discontinuities in shear and static stability at the model tropopause is found to give rise to increased growth rates in some cases; in general the results are highly dependent on the detailed structure of the basic flow. The typical length scales are, however, unaltered, providing further evidence that baroclinic instability does not describe the long waves which extend throughout the winter stratosphere. The predicted instabilities will be difficult to distinguish observationally from the upward extension of tropospheric disturbances.

The techniques developed for Murray's problem have been adapted to investigate a simple model of the decrease in static stability at the stratopause. In the presence of an eastward shear such as occurs in winter, quasi-geostrophic theory, with the inclusion of a Newtonian cooling mechanism, predicts instabilities with doubling times of the order of three days. The length scales are much as found for the lower stratosphere, and are probably too small to be resolved by present observational techniques.

Matsuno (1970) has successfully reproduced the mean structure of the long-wave disturbances in a numerical calculation of the steady response to forcing by waves excited in the troposphere by thermal and topographic asymmetries. The linear time-dependent problem has been studied by means of a simple analytical model, and gives a reasonable agreement with observation. The resonances predicted by Matsuno are found, but appear of little significance as the resulting wave disturbances do not differ much from the general case when the time scale of the forcing is around two weeks. The growing waves are maintained not only by the energy input by the forcing,

but also by the conversion of zonal available potential energy into the eddy form, The associated northward transport of heat provides a mechanism which can compensate for radiational cooling in polar regions.

References

- Matsuno, T. 1970 Vertical propagation of stationary planetary waves in the winter northern hemisphere. J.Atmos.Sci., 27: 871.
McIntyre, M. E. 1971 Baroclinic instability of Murray's continuous model of the polar-night jet. (submitted to Q.J.R.M.S.)
Murray, F. W. 1960 Dynamical instability in the stratosphere. J.G.R. 65: 3273.

NUMERICAL SIMULATION OF THE TROPICAL CIRCULATION (Abstract)

Joseph Smagorinsky

An updated picture will be given of the numerically simulated behavior in the tropics in global calculations. The climatic equilibrium will be discussed, as well as the structure of the individual phenomenological instabilities and their energetic properties. Some examples will be shown of actual prediction experiments involving the tropics as a measure of the practical level of predictability now obtainable in very limited tests.

A SIMPLE NUMERICAL GENERAL CIRCULATION MODEL (Abstract)

R. Terry Williams

The quasi-geostrophic equations are employed in a two-level model of the atmosphere. The model includes friction, and heating which is a linear function of y . The model is further simplified by restricting the disturbance to one wave in the x -direction, The wave amplitude and phase, and the x -averaged wind velocity are functions of y and t . The motion is confined between walls at $y = \pm W/2$. The equations are solved numerically with a Δy which is sufficiently small to resolve the barotropic damping or

barotropic instability which may arise from the mean wind profile. The wave number is taken as the wave number from the linear baroclinic instability theory which gives the highest growth rate. The initial mean wind field contains a sinusoidal jet at the upper level and zero speed at the lower level, The initial disturbance is sinusoidal in y and independent of height.

Each numerical experiment is extended to 300 days and all of the experiments attain approximate statistical equilibrium after about 100 days. The experiment with $w = 8000$ km showed large fluctuations in disturbance energy. One period of very rapid growth is attributed to barotropic instability of a double jet structure in the mean wind. The experiment with $w = 4000$ km. produces a constant amplitude propagating a baroclinic wave. This work was carried out by Frank H. Taylor.

AN EPISODE FROM THE STUDY OF **THE** SOLAR SPIN-DOWN PROBLEM (Abstract)

Takeo Sakurai

A characteristic property of the solar interior is its high degree of stratification. In these circumstances, the effect of the Ekman's pumping mechanism is restricted to a thin layer near the interface between the radiative and the convective region. The spin down of the radiative region is brought about by the Eddington-Sweet circulation in a time long compared with the usual spin-down time, but short compared with the viscous diffusion time,

We first examined this situation in cylindrical geometry, using the linearized Boussinesq equations to describe the rotating stratified

fluid, We obtained an estimate of the Eddington-Sweet time, determined the parameter range for which this Eddington-Sweet mechanism is relevant, and discussed the quasi-steady asymptotic state. We also examined the case of a non-Boussinesq fluid for the same geometry, and discovered the existence of a thermal wind effect.

We next considered the effect of the Eddington-Sweet circulation on the evolution of the rotation of the sun's deep interior under the influence both of the solar wind torque and a molecular weight gradient. We obtained the rather paradoxical result that, because of the inward transport of angular momentum by the Eddington-Sweet circulation, the surface angular velocity decays faster when this circulation is present than is the case when the convective region alone is spun down.

The main part of the above study was finished while I was at the National Center for Atmospheric Research* as a Long Term Visitor of the Advanced Study Program;

*The National Center for Atmospheric Research is sponsored by the National Science Foundation.

FRONTOGENESIS (Abstract)

R. Terry Williams

A front is a sloping zone of rapid potential temperature change. The tangential horizontal wind component also displays a rapid change through the frontal zone in the sense that the vertical component of the vorticity is large and positive, The frontal scale is about 100 km, whereas baroclinic instability injects disturbance energy into the atmosphere on scales of about 1000 km, The explanation of frontogenesis

requires a mechanism which can produce a small-scale zone from an **initially** smooth large-scale temperature field,

The operation of horizontal wind deformation fields can cause temperature gradient increases at least near the surface where the vertical motion is zero. We shall consider the stretching deformation field which was proposed by Bergeron (1928). Shearing deformation is also important but it will not be considered here, Stone (1966) carried out the first analysis of this effect with the quasi-geostrophic equations. A similar problem was solved by Williams and Plotkin (1969). In both studies the deformation fields remain constant in time, and the quasi-geostrophic equations become linear. These studies used the Boussinesq approximation and confined the motion between two rigid horizontal planes,

Williams and Plotkin showed that the solution can be obtained at any time if the principle of conservation of quasi-geostrophic potential vorticity is used. The potential vorticity is known at all points as a function of the initial fields, and this leads to Poisson's equation for the pressure field, The boundary conditions are obtained from the **conservation** of temperature along the upper and lower boundaries. The solutions show temperature discontinuities at the upper and lower boundaries which occur in the limit of large time. Except for these two points the temperature is everywhere continuous, and scale of the temperature variation away from the boundaries is equal to the Rossby deformation length divided by π . The region of maximum temperature gradient has no **tilt** in the vertical and the tangential velocity has logarithmic singularities at the two points where the temperature is **discontinuous**. Certain features of

this quasi-geostrophic frontal zone are not realistic. This frontal zone does not **tilt** with height as atmospheric fronts do. The tangential velocity is such that the vorticity in the center of the frontal zone is zero, with large positive and negative values on each side. Atmospheric fronts are found in regions of large positive **vorticity**. The quasi-geostrophic equations cannot describe the entire frontogenesis process because as the frontal scale becomes small the local Rossby number becomes large.

Hoskins and Berrherton (1971) and Williams (1971) have shown that the unrealistic features of the quasi-geostrophic frontal zones can be removed if more complete equations are used. Hoskins and Bretherton assumed geostrophic balance for the tangential wind component and they also assumed that the initial temperature gradients were very small. They transformed the equations using a quasi-Lagrangian horizontal coordinate which is proportional to the absolute momentum. Their transformed potential **vorticity** equation has exactly the same form as with the quasi-geostrophic equation and the boundary conditions are also identical. Thus the exact solution can be obtained by transforming the quasi-geostrophic solution from the Lagrangian coordinates back to the original cartesian coordinates. The transformation depends on the tangential wind component predicted by the quasi-geostrophic theory. The non-geostrophic solutions show the formation of discontinuities in temperature at the upper and lower boundaries within a finite period of time, and in general a more rapid frontogenesis than in the quasi-geostrophic case. The frontal zone develops a **tilt** in the proper sense, and large positive vorticities occur in the frontal zone. These frontal zones are quite realistic up to the

time when turbulent diffusions of heat and momentum would limit the frontal scale. Williams (1971) performed numerical calculations which gave the same results without the assumptions which Hoskins and Bretherton used.

References

- Bergeron, J. 1928 Uber die dreidimensional verknupfende Wetteranalyse I. Geofys.Publikasjoner, 5(6): 1-111.
- Hoskins, B. J. and F. P. Bretherton 1971 Atmospheric frontogenesis models: Mathematical formulation and **solution**. (unpublished-manuscript) .
- Stone, P. H. 1966 Frontogenesis by horizontal wind deformation fields. J.Atmos.Sci., 23: 455-465.
- Williams, R. T. 1971 **Linear** versus non-linear frontogenesis, (unpublished manuscript).
- Williams, R. T. and J. Plotkin 1968 Quasi-geostrophic frontogenesis. J.Atmos.Sci., 25: 201-206.

THE PROBLEM OF OXYGEN IN THE EARTH'S ATMOSPHERE (Abstract)

Saiyed I. Rasool

The presence of free O_2 in the atmosphere of the Earth, as much as 20%, is unique in the Solar System, This relatively large abundance of free oxygen in the atmosphere is all the more intriguing because not only the whole Earth but even the upper crust is in a partially reducing state.

It is well-known that the major source of present-day oxygen in the atmosphere is the photosynthetic conversion of CO_2 and H_2O into carbohydrates and oxygen. The oxygen thus produced is almost immediately used up in respiration, However, a small residual amount, which can be accounted for by the total organic carbon buried in the crust, has slowly accumulated at the surface and in the atmosphere of the Earth. Another source of free O_2 is the photodissociation of H_2O and the subsequent escape of H_2 . At the present time, this rate of dissociation is small

$\sim 10^8/\text{cm}^2/\text{sec}$ and the rate of H_2 even smaller $10^7/\text{cm}^2/\text{sec}$. However, in the early history of the Earth before the commencement of photosynthesis, this rate of photodissociation should have been much higher, at the rate of 10^{11} particles/ cm^2/sec as has been suggested by Brinkman. This is so because of the absence of free O_2 in the Earth which now screens the solar ultraviolet from penetrating into the lower atmosphere. If this were true, free O_2 would have accumulated quickly and oxidized the early atmosphere. In the present study, it is shown that 10^{-6} mixing ratio of ammonia would inhibit photodissociation of H_2O and accumulation of O_2 . A balance sheet for the sources and sinks of O_2 both in the early atmosphere and the present-day atmosphere is presented.